UNIVERSITÀ DEGLI STUDI DELL'AQUILA
DIPARTIMENTO DI INGEGNERIA INDUSTRIALE E DELL'INFORMAZIONE E DI ECONOMIA

Dottorato di Ricerca in Ingegneria Industriale e dell'Informazione e di Economia

Curriculum in Ingegneria Elettrica, Elettronica e dell'Informazione

XXXV ciclo

Titolo della tesi

SENSORS AND ELECTRONIC SYSTEMS FOR STRUCTURAL AND ENERGY MONITORING

SSD ING-INF/01 (Elettronica)

Dottorando

Romina Paolucci

Coordinatore del corso

Prof. Giuseppe Ferri

Tutor

Prof. Giuseppe Ferri

a.a. 2021/2022

Table of Contents

Abstract

Safeguarding human life and, more generally, the well-being of the individual are probably some of the highest and most noble goals that research pursues on a daily basis. Topics (and goals) of this thesis are on the one hand structural monitoring, on the other energy/environmental monitoring. Each of the two, albeit from different points of view, contribute precisely to place human being at the centre, safeguarding his life and health. For this purpose, innovative electronic systems have been developed. The common denominator is the basic structure of the system: a series of nodes that communicate with the master which in turn interfaces with the PC. From time to time, however, each system has been configured in an optimal way to respond to the specific need, through the careful choice of the particular devices used.

To this aim, specific sub-topics have been addressed. From the point of view of structural monitoring, the focus was on the study of synchronization, damage index and modal frequencies. As far as synchronization is concerned, the experimental results have shown that, thanks to the use of the RS485 protocol, the developed system is able to monitor the structure with data synchronization from each node. From the point of view of the damage index, the experimental results show that the estimated damage index increases when the structure is disturbed. In particular, the damage indicator is increased to a maximum value of 24.65 when the structure is disrupted by a 2.5mm incision. As far as the study of modal frequencies is concerned, the novelty of the developed system lies in the fact that the data processing starts directly on board the nodes. The experimental results have shown that there is actually a significant variation of the modal frequencies when the conditions of the structure vary.

In relation to energy/environmental monitoring, an interesting and innovative study was carried out on the potentially dangerous emissions of fine particles into the atmosphere within a building site. The experimental results show that the emissions of PM 2.5 and PM 10 detected during the demolition activity far exceed, in some moments, the threshold values. In fact, peaks as high as about 123 $\mu g/m^3$ for PM 2.5 and over 1000 $\mu g/m^3$ for PM 10 have been detected.

Keywords

Accelerometer system
Construction Site
Damage Detection System
Damage Indicator
Dust Level
Dust Sensor
Electronic System
Intelligent Structure
IoT Structural Monitoring
Sensor Networks
Smart Buildings
Structural Health Monitoring
System Monitoring

Chapter 1: Introduction

Safeguarding human life, health and, more generally, the well-being of the individual are probably some of the highest and most noble goals that research pursues on a daily basis.

There are many ways and many points of view to do this. Although, probably, what immediately comes to mind is the medical field, this need is also strongly felt in the engineering field.

The objective of this research work is precisely the development of systems capable of operating in this sense. In particular, in the past three years, I have essentially dealt with two topics: on the one hand, structural monitoring, on the other, energy monitoring, with particular reference to the environmental field.

1.1 STRUCTURAL MONITORING

As far as structural monitoring is concerned, the continuous succession in recent years of large-scale seismic events, of tragedies such as that of the Morandi bridge, and, last but not least, of climatic upheavals which make phenomena such as landslides and floods more and more frequent, should today more than ever, make us reflect on the absolute need to take care of the built environment. This means paying the utmost attention so that critical situations are not created which lead the structures to be extremely fragile, and such as to constitute a potential danger to human life. To prevent this from happening, therefore, it is necessary to keep the "state of health" of the structure under control (whether it is a building, a bridge, etc.).

Structural monitoring, known in the literature as SHM (Structural Health Monitoring), is aimed precisely at this.

SHM is certainly a multidisciplinary subject that affects electronic and mechanical engineering as well as civil and infrastructure engineering. So far the most monitored structures have been bridges, dams and public buildings, but recently the attention has also extended to residential buildings.

The difficulty of structural monitoring lies in the fact that, except in rare and particular cases, each structure is unique and unrepeatable, both in terms of

construction technology and age. It is therefore necessary to develop non-rigid systems, but also able to easily adapt to the particular building being evaluated. For this reason, the development of an optimal monitoring system is still an open challenge [1]: establishing which of the existing ones is the most appropriate is by no means trivial, and also the aforementioned interdisciplinarity makes it extremely complex to take into account all the variables involved.

Structural monitoring systems encounter two types of challenges: aging, with consequent and gradual loss of operating conditions, and the occurrence of a sudden and unexpected event, as an earthquake or a landslide[2]. However, there is a certain heterogeneity in the methods of applying structural monitoring. The objectives go towards a more precise detection capacity, easier management, and storage of data (even when they are in large quantities), timeliness, and reliability of the information provided [3].

1.2 ENERGY/ENVIRONMENTAL MONITORING

As far as environmental monitoring is concerned, the focus of the work carried out during the PhD was the study of the emissions of fine particles emitted into the atmosphere during the demolition of buildings. Given that the writer has personally experienced the devastating earthquake that occurred in L'Aquila, Italy, on April 6, 2009, she has also been able to ascertain that, in the aftermath of such destructive events, we find ourselves having to manage an intense reconstruction activity . This translates into the simultaneous presence of many construction sites. As can be easily understood, by its very nature, the construction site is an environment in which one of the risks to which workers are most exposed is that of dust. From this, it follows that this risk is enormously amplified in the event that it is necessary to proceed with the total demolition of the building subject to intervention. Hence the need to study these emissions, and to develop any corrective actions, in order to safeguard the health of workers and anyone involved in the construction site for various reasons.

Moreover, the continuous and heavy emission of fine particles constitutes a potential source of pollution, an issue which has also been particularly felt in recent years. Not surprisingly, the level of dust present in the air is an increasingly important problem in industrialized countries due to their impact on human life and the environment [4].

From the point of view of human health, these particles can cause problems such as asthma, respiratory issues, and even cancer. From a more strictly environmental point of view, they have a major impact on global warming, thus worsening the quality of life.

The most dangerous are the so-called “fine particles”, in particular PM 10 (formed by particles with a diameter of less than 10 μm) and PM 2.5 (formed by particles with a diameter of less than 2.5 μm).

In this sense, both Europe and theWorld Health Organization (WHO) have set very specific limits. The European daily limit of PM 10 is 50 $\mu g/m^3$, not to be exceeded more than 35 times a year with an annual average limit of 40 $\mu g/m^3$. The WHO allows only three surpluses per year of the daily threshold of 50 $\mu g/m^3$, lowering the annual average to 20 $\mu g/m^3$. For PM 2.5, Europe sets a limit of 25 $\mu g/m^3$ and the WHO sets a limit 10 $\mu g/m^3$.

The presence of PM 2.5 and PM 10 is due, on the one hand, to natural phenomena (for example, forest fires); on the other hand, it is also due to the increasingly numerous presence of vehicles, industries, etc [5]. These aspects give importance to developing flexible, economical, and easy-to-use systems to control emissions in this second case. Systems with these characteristics are quite widespread in the literature, especially from the point of view of effective structural and environmental monitoring [3,6-25].

Given the topics covered and previously introduced, this thesis is structured in two sections: structural monitoring (Chapter 2:), and environmental monitoring (Chapter 3:).

Chapter 2: Structural Monitoring

This chapter deals in detail with the issue of Structural Monitoring, introduced in the previous chapter (section 1.1). After a paragraph dedicated to the literature review (section **Errore. L'origine riferimento non è stata trovata.**), three main topics were addressed: synchronization (section 2.2), the damage index (section 2.3), the study of modal frequencies (section 2.4), showing contextually the scientific results achieved for each of them.

2.1 LITERATURE REVIEW

As mentioned in the first chapter, and in particular in the section 1.1, the application of a system that allows structural monitoring has a specific name in the literature, which is Structural Health Monitoring (SHM) and it is an extremely widespread theme in the literature, due to the interdisciplinarity of the theme.

Indeed, Schubel et al. [26] presented a review of structural health monitoring techniques for wind turbine blades. With reference to this specific area, the application of structural monitoring makes it possible to save on production time and to reduce the cost of the quality control phases. Furthermore, the complete knowledge of the behavior of the structure through monitoring permits better design and manufacturing. An essential other application of structural health monitoring is for aircraft. Diamanti et al. [27] presented an SHM technique for composite structures of the aircraft. The size of the critical damage has been determined by the defect of the composite structures that can be found with a visual inspection, electromagnetic testing, ultrasonic inspection, and other methods. Furthermore, fiber optic sensor technology is increasingly used for aircraft monitoring to reduce the cost of maintenance and to identify damage in the structure [28].

There is a wide variety of monitoring solutions, in addition to the number and complexity of sensors. Indeed, there are methods based on the study of natural frequency [10], which allows the study of vibrations. Furthermore, there are methods widely used in the case of sudden structural degradations [8]. Other methods are based on the study of modal forms [29], where a system is capable of limiting false alarms. Then, there are the so-called “hybrid” methods because they are based on the study of

approaches [11]. Methods based on the use of artificial neural networks, capable of learning from past data and formulating predictions on future evolutions of the structure, are also an object of study [3,12].

The structural monitoring, in addition to ensuring that the structure is always in excellent health, also exempts from the need to carry out visual inspections and substitute the use of more conventional methods (for example ultrasound methods). The advantage of the SHM is related to a very promising alternative and efficient with respect to the conventional methods. Indeed, visual inspections are not always possible and are, in any case, expensive in terms of time and money, while the use of conventional methods cannot give up on the operator experience [30].

Therefore, SHM is generally characterized by a non-destructive approach allowing continuous and autonomous monitoring thanks to the use of integrated sensors [31-32]. A typical structural monitoring system, then, is made up of a sensor system, a data processing system, and a health evaluation system [33].

Furthermore, there were different ways in which SHM has declined over the years, also in reference to different degrees of complexity. In [6], for example, an SHM system was born practically by chance because the rather poor sensors installed at the Meazza Stadium in Milan, were not originally intended to monitor the structure. Only later, it became clear that the information returned was also interesting from that point of view. In [7], on the other hand, a much more complex system is presented, which makes use of more than 600 sensors, testifying how wide and varied this field of research is.

Wang et al. [34], proposed a wireless structural health monitoring system for real-time data acquisition. This kind of system is limited in the number of sensors and the capability of the synchronization of the samples. Indeed, to increase the sampling rate, the number of sensors connected in the same network decreases. Therefore, with a sampling frequency of 100 Hz, the number of nodes is equal to 12. Furthermore, to use a wireless monitoring system in a large structure, such as a bridge, a peer-to-peer wireless sensor network must be designed and improved. Hu et al. [35] developed a wireless monitoring system integrated into the Zhengdian Highway Bridge for structural health monitoring. This system is able to acquire samples in continuous mode using a microcontroller and ADC to acquire analog accelerometers. The main problem of analog accelerometers is the output drift due to the temperature, and

compensation circuits are needed. The work shows the limitation of the proposed wireless system in terms of output data. Indeed, the results are limited due to the noise interference of the analog circuits and data losses of the transmission.

One of the most popular components in the field of structural monitoring is the ADXL355 accelerometer [36], and this work is no exception, as we will see later. This is a digital sensor that is able to acquire the three-axis accelerations internally and send them to an external microcontroller.

Effectively, multiple works in the literature [16-18,37-41] present a monitoring system for structural health monitoring using the accelerometer ADXL355. These works are divided into the system based on a wireless sensor network (WSN) and wired monitoring systems. Valenti et al. [18] proposed a low-cost WSN for SHM and the system has been used for identification of modal frequency. The problem of this system is the synchronization of the samples. Indeed, the only synchronization refers to the start time and stop time that the master sends to the node. Other work that used a WSN was proposed by Wondra et al. [40]. The WSN was also used for monitoring the wind turbine tower to wind excitation. The limitations of this system ~~is~~ are the maximum sample rates (31 Hz) and the maximum number of nodes (three), respectively. Furthermore, synchronization is also a critical problem for this WSN.

The wired sensor monitoring system is an alternative to a WSN. An application for a wired system that used the ADXL355 is for earthquake detection [37-38]. Microseismic events is an important research field, and this kind of system can send warning messages when an event occurs. The limit of these systems is the small number of sensors that can be used. Indeed, the system is composed in general of one node that sends data to a web server. Other nodes are disconnected from each other and positioned at distances of kilometers. Pierleoni et al. [39] proposed a wired monitoring system with 64 samples per second without synchronization from each node that communicates the data through an ethernet connection. This system can appreciate the lowest modal frequency of the structures but not the highest due to the low sampling frequency. Quqa et al. [17], instead, realized a single node wired monitoring system for structural health. The system is able to identify the natural frequency and modal parameters in real-time. The system is based on a single-board computer and accelerometer ADXL355 that limits the synchronization and the maximum number of nodes connected in the same network. Navabian et al. [41]

proposed an event monitoring system for structural health. This system acquires data if the event exceeds the threshold, and the duration of the acquisition is about 70 s. Although, like [18], the synchronization is also available from the start and stop acquire campaign.

Based on the literature review of the monitoring system that used the same accelerometer of the system proposed in this work, a summary of the comparison between wired and wireless can be done. The existing wired monitoring system has a very high cost, a typically low number of sensors that can be connected in the same network, high bandwidth, high sensor data rate, and very high sensor synchronicity. On the other side, the wireless monitoring system has a low cost, a high number of sensors that can be connected in the same network, limited bandwidth, low sensor data rate, and critical synchronization of nodes [42].

Concerning the used methodology, the heart of SHM is damage detection. The occurrence of damage, in fact, can entail, and often does, changes in the characteristics of the structure (for example with regard to stiffness) [13] which, properly detected, needs maintenance work to avoid the aggravation of the situation since, in the long run, the structure itself collapses. It follows that the rapid identification of the damage is a fundamental step in SHM. A fully developed system should be capable of detecting and evidencing in near real-time the occurrence of a structural anomaly, identifying its location, and associating it with a type of structural damage and intensity [43]. There are two ways to monitor a structure. When its global behavior is analyzed, and the structure is considered as a single system, we speak of global damage identification. On the other hand, when we focus only on certain elements considered critical or already weakly damaged we speak of local identification of the damage [44].

The damage index is a problem that has been studied using various methods [14-15,25,45,57]. A fuzzy neural network for two-stage damage detection is presented by Jiang et al. [45]. A damage assessment based on a fuzzy neural network for the first stage has been performed. Whereas in the second stage, thanks to the use of the union of data fusion and fuzzy models, a final evaluation has been achieved. This approach can identify more patterns than the single-stage fuzzy model. Gui et al. [46] illustrated a three optimization algorithm for Gaussian kernel function parameters. These optimization algorithms are based on vector machines and are allowed to use them for damage detection. Other methods used the Particle Swarm Optimization algorithm

[47], Operational Modal Analysis with dynamic measurements [48], frequency response functions with artificial neural network-based for damage detection [49], and 1D Convolutional Neural Networks for vibration-based damage detection and localization in real-time [50].

One of the first works on the identification of the damage index addressed from the one-dimensional point of view is that shown in [51], in which a method to evaluate the integrity of the structures non-destructively is shown. In particular, it is described how the measurement of vibrations carried out in a single station in the structure can be used, in combination with a suitable theoretical model, to indicate both the position and the extent of the damage.

In [25] an application of the system for structural health monitoring using a damage detection method based on Stochastic Subspace Identification concepts [52] is shown. The method, being based on a non-parametric test, does not require to explicitly know system parameters and is suitable for automatic data-driven damage detection monitoring of in-service structures.

Any damage diagnosis method requires the extraction of damage-sensitive features from the measurement data of the monitored system. The feature vector is generally defined in a way that it is approximately Gaussian distributed with zero mean in the reference (undamaged) state and non-zero mean in the damaged state, hence the designation of the residual vector [53-54]. Many residuals have been used in the literature [55-56]; in this work, the subspace residual, representing the orthonormality defect between subspaces characterizing the dynamic response in the current state of the structure with respect to its reference, is adopted, specifically the robust subspace residual [57] less prone to changes in excitation covariance.

Measures of the dynamic response of the structure in its reference state are acquired over time to produce a statistical model of the residuals under changing environmental conditions [14]. If no structural damage occurs, the orthonormality assumption between the mentioned subspaces, evaluated for different data sets, remains approximately valid according to small residues. However, possible structural damage causes an increase in residues. This increase involves, with the choice of an adequate metric, a significant rise in the scalar damage indicator. Therefore, if this value falls beyond an appropriate threshold, it indicates the presence of damage [15].

Finally, the SHM, combined with environmental monitoring [58-21,58,60-62] and energy monitoring [22-24,63-66], makes it possible to achieve the so-called "completely intelligent structure".

2.2 SYNCHRONIZATION

The synchronization of the communication between the nodes and the master is one of the fundamental themes within the SHM. In fact, we typically have several nodes all connected to a master. Obviously, it is fundamental that the communication between nodes and masters takes place in the most orderly way possible, and therefore that the nodes are perfectly synchronized.

To do this, a particular electronic sensory system has been developed. It is based on one master device and N nodes that are synchronized through RS485 bus. The main component of the node is a microcontroller Sam3X8E Arm cortex-M3 [67] that is able to read a 3-axes accelerometer ADXL355 [36] via SPI communication. Thank to the use of a memory flash, the system can acquire up to 2 Mega-samples with high speed. An evaluation board based on Sam3X8E (on which, as we will see, the Arduino Due, used in this work, is based in turn) is used for the prototyping phase and the designed board is connected to it. Compared to [9], the proposed system uses flash memory to save data. The monitoring system has been tested with one master and two nodes to verify the synchronization between the samples.

2.2.1 General System Overview

The proposed monitoring system is composed of one master and N nodes that communicate through RS485 bus. The principle of operation of the designed monitoring system is the employment of the RS485 communication protocol to synchronization the nodes. The master device generates the clock signal used for synchronization. Indeed, thanks to the use of the RS485 protocol, the clock signal from master is able to reach each node, even hundreds of meters away. The scheme of the proposed monitoring system used for structural health is shown in Figure 1. Therefore, the master generates the clock signal to start the acquisition and at each rising edge the nodes sample.

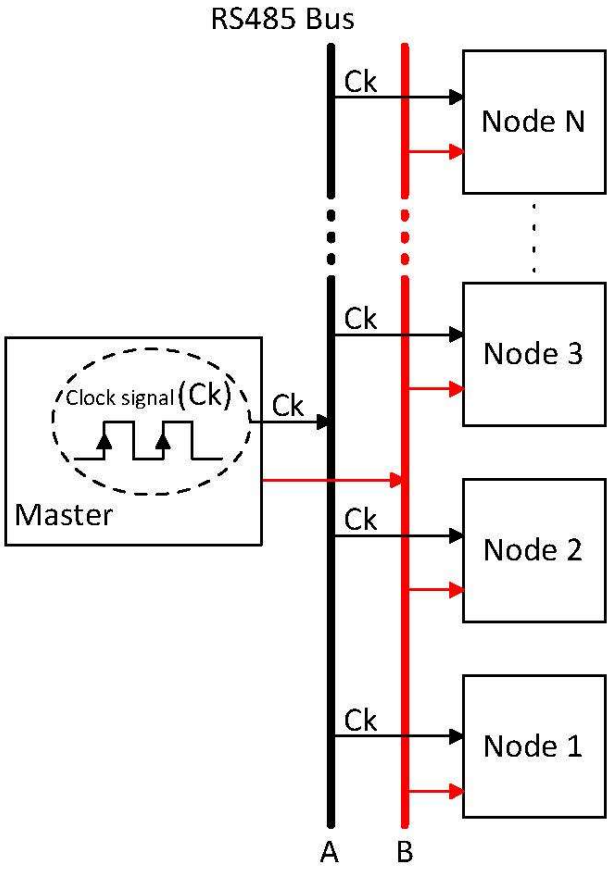

Figure 1: Typical scheme of the proposed monitoring system.

The proposed node is based on a microcontroller and a board with various blocks. In the prototyping phases, an Arduino Due board has been used and the node is a board that is plugged. The Arduino due is based on microcontroller Atmel SAM3X8E Arm Cortex-M3 [67]. The microcontroller has a 32-bit ARM core and runs at 3.3V with 12 ADC (analog to digital converter), 2 DAC (digital to analog converter), 54 digital input/output and an 84 MHz clock. The block diagram of the proposed monitoring node is shown in Figure 2.

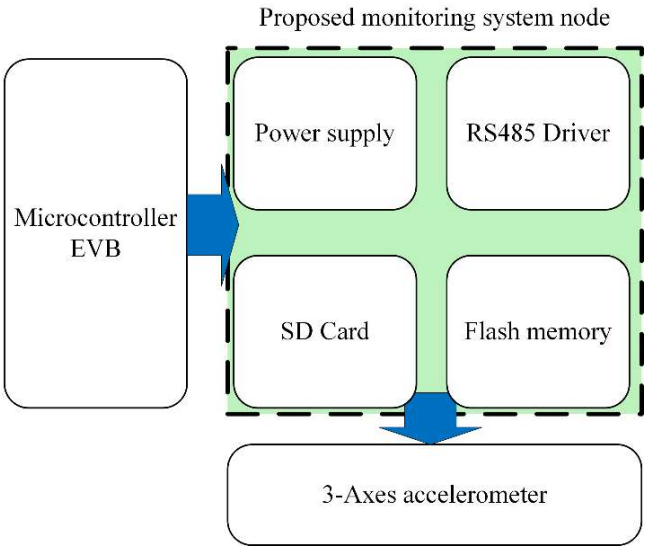

Figure 2: Internal proposed node architecture.

The designed node is a board able to plug directly on the microcontroller evaluation board (EVB). The node is composed of four main blocks. The first block is the power supply. Indeed, this block converts the 5V input voltage to 3.3V used for supply all blocks. The RS485 block is the driver connected to a digital pin of the microcontroller. The RS485 driver is able to convert the differential signal from bus to single-ended signal. Each time a rising edge of the synchronization clock occurs, an interrupt service routine is activated on the microcontroller. Therefore, the nodes acquire the same sample at the same time, thanks to this clock.

Furthermore, flash memory has been used to save the samples. The flash memory is S25FL256S with 32Mbytes from Spansion [68] connected through SPI with microcontroller. In addition to the flash memory, an SD memory has been inserted as a data backup.

Finally, a digital triaxial accelerometer ADXL355 [36] is used in the proposed system. This accelerometer from Analog Device is a low noise, low drift, and low power with 20 bit internal ADC. With the sensitivity of 400 mV/g at ±2g scale, the ADXL355 is suitable for the structural health monitoring. The accelerometer has been connected with the microcontroller through I2C communication.

Figure 3 shows an algorithm that ensures the functionality of the complete system. It provides information about the steps necessary for the operation of the single node. When the entire system is switched on, the system is initialized. Initialization involves the configuration of the communication buses, the setup of the digital pin as interrupt and the definition of the maximum waiting time between one period of the

clock and another. After the system initialization, the nodes wait for the clock signal from the master device. Once the master device generates the clock signal, the nodes are starting the acquisition phase. At each rising edge of the clock, the microcontroller reads the three axes from the accelerometer and saves them in the flash memory. Thanks to the flash memory and the use of the DMA of the microcontroller (direct memory access) it is possible to save three 32-bit data in a short time. The system is able to read the values from the accelerometer and save them on the flash memory up to 2.5 ms.

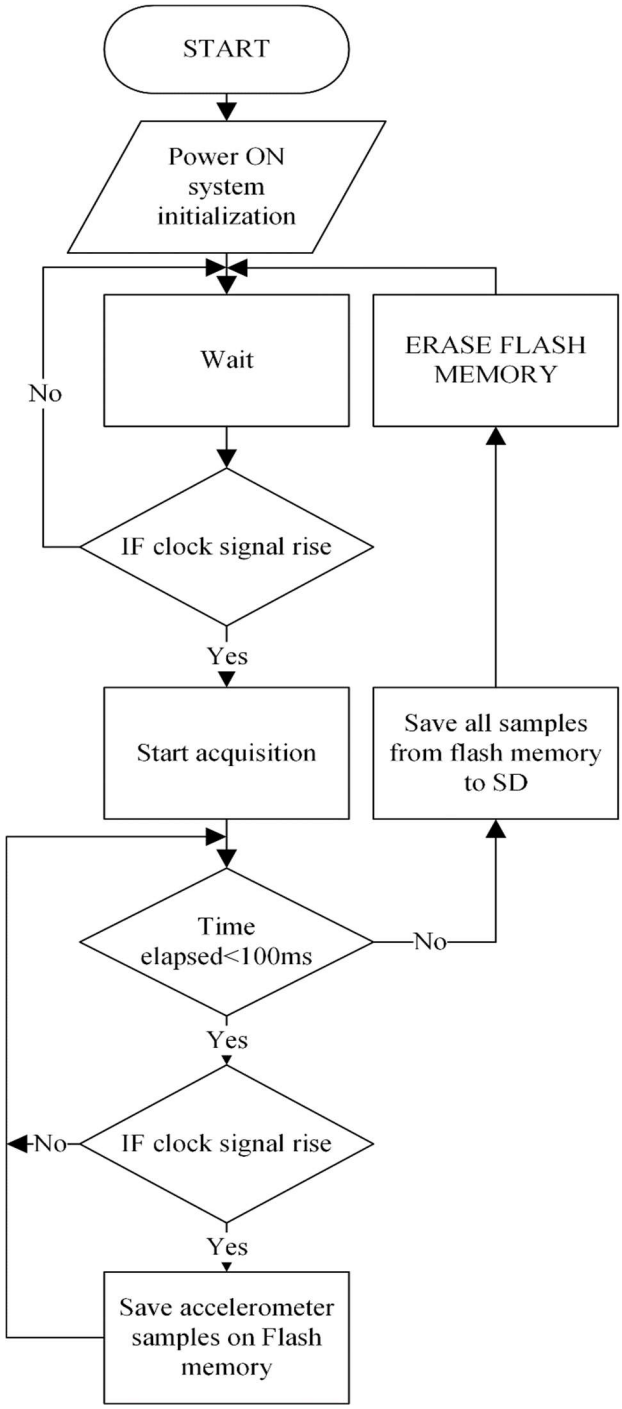

Figure 3: The algorithm that describes the operation of the proposed sensory monitoring system.

At each acquisition, three 32-bit values of the 3-axes and the time elapsed between sampling are saved. With four 32-bit data it is possible to save up to 2 Mega-samples in the flash memory. Indeed, it is possible to continuously acquire up to 84 minutes with a sampling frequency of 400 Hz.

However, when the master deactivates the clock to finish the acquisition, the node stops acquiring and transfers the data to the SD memory. In the present study, an interval of 100 ms was set. From this it follows that, if more than 100 ms elapses from

the last rising edge of the clock, the node ends the acquisition and transfers the data to the SD memory. Once the data transfer to the SD memory is finished, the microcontroller erases the flash memory.

Two pictures of the final prototype are presented in Figure 4 and Figure 5. In Figure 4 the board without the accelerometer with microcontroller board is shown. The accelerometer is connected to the white connector on the board. Figure 5 shows the final connection of the proposed monitoring system with a microcontroller board.

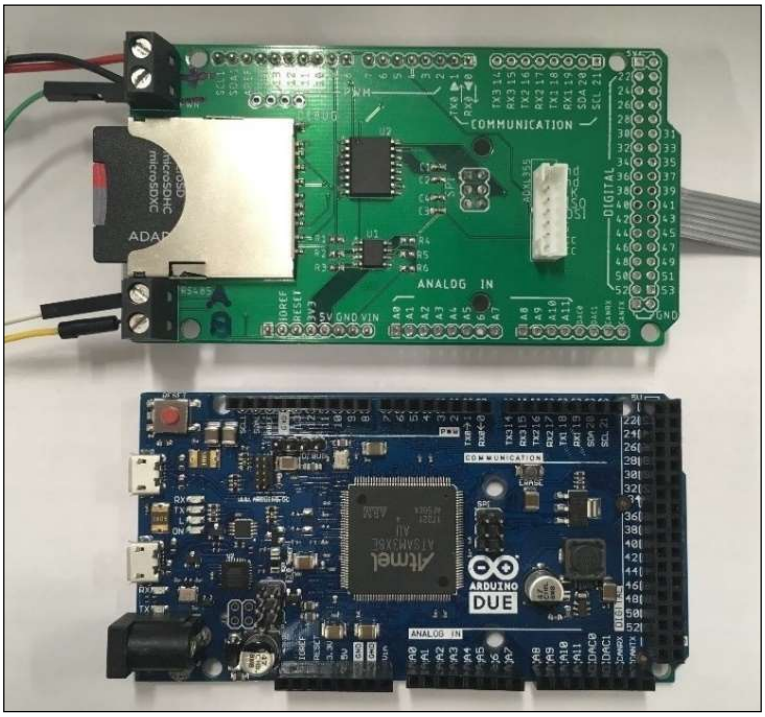

Figure 4: The prototype of the proposed monitoring system. The green board is the node, and the bottom one is the evaluation board of the microcontroller.

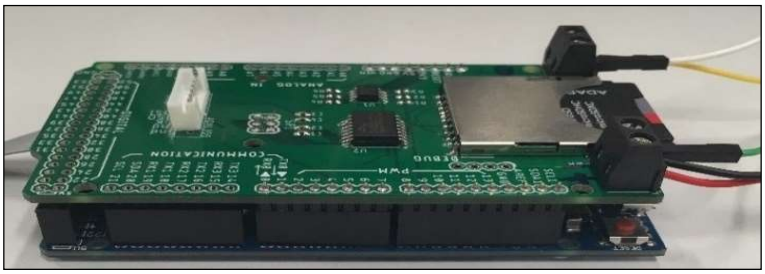

Figure 5: Final connection of the proposed monitoring system with a microcontroller board.

2.2.2 Experimental Set Up

The proposed monitoring system has been tested in the laboratory with one master device and two nodes. Synchronism between the nodes has been checked. The nodes were placed on the same test bench with the same orientation but at 2 m distance. External excitations check the samples synchronization on the two nodes.

The sampling frequency of 400 Hz has been chosen. The length of the test was about 2 minutes with total samples equal to 47656. When the master device is starting acquisition with the generated clock signal, the two nodes acquire at the rising edge saving the sample on the flash memory. Finally, the microcontroller transfers all samples from flash memory to SD for post processing when the clock signal was switched off from the master.

2.2.3 Results

Experimental results are shown in Figure 6. All samples of the nodes of the proposed monitoring system are synchronized. X1, Y1 and Z1 are the axes of the first node and X2, Y2 and Z2 are the axes of the second node. The enlargement of Figure 6a from sample 19300 to sample 20000 is shown in Figure 6b, Figure 6c, Figure 6d and Figure 6e.

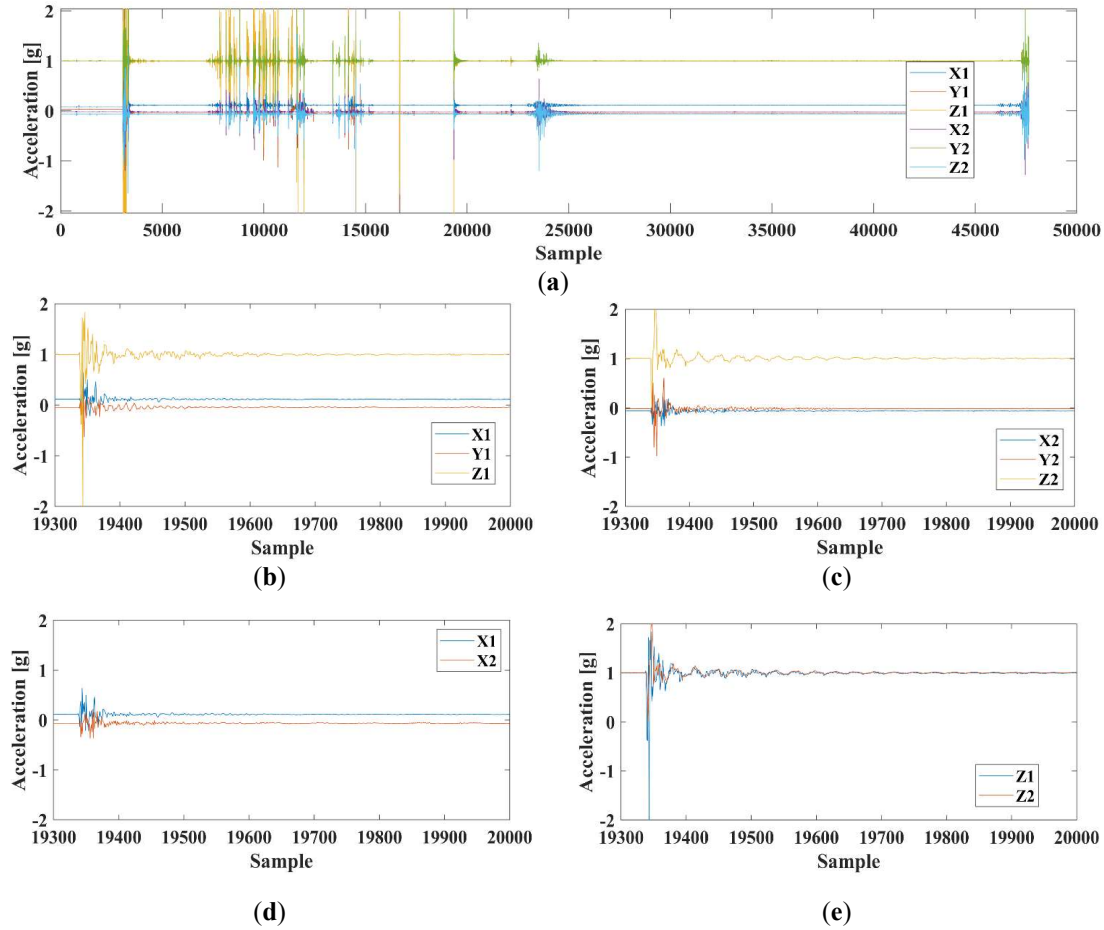

Figure 6: Experimental results with two nodes. The axes X1, Y1, and Z1 corresponding to the node one. The axes X2, Y2, and Z2 corresponding to the second node. **a**) All samples of the nodes of the proposed monitoring system. **b**) part of the samples of node one. **c**) part of the samples of node two. **d**) comparison between the X-axes of the nodes. **e**) comparison between the Z axes of the nodes.

2.3 DAMAGE INDEX

As mentioned in the introduction, another important issue within the SHM is the damage index. This is is a number whose variation certifies that the structure has been affected by a change in its structural characteristics.

In particular, an innovative electronic system has been developed whose strengths (and innovations) are the following:

1. the high number of nodes that can be connected in the same network, the only limitation is due to the RS485 protocol;
2. high bandwidth;
3. high data rate;
4. high synchronization between nodes;
5. low-cost system.

This system is based on the same microcontroller used for synchronization (Atmel SAM3X8E Arm Cortex-M3), but has obviously been optimized for damage index detection. For example, in synchronization each node was equipped with a single accelerometer. For the study of the damage index, on the other hand, two accelerometers were positioned on each node. This allows to optimally detect any change in the structure of interest.

2.3.1 Materials and Methods

In the present work, for the detection of the damage on the beam model, we proceeded “by comparison”: first, some measurements were performed on the intact test structure, assuming this as the reference state; subsequently, they were repeated on the same structure deliberately perturbed through an incision of 2.5 mm.

The conducted test has been divided into three phases: in the first phase, the sampling frequencies and the duration of the test were chosen; in the second one, we proceeded to start the system, acquire the samples, save them in an SD card, stop the acquisition, and send the data to the PC; the third and final phase consisted of the post-processing of data through Matlab. The test operating phases to derive the damage indicator are shown in Figure 7 as a sort of flow-chart. Phase 2 consists of two tests: the first is the test with a healthy structure and the second is with a damaged structure. At system startup, N = 1. Therefore, the system acquires and saves to the SD card

repeatedly for the test time. After that, the acquisitions were stopped, and data was sent to the PC. Instead, the second test consists of N = 2 and with the damaged structure. The system started and acquired the samples, saved them on the SD card, and then sent the data to the PC after the test time. The final phase is the post-processing of data for damage indication.

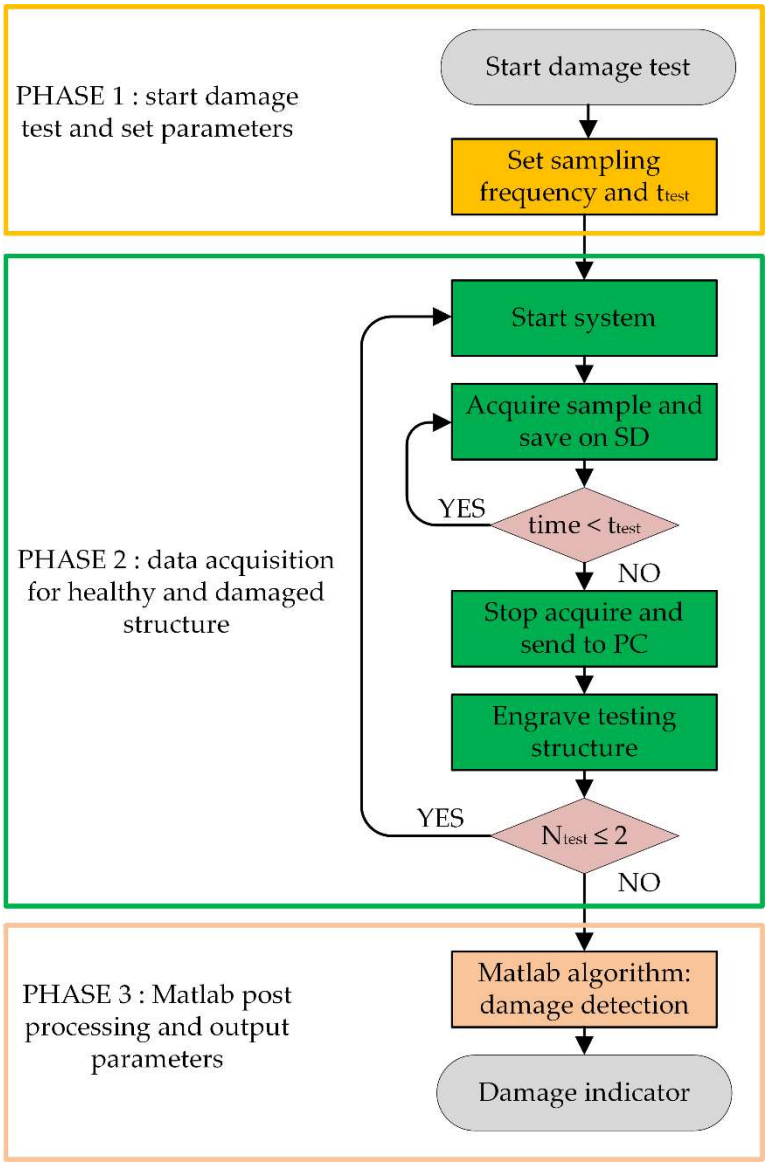

Figure 7: Damage indicator test operating phases.

2.3.1.1 System Description

The whole general scheme of the proposed monitoring system, with typical connection and node architecture, is shown in Figure 8.

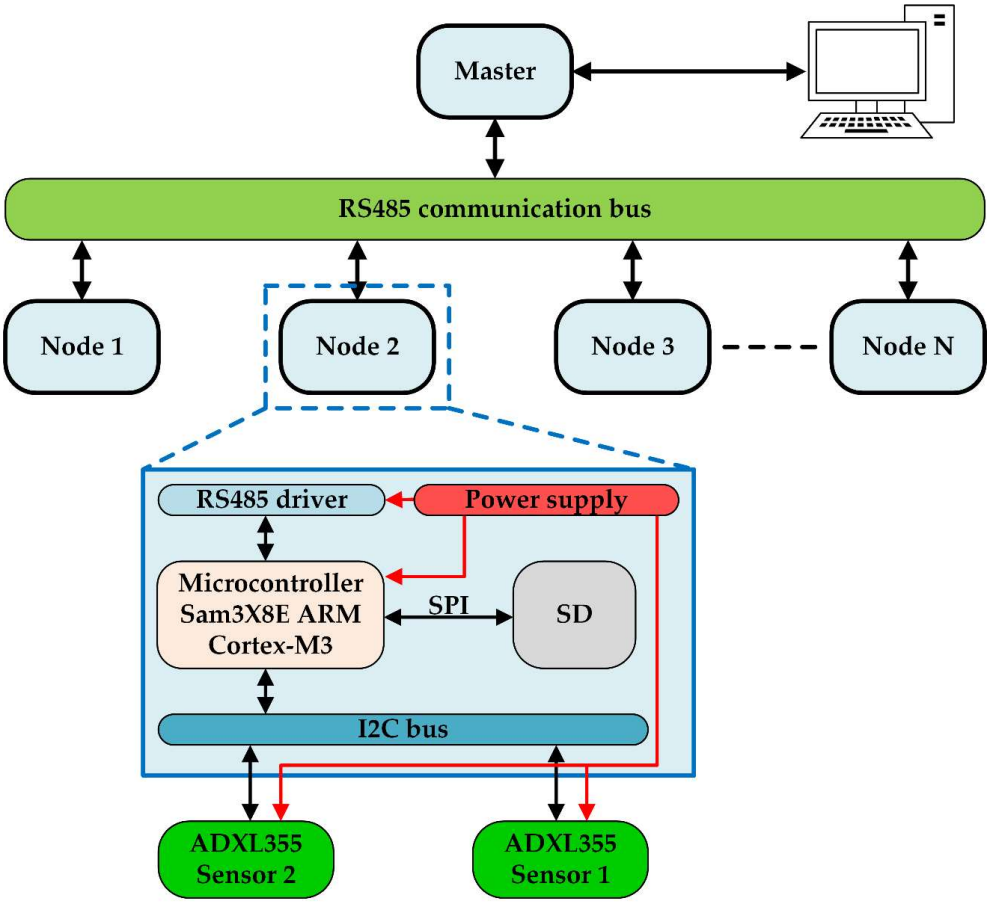

Figure 8: The scheme of the proposed monitoring system. In this scheme, the architecture of the node is presented.

The system is composed of nodes, described in more detail below, which, via the RS485 protocol, communicate with a master. The choice of this protocol is not casual: thanks to its characteristics, in fact, the nodes can be positioned even at a distance of hundreds of meters, without compromising their capability to communicate correctly with the master. This aspect is fundamental, as it allows the master to synchronize the various nodes, to recover the data sent by them and to forward them to the PC for post-processing via Matlab.

The single node, as seen in the previous figure, is made up of a microcontroller, the SAM3X8E ARM Cortex-M3 [67], equipped with an integrated Direct Memory Access (DMA). One of its tasks is to manage communication with the master.

The microcontroller, of course, needs to be powered. However, since the total current consumption of the node is only 100 mA, it is configured as a low power

system. This allows it to be powered also through photovoltaic panels with a battery and, then, the possibility of positioning the nodes even at great distances and in environments with no electricity.

In addition, the microcontroller provides data storage on an external SD (Secure Digital) card, whose presence is necessary considering that the number of samples acquired can quickly reach the order of millions. Therefore, at the end of the single acquisition, it is particularly useful to store the data on an SD card so that it can also be sent to the master later.

Another critical point of the system is related to the fact that the code execution time on the microcontroller for data acquisition and saving is much longer than the time occurring between one sample and the next. This always happens, even for sampling frequencies equal to 1 kHz, and makes it impossible to acquire and save all data sequentially. To avoid data loss, the integrated DMA has been used on the microcontroller, which, through direct access to memory, allows the bypassing of the control unit of the microcontroller itself and to store the data directly in the SD card memory.

To complete the description of the system, and in particular, of the nodes, it should be emphasized that, as can be seen in Figure 9, each of them is made up of two accelerometers, both connected to the same microcontroller. This is made possible by the fact that communication, in this case, is managed via the I2C protocol, which allows for connection of more than one device to the same bus, each with its own address, chosen via external hardware settings. In particular, the sensors used are integrated triaxial digital accelerometers. The fact that they are integrated makes it possible to calm the price of the system, making it effectively competitive even from a purely economic point of view. Specifically, the sensor model used is the Analog Device ADXL355, whose basic characteristics are voltage supply range equal to 2.25–3.6 V, settable range ±2, 4, 8 g for each axis, for ±2 g the sensitivity is 3.9 μg/LSB, low power device with 200 μA consumption in measurement mode and 20-bit internal analog-to-digital converter (ADC). The sensitivity of this sensor changes, according to the temperature, of ±0.01%/°C, with respect to the ambient value of 25 °C. The accelerometer has an internal temperature sensor that the microcontroller can read for the data compensation.

2.3.2 Experimental Set-Up

The proposed monitoring system has been tested utilizing the experimental setup shown in Figure 9, where the identification of damage indicator procedure has been applied. The environment temperature test was equal to 25 °C, and under these test conditions, the sensitivity of the accelerometers does not change. The cantilever structure (aluminum bar) has been anchored with a bench vice. The two accelerometers of the acquisition node have been put on the aluminum bar. The first accelerometer has been mounted at the end of the bar and the second is positioned at 16.6 cm distance from the blocking point.

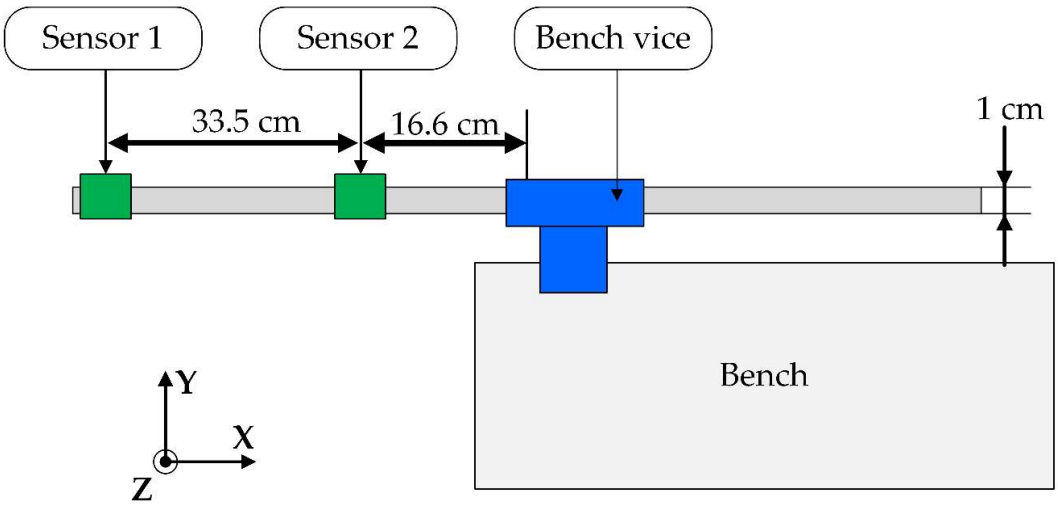

Figure 9: Testing the structure for the identification of the damage indicator.

For this test, one master and one node that communicate through the RS485 bus were used. The node acquires the data from two three-axis accelerometers, saves them on an SD card, and at the end of the test, transmits to the master device. Moreover, an external power supply for the node and master is required. A picture of the complete testing system is shown in Figure 10.

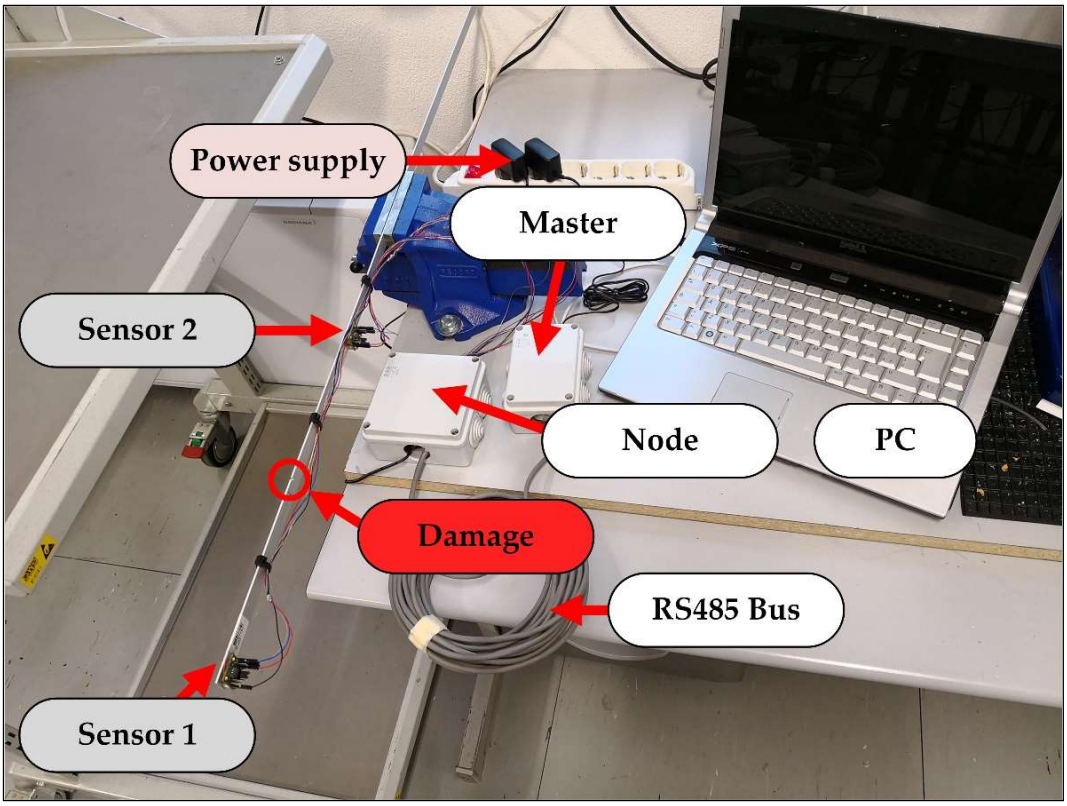

Figure 10: Experimental set-up of testing structure for the identification of the damage indicator.

Having adapted the sampling frequency of 200 Hz, two tests have been carried out. The first test concerned the acquisition campaign with the healthy structure, and after that, the aluminum bar was damaged for the second experiment. For damage detection, a perturbation to the structure was induced. Indeed, on the testing structure (Figure 11), a 2.5 mm engrave was realized. For both the tests, the bar was stressed with only ambient noise. The approach of damage detection is based on an algorithm that processes the output data of the acquisition system when the structure is subjected to external excitations. These output data represent two measurements lasting 15 min of the healthy and damaged structure. The algorithm allows the evaluation of the damage indicator of a structure.

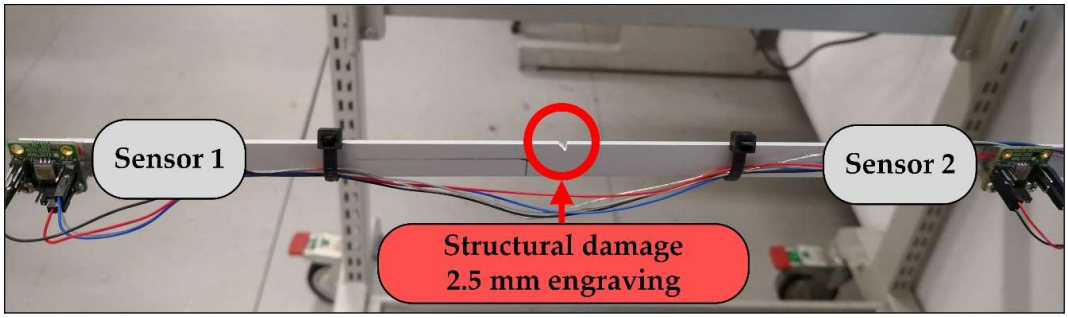

Figure 11: Engraved aluminum bar anchored in the bench vice for the damage detection test.

2.3.3 Results and Discussion

Measurements have been performed on six axes, three for each triaxial sensor. In Figures 12 and 13, the acceleration measurements relative to all axes located on the structure for the two tests are shown.

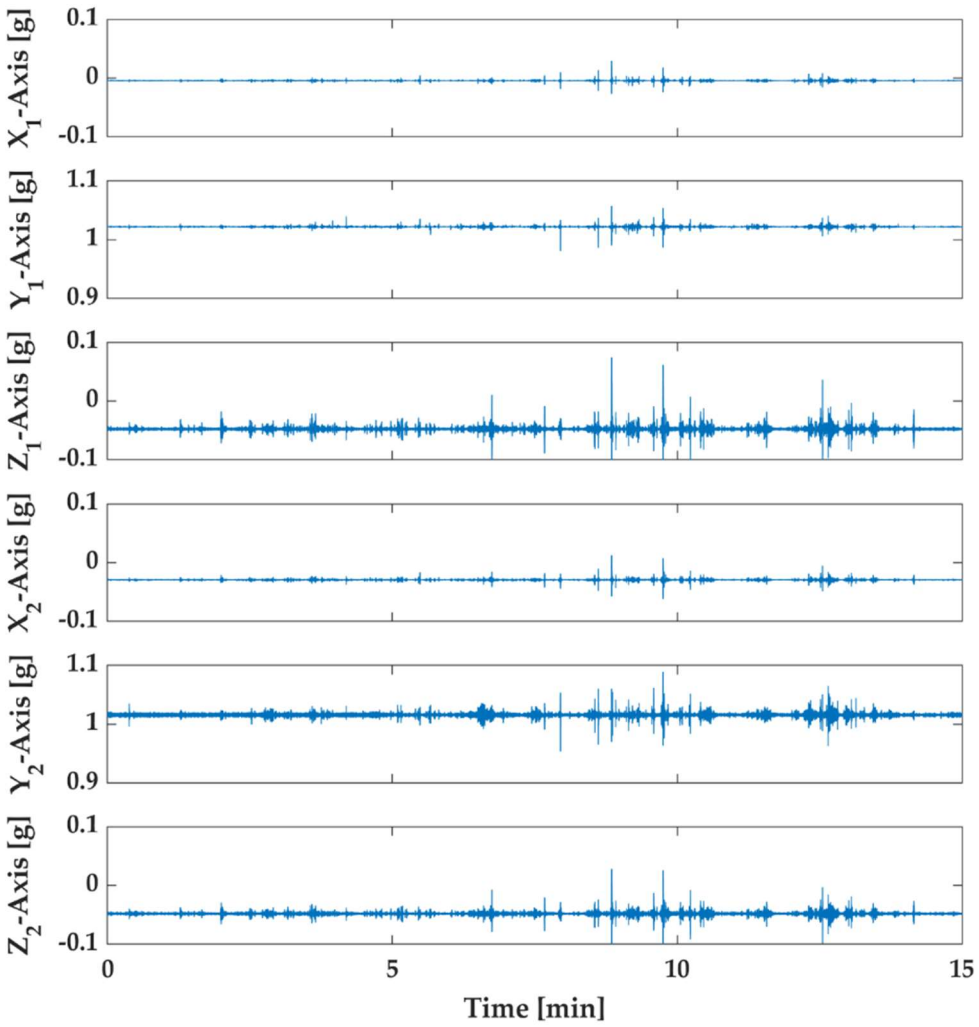

Figure 12: Six axes acquired data through the proposed monitoring system of the undamaged structure. The first three measurements are related to sensor 1 (X_1, Y_1, Z_1), and the others are from sensor 2 (X_2, Y_2, Z_2).

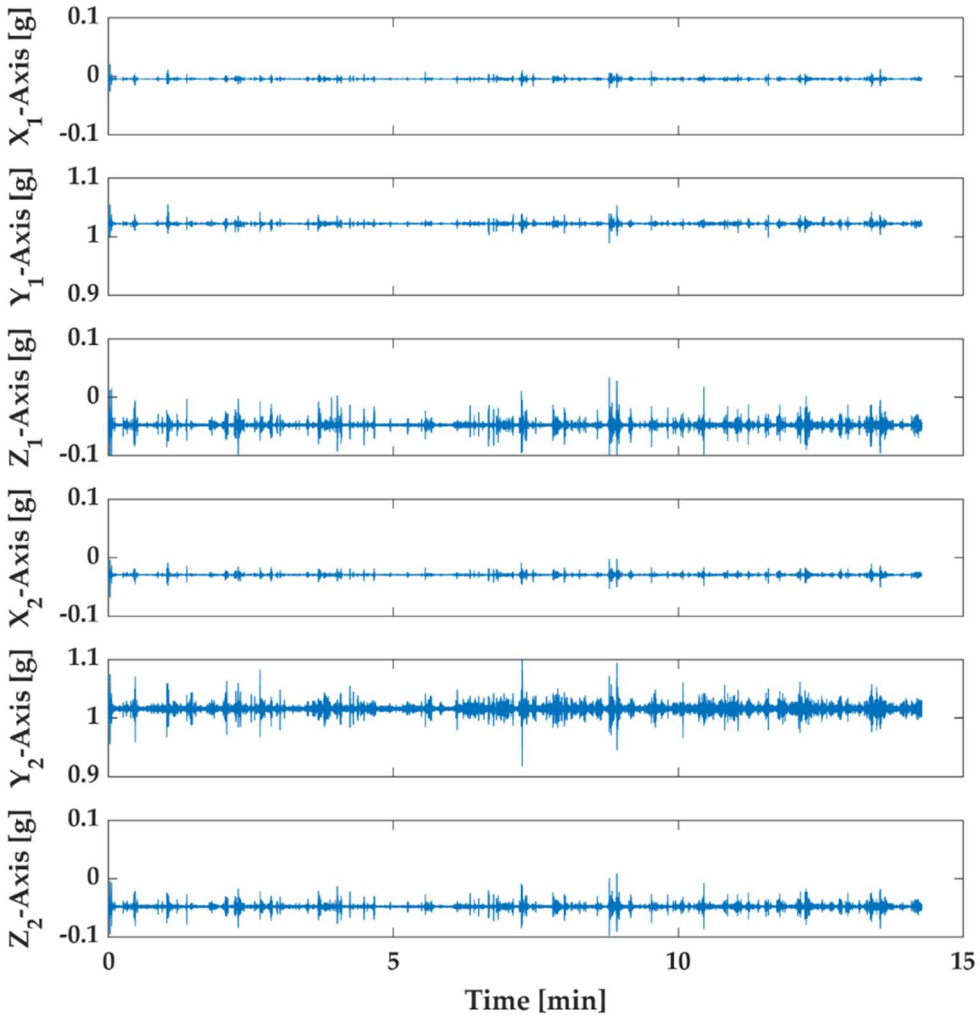

Figure 13: Six axes acquired data through the proposed monitoring system of the damaged structure (engraving of 2.5 mm). The first three measurements are related to sensor 1 (X_1, Y_1, Z_1), and the others are from sensor 2 (X_2, Y_2, Z_2).

The acquired samples were 224,400 for the healthy structure and 213,602 for the damaged structure. Indeed, with sample time equal to 5 ms, the whole experimental time is about 15 min for the healthy structure and approximately 14.27 min for the damaged structure. In order to estimate the damage indicator, the first measurements have been divided into four series with about 50,000 samples each. These series have been called UD1, UD2, UD3, and UD0. The latter series UD0 has been used to calculate the damage indicator as the reference subspace. Similarly, the measurements of the damaged structure have been divided into four series called D1, D2, D3, and D4 with the same number of samples.

Therefore, with the reference subspace UD0, the algorithm returns three damage indicator values for the healthy structure and four for the damaged structure. These

values are smaller in structural health condition than the structural damage condition. The values of the damage indicator are shown in Figure 14.

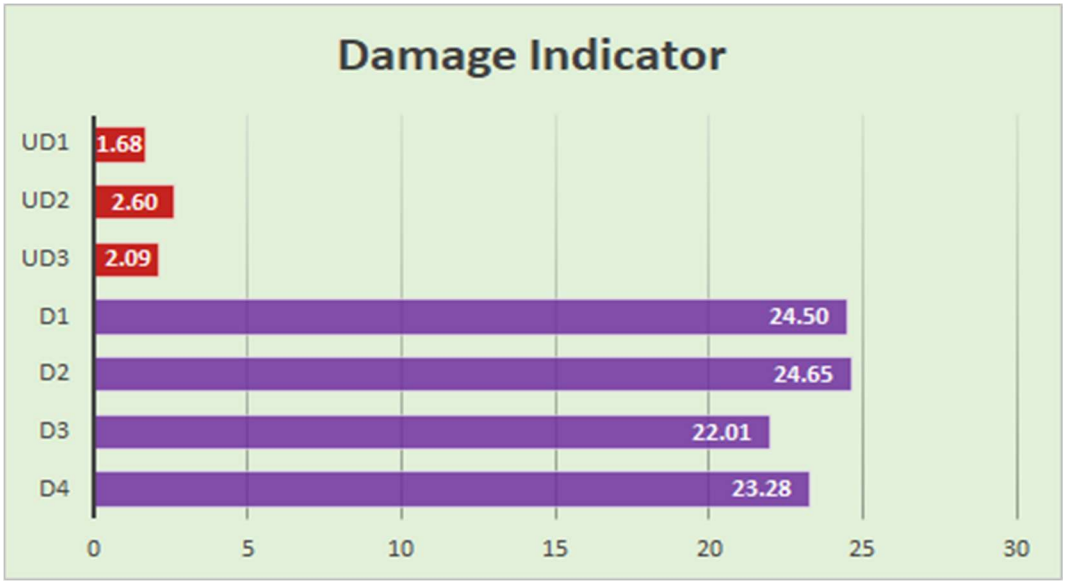

Figure 14: Values of the damage indicator. The red bars represent the structure in a healthy condition and the violet bars show the damage indicator with the engraved structure.

Finally, in Table 1, the calculated damage indicators have been reported. The values of the damage indicator have an increase of ten times, with only a 2.5mm engrave. The results show that the proposed system, with synchronous samples between the two sensors, is able to detect damages in a monitored structure. However, the proposed monitoring system with a damage indicator approach will detect structural defects or damage after events such as earthquakes or landslides.

Table 1: Damage indicator values for all measurements in undamaged and damaged structures.

Condition	Series	Damage indicator
Healthy structure	UD1	1.68
	UD2	2.60
	UD3	2.09
Damaged structure	D1	24.50
	D2	24.65
	D3	22.01
	D4	23.28

2.3.4 Node improvement

The node presented in the system just described was subsequently improved [69]. In particular, a new type of node has been developed. Specifically, each single node has been equipped with a very large flash memory, capable of storing a large number of data.

In Figure 15 the internal architecture of the proposed node is shown.

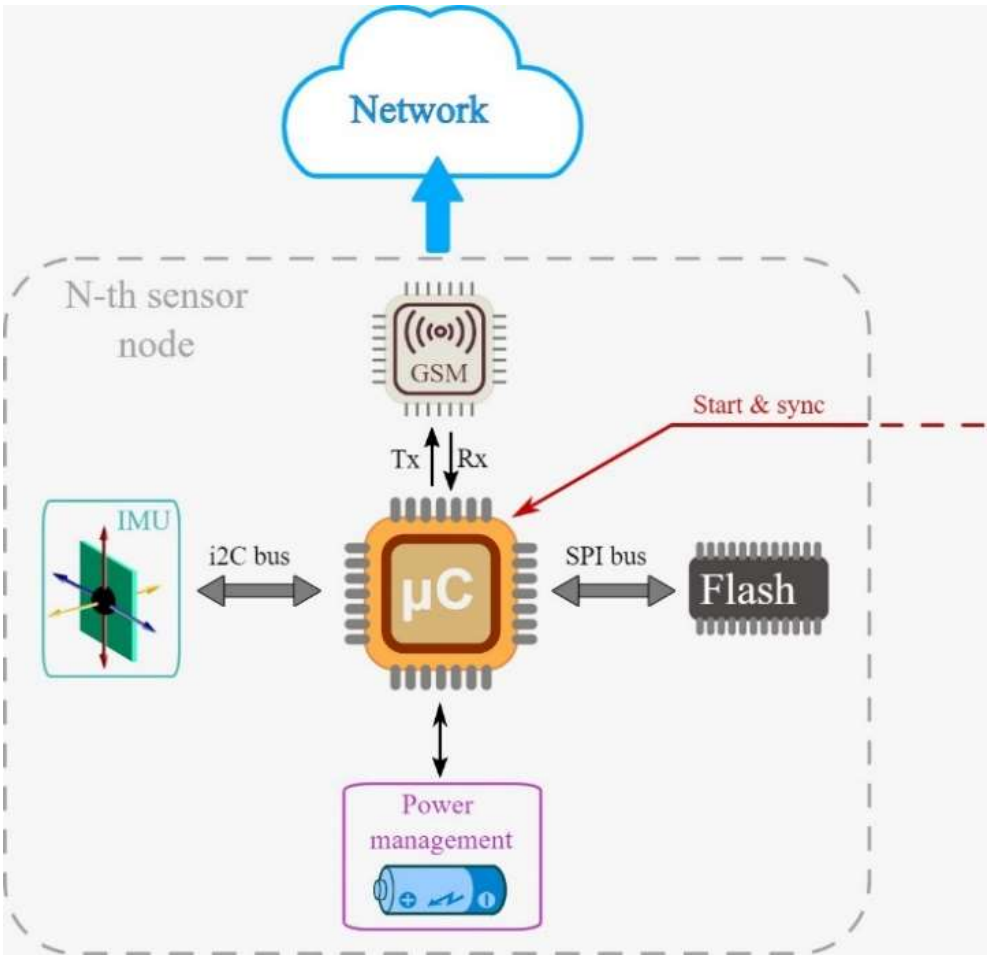

Figure 15: Internal architecture of the proposed node.

The heart of the node is the microcontroller, which constitutes its intelligent part. The microcontroller (AtMega 328p) receives a synchronization which gives the start to the signal. This signal can come from the outside, or, alternatively, from a master microcontroller. During sampling, the microcontroller takes data provided by the accelerometer and save them locally on the flash memory via an SPI bus. Specifically, the memory is a 512 Mbit NOR Flash (IS25LP512M). Furthermore, at the end of the acquisition period, the microcontroller transfers the data to the cloud using the GSM module (SIM800C type) with which it communicates via the TxRx serial. The returned data is then post processed appropriately.

The microcontroller power management consists of a voltage regulator and a charging chip (MCP7383) that manages the charging phase of the LiPo battery.

Through an Inertial Measurement Unit (IMU) it is possible to detect the 3D displacement of the node. In particular, accelerometer is of the LISDW12 type, configured with a range between ± 2g and a sensitivity of 6.1·10-5 g / LSB. The sampling rate is 400 samples per second, with a Nyquist frequency of 200 Hz.

2.4 MODAL FREQUENCIES

Modal frequencies are those frequencies at which a given structure is free to move. Any change in the structure instantly translates into a change in modal frequencies.

In the context of the following study, which however was merged into a thesis of which I was co-supervisor, a suitably optimized system was developed for the detection of modal frequencies and their variations.

2.4.1 System Overview

The scheme of the data acquisition system and the relative node is shown in Figure 16. Given the structure to be monitored, we therefore have a series of nodes of the type shown in the figure and positioned in strategic points and connected to a master.

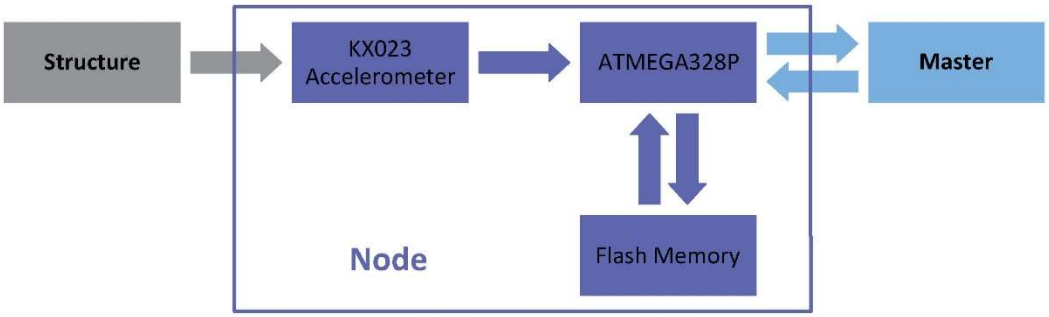

Figure 16: Data acquisition system and relative node scheme.

Figure 17 shows the photos of the master (a) and of the node (b) used here.

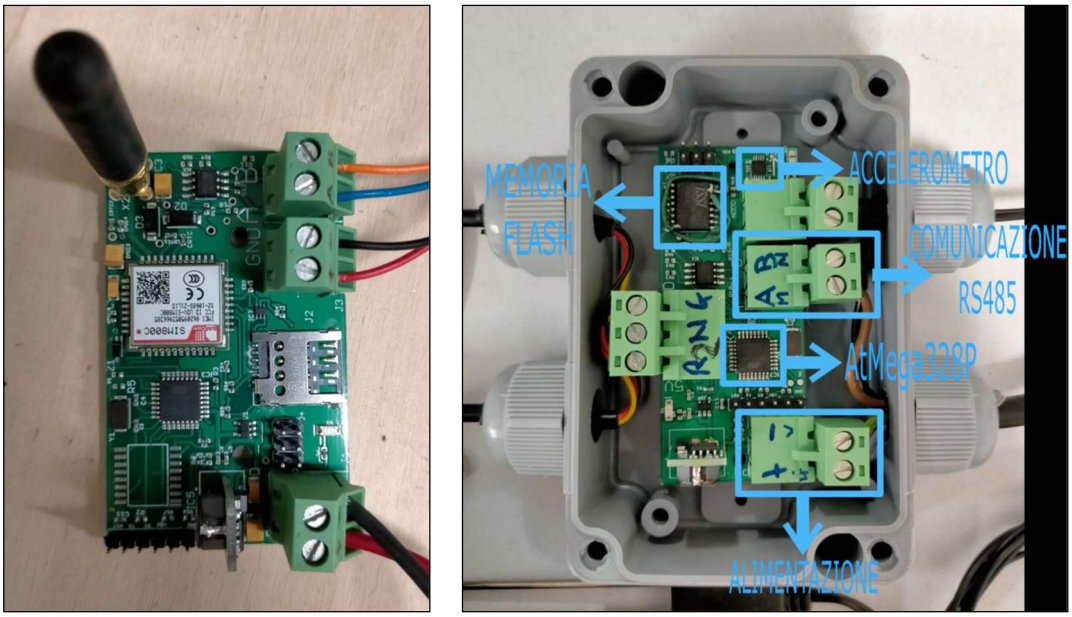

(**a**) (**b**)

Figure 17: Photo of the master (**a**) and node (**b**).

Each node is then, in turn, composed by an ATMEGA328P microcontroller, a KX023 triaxial accelerometer and a flash memory.

The novelty of this system is that the data processing takes place directly on board the individual nodes, thanks to an Arduino library created ad hoc. This allows the amount of data sent to the master to be greatly reduced, making communication with it considerably more fluid. In fact, the acquisition by the master takes place for a pre-set time (decided by the operator) simultaneously by all the nodes and in response to a signal that the master itself sends. The data acquired are those detected by the accelerometers of the single nodes, processed by the relative microcontroller and saved in the memory. Once the acquisition has taken place, the master will interface with the end user.

2.4.1.1 Microcontroller

A microcontroller, in general, constitutes the "intelligent part" of a system, because it is the component dedicated to putting the various parts in communication, to processing the data, to setting the times.

In this work we have chosen the Atmel ATMEGA328P microcontroller. It is an 8-bit megaAVR device, based on AVR's advanced RISC architecture. It features picoPower technology that offers ultra-low power consumption and low-power sleep modes. This makes it ideal for battery-powered applications. The version mounted on

the node board is powered at 3.3V, the clock has a frequency of 8MHz, there is an internal EEPROM memory of 32kB and a SRAM of 2 kB.

2.4.1.2 Accelerometer and communication protocol with the microcontroller

In this work the triaxial accelerometer KX023 was used. It is a digital accelerometer with user-configurable 8 or 16 bit resolution. It can be programmed with both the SPI (Serial Peripheral Interface) protocol and the I2C (Inter Integrated Circuit) protocol. In the node under examination, the communication between the accelerometer and the microcontroller occurs through the I2C protocol.

In particular, the I2C protocol is a two-wire serial communication system used between integrated circuits. The classic I2C bus is composed, as in this case, of a master and a slave. The most frequent situation instead sees a single master and several slaves, even if multimaster and multislave architectures can also be used in more complex systems. From the hardware point of view, the I2C requires two serial lines of communication:

- SDA (Serial DAta) for data;
- SCL (Serial CLock) for the clock (due to the presence of this signal, the I^2C is a synchronous bus).

A GND reference connection and a Vdd power line must be added.

Figure 18 shows the general usage scheme of this protocol.

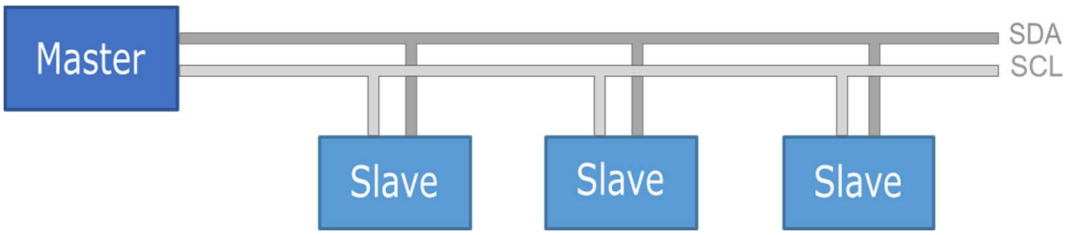

Figure 18: General usage scheme of I2C protocol.

Communication is initiated by the master, who also indicates which slave he wants to communicate with. The master also informs if the communication consists in sending or receiving data.

In the present work, the I2C protocol has been implemented using the Arduino "Wire" library, which allows to extract the accelerations detected.

2.4.1.3 Flash memory and communication protocol with the microcontroller

The memory used is a 512 megabit flash connected to the microcontroller via SPI protocol.

This protocol is a communication system used for serial communication between a microcontroller and other integrated circuits or between multiple microcontrollers. It is synchronous due to the presence of a clock which coordinates the transmission and reception of the individual bits and determines the transmission speed. It is full-duplex as the "conversation" can take place simultaneously in transmission and reception. It is based on 4 signals:

- SCLK: Serial Clock (issued by the master)
- MISO: Serial Data Input, Master Input Slave Output
- MOSI: Serial Data Output, Master Output Slave Input
- CS or SS: Chip Select (Slave Select), issued by the master to choose which slave device it wants to communicate with.

Data transmission on the SPI bus is based on the operation of shift registers.

Figure 19 shows the general use scheme of this protocol.

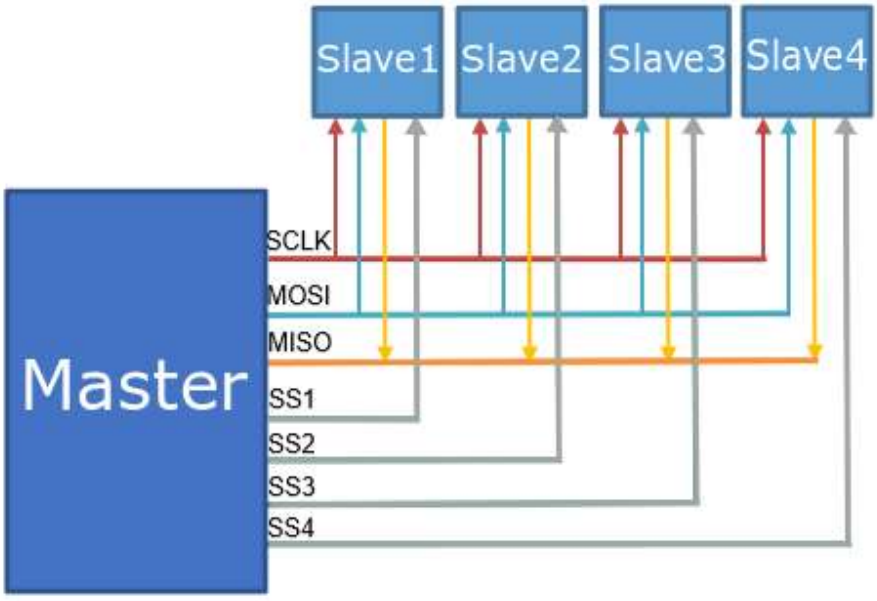

Figure 19: General usage scheme of SPI protocol.

In the present work, the SPI protocol has been implemented using the Arduino "SpiFlash" library, which allows to simplify the communication between memory and microcontroller.

2.4.2 Application of the Fourier transform to the SHM

Given the components just described, and the specifications of each of them, the aims of this work are summarized below.

1. Develop a library written in C++ (in the Arduino programming environment), which allows to carry out a frequency analysis through an FFT (acronym of Fast Fourier Transform) of the data acquired ON BOARD. This choice makes it possible to drastically reduce the amount of data to be processed in the case of subsequent post processing. This library must also be such that it can be implemented in poorly performing processors. The RAM provided in the ATMEGA328P, in fact, is only 2048 bytes, which is very limiting if you want to perform an FFT. This is because two vectors of N elements are required to perform an FFT of N samples. Given that a float type number (floating point number) in Arduino occupies 4 bytes of RAM, it is enough to do an FFT of 256 samples to saturate the memory, not to mention the fact that a part of RAM is used to perform the other operations and therefore the maximum number of usable samples drops to 64.
2. Use the library written in specific software for the data acquisition system, which must be able to:
   - retrieve data from the accelerometer;
   - perform a frequency transform of the sampled data;
   - save and retrieve data in flash memory.

2.4.2.1 Existing libraries

For this purpose, the libraries for FFT algorithms already available on Arduino have been reviewed. The most used, which was also the starting point for this work, is the "arduinoFFT", which however presents some critical issues, essentially related to the use of RAM and accuracy.

As far as the RAM is concerned, in fact, the library provides input vectors of the float type. This involves the rapid saturation of the RAM itself. Furthermore, this library is not very "lean", and therefore not suitable for use in large programs in which several libraries are used. In fact, the maximum number of samples that can be used in performing an FFT on the AtMega384p with this library is 64, too few for the purposes of this work.

As far as accuracy is concerned, the tests carried out showed that signal windowing leads to a result that does not respect the real one. Indeed, in the case of transforms with a few high amplitude peaks and many small amplitude peaks, the smaller amplitude peaks become less visible. This leads to an insufficiently reliable result, considering that, in the case of structural monitoring, there is usually a first peak of high amplitude and much smaller peaks at subsequent frequencies.

2.4.2.2 Radix-2 algorithm

One of the main problems, therefore, remains that of having to manage huge amounts of data.

In reality, in the context of the Discrete Fourier Transform, which is the one from which the FFT was born, at the basis of this work, this is a rather generalized problem. However, thanks to the Radix-2 algorithm, which allows the continuous splitting of the representative summation of the original signal, the computational cost decreases enormously.

The only notation: in order to have a vector whose indices are ordered in the best possible way for subsequent operations, before executing an FFT, it is useful to execute a bit operation Reversal (an operation for which, in the context of binary code, the most significant bit becomes the least significant and vice versa).

In order to exploit this algorithm, in the present work reference has been made to a code originally written for the C language and suitably adapted to C++.

Even in this case, however, the problem of having two float-type inputs persisted, which, as already mentioned, quickly bring the ATMEGA328 into saturation. Specifically, in fact, it has 2048 bytes of memory, which, of course, cannot be used exclusively to save the input/output vectors. Such an algorithm, albeit very simple, easily saturates the microprocessor's RAM. A float type number occupies 4 bytes (in the processor considered) and the maximum order of the FFT (and therefore of the input/output vectors) is equal to 64. It is necessary to use two input vectors since, even if the input is real, the output signal is not. In the same way it is not possible to save the vectors in the non-volatile memory (in this case the Flash memory connected to the processor) since the data contained in it cannot be freely erased but must be eliminated in groups of 1 kb. It is therefore necessary to find a way to decrease the use of RAM and increase the number of samples of each operation.

2.4.2.3 Memory optimization

For all that has been said, one way to decrease the use of memory is certainly to decrease the space occupied by the input vectors. As we have seen, all the codes mentioned refer to inputs of the float type (4 bytes each). On the other hand, a vector of type int (integer), however, occupies 2 bytes. Therefore, the first step to achieve the goal is undoubtedly to convert the float data into int data, using the "foatToInt" function and its inverse "intToFloat".

For this purpose, a new function for calculating the FFT has been developed which, however, requires that the data involved be of integer type. Its operation is schematized in Figure 20.

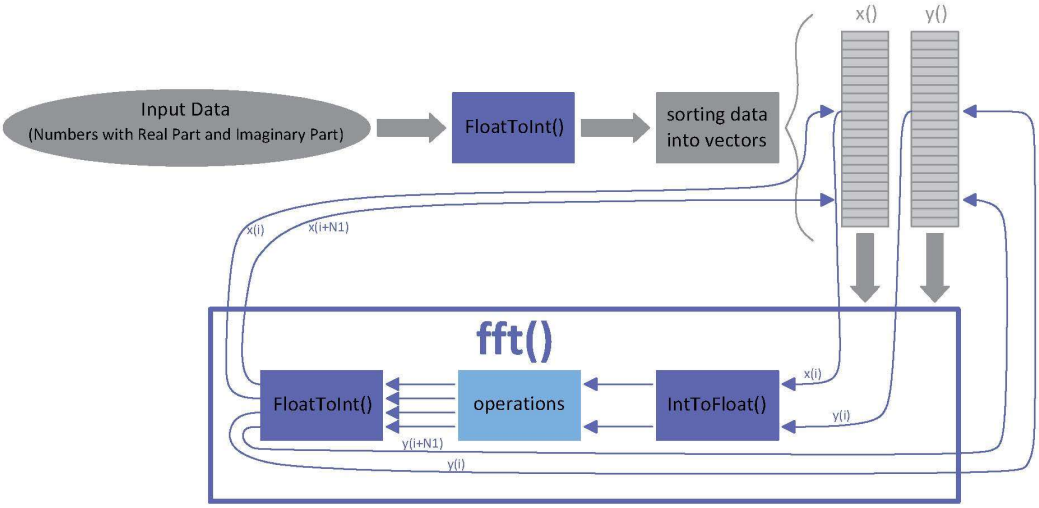

Figure 20: New function for calculating the FFT.

Basically, therefore, keeping in mind that each element of the input vector is composed of a real part and an imaginary part, the input data are all transformed into integers and allocated in the relative 2 bytes of memory. When it is necessary to calculate their FFT, they are recalled from memory and transformed into float data. At the end of the FFT operations, the relative results are retransformed into integer type data and appropriately reallocated in memory.

Using this method, therefore, the arrays of the real and imaginary parts of the vector components are always of type int and do not saturate RAM.

A further step forward can be taken using the "complexTo Magnitude" function, which, starting from the vector relating to the real component and from that relating to the imaginary part, saves the magnitude of the two in memory.

2.4.3 Use of multiple nodes and communication protocol with the master

The code presented can be adapted for communication between multiple nodes and a master. Communication takes place via the RS485 protocol.

The RS485 standard is a very widespread serial communication protocol. Through this protocol, information can be transmitted to up to 32 devices connected via two lines (A and B).

The two states of each line are defined as follows:

- when terminal A is negative with respect to B, the line represents a binary one (this state also represents no signal;
- when the A terminal is positive with respect to B, the line represents a binary zero.

The system is the evolution of the RS422 protocol used for point-to-point communication, i.e. to connect a single transmitter (Tx) to a single receiver (Rx), as represented in the diagram shown in Figure 21.

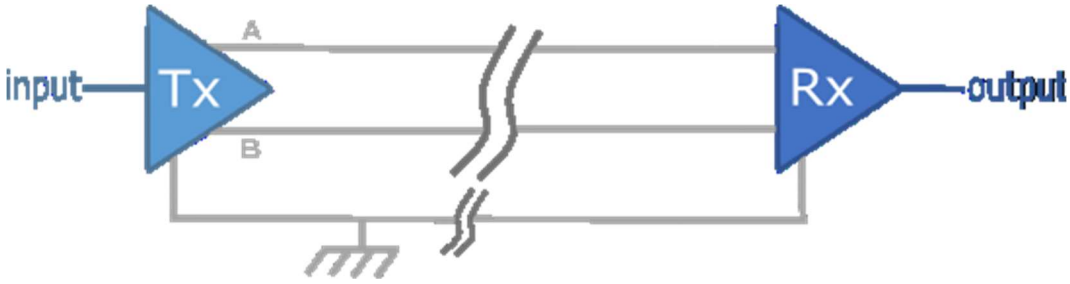

Figure 21: Point to point connection diagram.

The substantial difference between the RS422 protocol and the RS485 protocol is the support of multi-drop lines, i.e. those lines in which multiple receivers and transmitters coexist on the same pair of wires. In order to avoid conflicts it is obviously necessary that only one transmitter at a time is active. This implies the use of transmitters which, in addition to the outputs corresponding to zero and one, can also manage a "third state" in which the electronics appear as physically not connected to the line (state called high impedance, three-state or Hi-Z).

Instead, the receivers can all be active at the same time and in general they actually are. The most used topology with this protocol is the two-wire (in addition to ground) one shown in Figure 22.

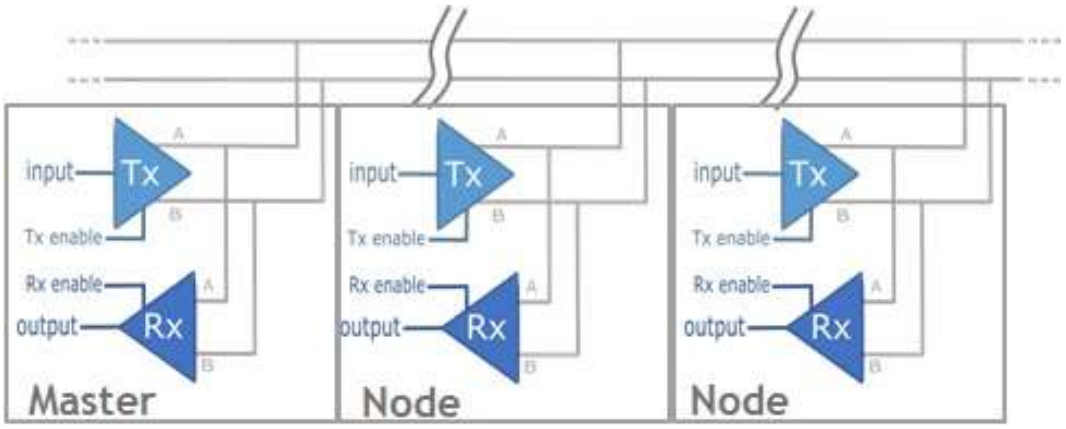

Figure 22: Multi/drop line: each node connected to the line is represented by an Rx receiver and a Tx transmitter.

This connection allows bidirectional (but obviously not simultaneous) transmission between two or more nodes which, from an electrical point of view, are equivalent to each other.

2.4.3.1 Using the RS485 protocol on the Arduino platform

The "SoftwareSerial" library allows you to use communication via the RS485 protocol in the Arduino environment. Once included in the project, it is necessary to define the pins used for communication.

In the present work, a digital pin (HIGH or LOW) has also been defined which, if high, activates the node transmitter, and if low, deactivates it so as to avoid errors.

2.4.4 The case study – Experimental set up

For testing the functions, Arduino Uno (which has the same processor as the acquisition system considered here) and Matlab were used.

The developed system was first tested in a simple case: determining the modal frequencies of a bar anchored to the bench and stimulated by white noise.

Subsequently, we moved on to a more complex case: a real structure (albeit small in size) made available to the University of L'Aquila.

2.4.4.1 Search for the modal frequencies of a bar

This type of test was made to test the effective functioning of the program written for the single node.

The test consists in identifying the modal frequencies of a metal bar fixed to a test bench by applying white noise to it (Figure 23).

Figure 23: Metal bar excited by white noise.

Preliminarily, given the characteristics of the busbar and the applied noise, the modal frequencies were calculated from a theoretical point of view, obtaining the values shown in Table 2.

Table 2: Theoretical modal frequencies of the bar.

Modal frequencies of the bar
11.7 Hz
28.3 Hz
45.5 Hz
86.7 Hz

As mentioned, the bar was then perturbed with white noise. Two methods were used to generate the noise:

1. an electrodynamic shaker, theoretically capable of generating a vibration at all frequencies;
2. the clicking of the fingers in random points of the beam for the whole duration of the test (this should generate a white noise).

The use of the two methods was necessary having observed that the shaker had difficulty in exciting the bar at low frequencies, and therefore it would not have been possible to detect the first modal frequency.

The program has also been set up as follows:

- sampling frequency=200 Hz;
- sampling time= from 30 seconds to 2 minutes;
- SAMPLES=128;
- Type of fft() performed= FFT_INT_NOCONST;
- INT_FLOAT_FACTOR=1000(precision of 3 decimal numbers);
- Since the accelerations detected are low, it was not necessary to activate the FITTING option;
- data sampling performed on the X axis only (perpendicular to the beam);
- SAVE_PEAKS has been activated.

2.4.4.2 Search for the modal frequencies of a hut

In this case the code had to be further improved to optimize it from the point of view of the simultaneous communication between several nodes and the master, which takes place according to what is reported in paragraph 2.3.

For simplicity, communication is not between multiple nodes and a master, but between multiple nodes and a serial monitor.

The core of the code used is the same as that relating to the case of a single node. What differs is the execution of the various parts that compose it (SAMPLE, FFT and READ). In particular, each node has a unique ID (1,2,3...) with which it can be recognized by the master. With a precise signal from the master, the various operations on the nodes begin: sampling, FFT, average of the FFTs, reading of the samples/FFT/averages of a single node, erasing the memory and setting the sampling period.

To verify the functioning of the system, three nodes were mounted inside a shed owned by the University of L'Aquila. This shed had previously been used for structural monitoring tests.

Also in this case, the objective of the test was to find the modal frequencies of the hut. In particular, a comparison was made between the case in which the door of the shed is tightly closed and the case in which the same door is open. The structure was energized with the aid of a rubber mallet. Four trials were performed: two with the door open and two with the closed door.

Figure 24 shows the structure being monitored (a) and the diagram of the positioning of the nodes within the structure itself.

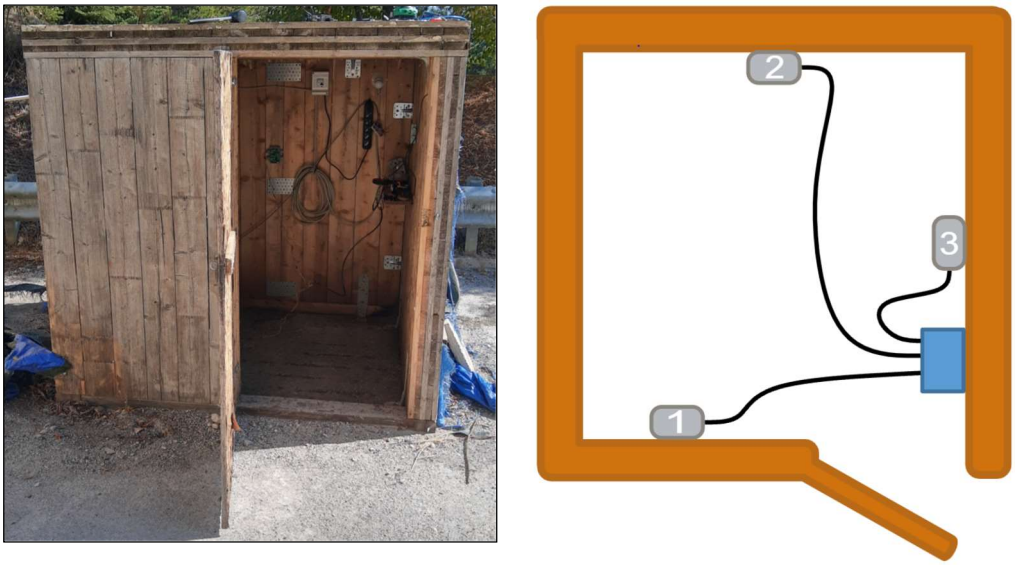

(**a**) (**b**)

Figure 24: Test with multiple sensors: structure to be monitored (a) and node placement pattern (b).

2.4.5 Results

This paragraph shows the results of the two case studies described above.

It should be noted that, in all the following figures, the frequency in Hertz is represented on the abscissa axis. The ordinate axis, on the other hand, is representative of the amplitude. However, the values shown are not intended to be absolute. In fact, the so-called "Fitting" operation was performed on the data. This technique allows to lighten the computational load on the single node because it allows to avoid the overflow. For a correct display of the amplitude, the data obtained should have been divided by an appropriate multiplication factor called "fitting Value". However, from the testing operations carried out, it emerged that, regardless of the exact value, the graphic amplitude become significant precisely in correspondence with the expected modal frequencies. Since, in the final analysis, the aim of this study was exactly this, we decided to omit this operation. In this way, we have also avoided making the system heavier, maintaining the characteristics of extreme slenderness mentioned above.

2.4.5.1 Modal frequencies of the bar

Four types of tests were performed.

The first type of test had a duration of 30 seconds. An electrodynamic shaker was used to generate the vibrations. Sampling produced 5966 samples. The transformations into frequencies combined with the search for the peaks produced 47 vectors, for a total of 1888 numbers saved in memory counting both the indices of the values (integers) and the values themselves (floats). The result can be visualized using Matlab. Figure 25 shows the overlapping results of the various samples for a single node (the X indicates the frequency relating to them).

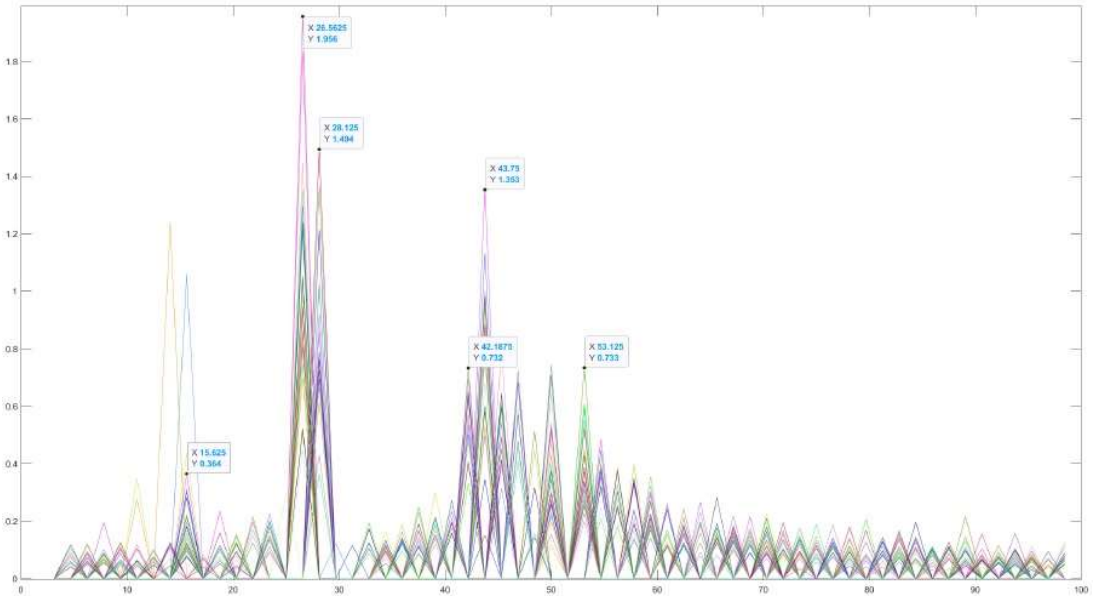

Figure 25: Graph of the results of test n.1.

As can be seen, important peaks can be seen between 26 and 28 Hz and between 43 and 52 Hz, approximately corresponding to the central modal frequencies of the bar. No wonder if the modes are slightly different from the theoretical ones, since the latter are the result of an analysis performed with accelerometers (having a different weight than the node used now) placed above the beam under examination. A different load on the bus leads, of course, to slightly different modal frequencies.

Furthermore, by performing an ON BOARD average of the transforms it is possible to:

- save a much smaller number of samples (at most 128 instead of 1600);
- better view frequencies with higher amplitude.

Figure 26 shows the graph resulting from the average operation (also in this case, the X indicates the relative frequency).

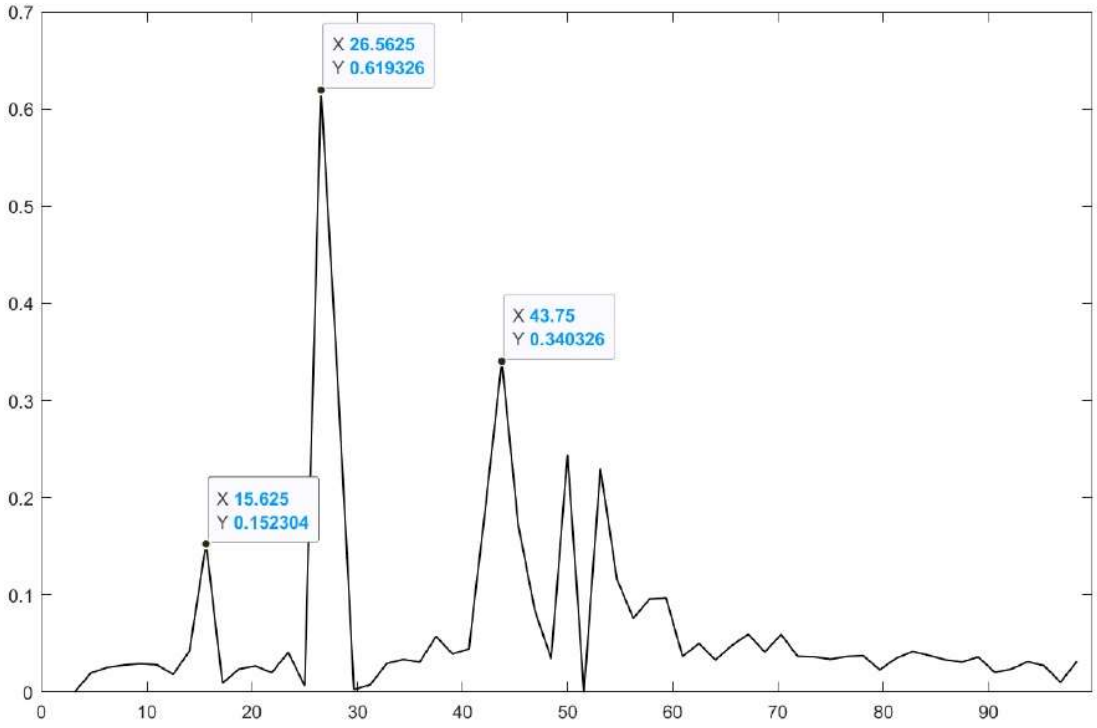

Figure 26: Graph of the average value of the results of test n.1.

The second type of test was conducted under the same conditions as the previous test. In this case, however, the node has been moved to a central position in the busbar in order to better detect high frequencies.

The result is shown in the following Figures. In particular, in Figure 27 the results relating to the overlap of all the samples are reported, in Figure 28 the average of the results.

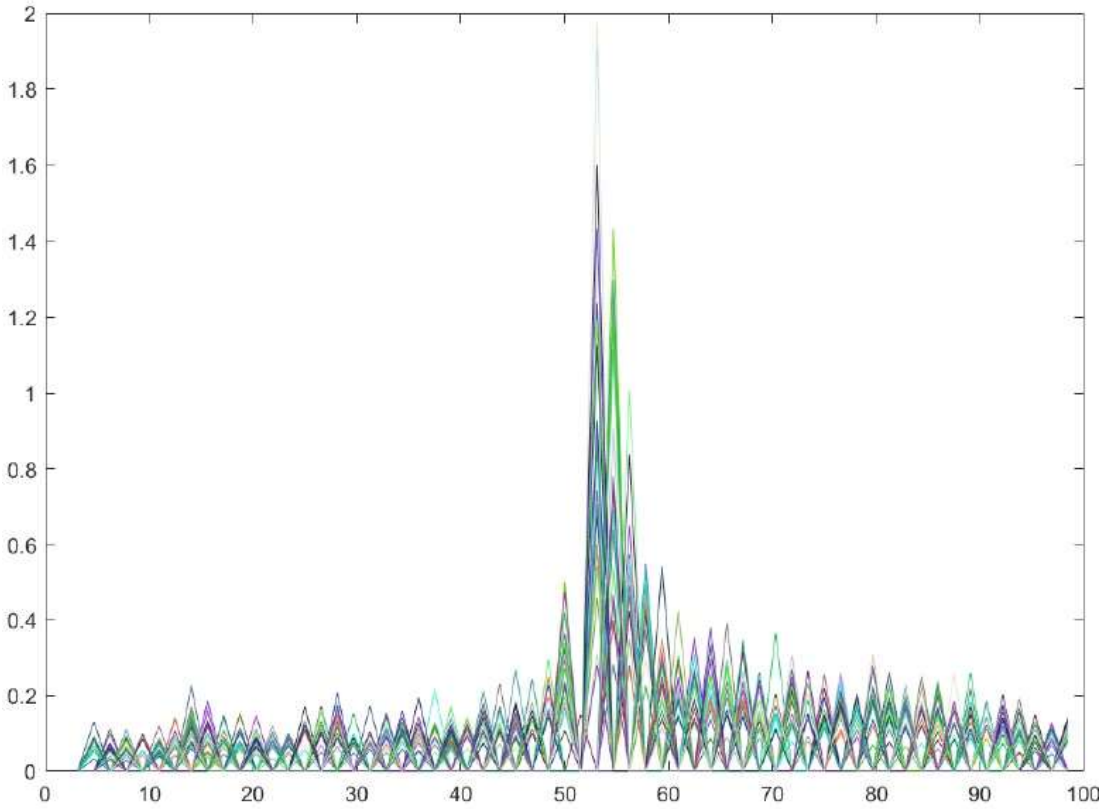

Figure 27: Graph of the results of test n.2.

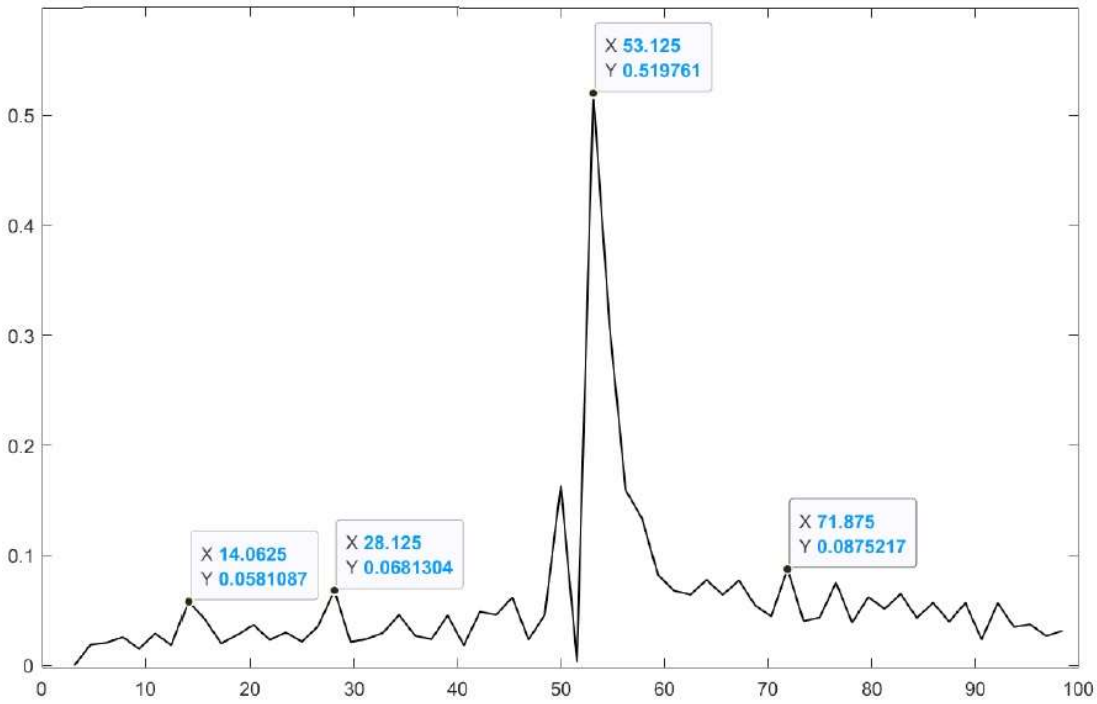

Figure 28: Graph of the average value of the results of test n.2.

In this case, the main frequency is 53Hz, while all the others are less visible. It can therefore be seen how the position of the node influences the frequencies detected by the sensor.

In the third type of test, also lasting 30 seconds, the bar was instead excited by randomly clicking the fingers on the bar in order to generate white noise. The amount of data saved in memory and passed to the monitor is always the same.

Figure 29 shows the set of results, Figure 30 shows their average.

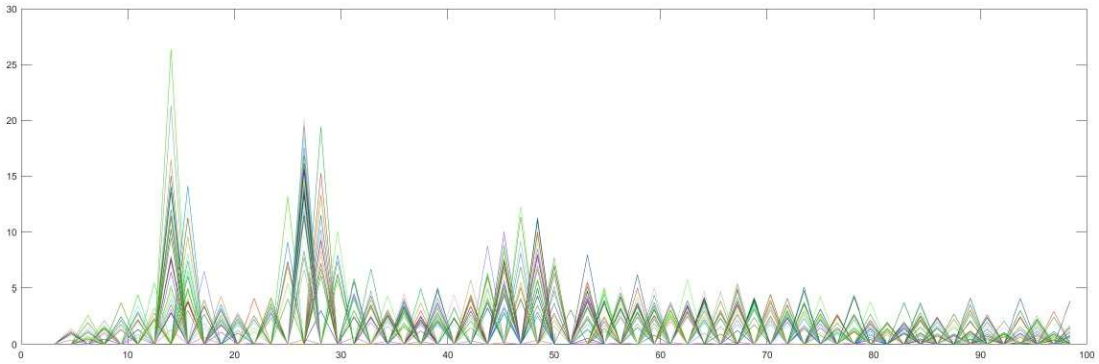

Figure 29: Graph of the results of test n.3.

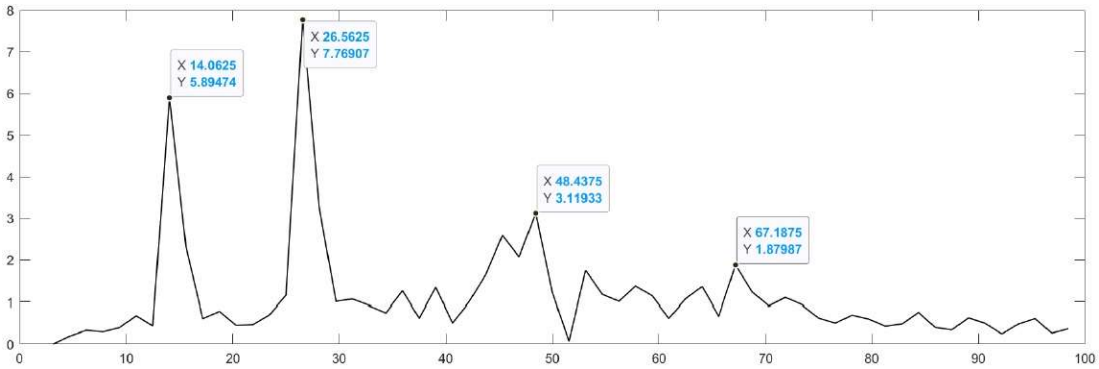

Figure 30: Graph of the average value of the results of test n.3.

In this case, as can be seen, the lower frequency also emerges strongly, while the detection of the higher one is a little more problematic (which could be associated with the peak at 67 Hz, which however is very far from the 80 Hz hypothesized; moreover, the peak at 67 does not particularly stand out).

Finally, a further test was performed. Starting from the same conditions of the previous test, a sampling period of 2 minutes was set. The results are shown in Figures 31 and 32.

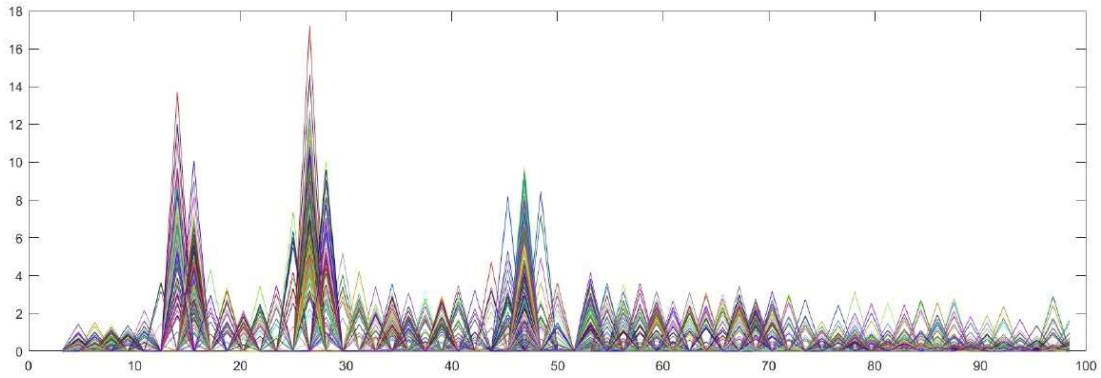

Figure 31: Graph of the results of test n.4.

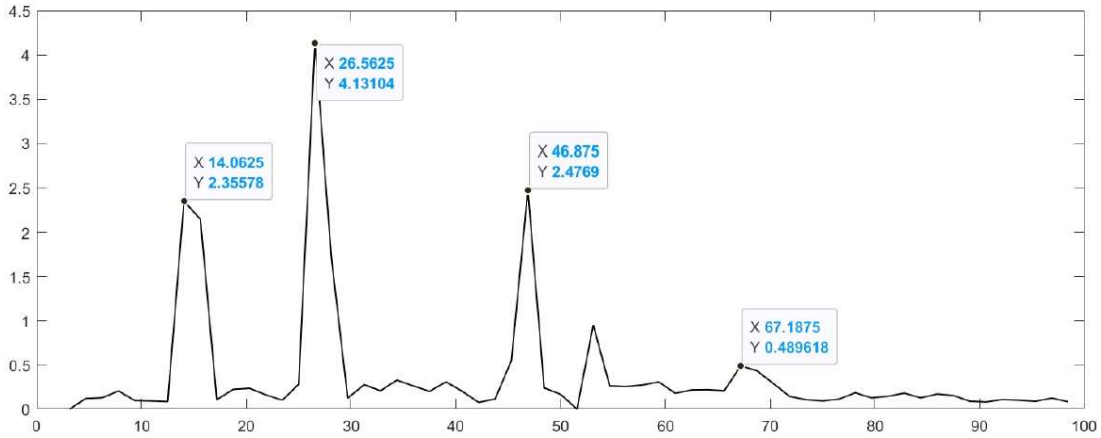

Figure 32: Graph of the average value of the results of test n.4.

From an examination of the graphs it can be seen that by increasing the number of samples the result becomes less corrupted by noise and the modal frequencies are more visible in the average of the signal.

2.4.5.2 Modal frequencies of the hut.

As regards the test with three nodes, Figure 33 shows the results of the tests relating to the case in which the door is closed. Figure 34, on the other hand, shows the results of the tests relating to the case in which the door is open. As can be seen, the peaks relating to the modal frequencies of the structure are clearly visible.

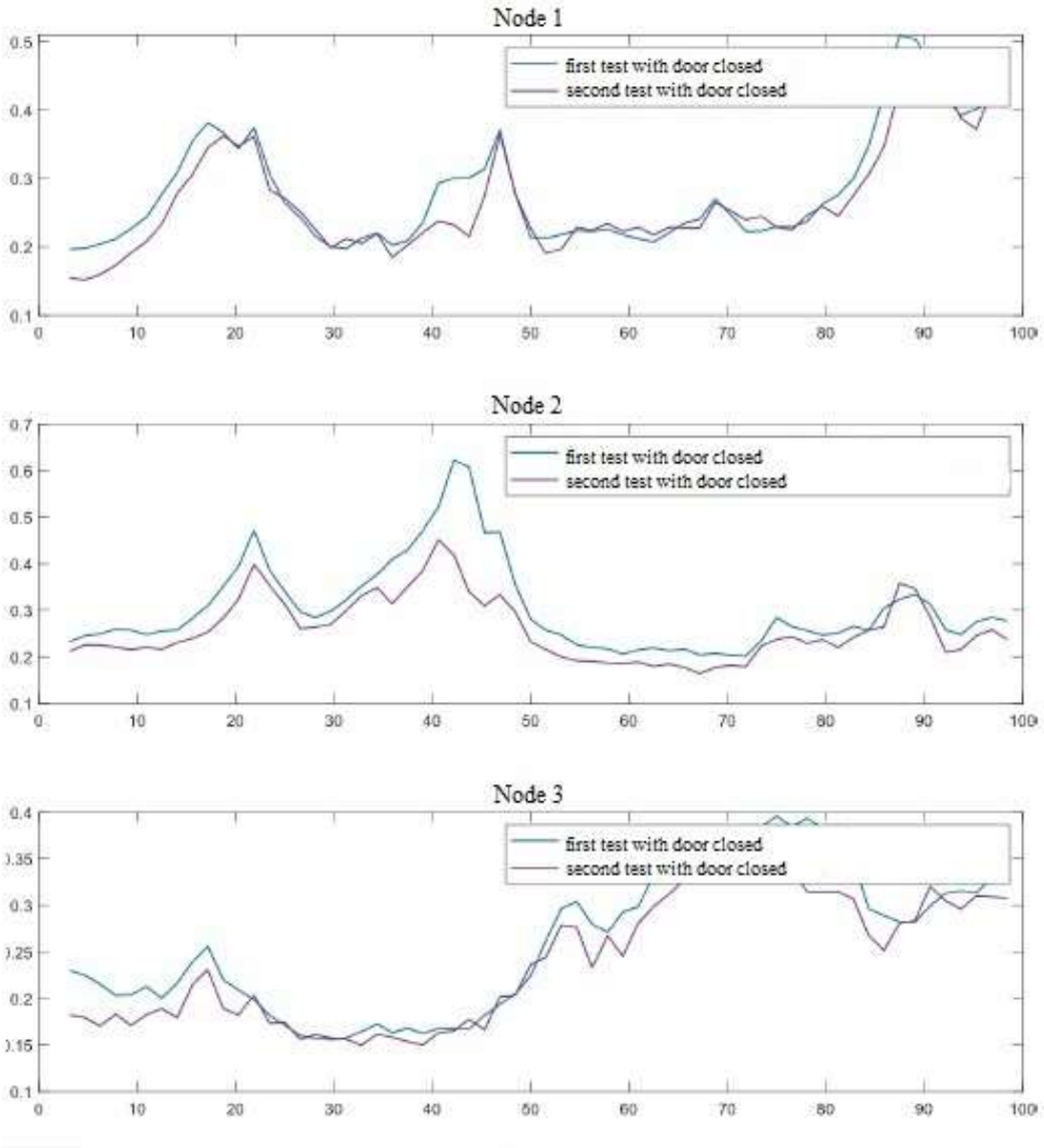

Figure 33: Graph of the tests carried out on the shed with the door closed.

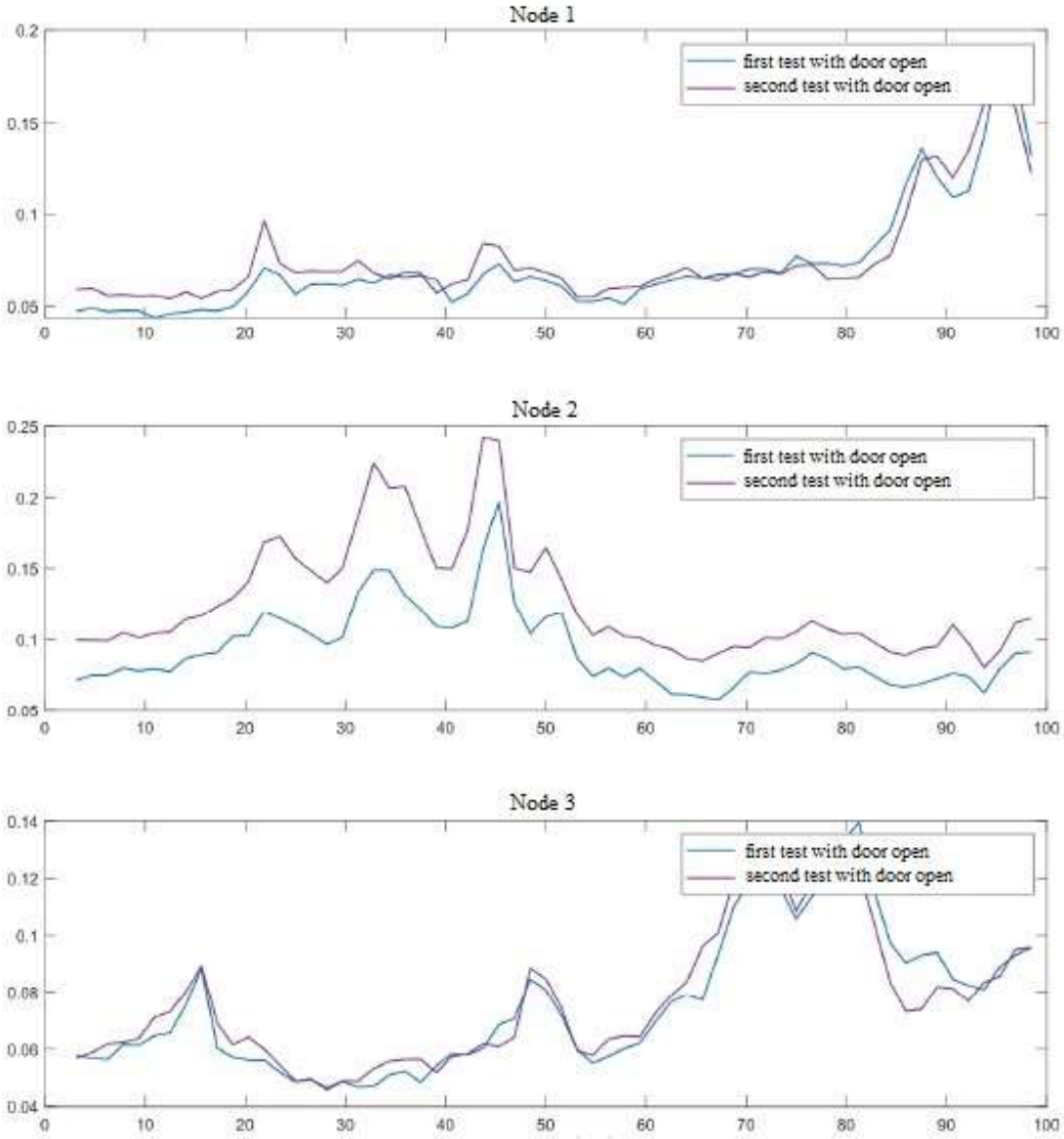

Figure 34: Graph of the tests carried out on the shed with the door open.

Finally, Figure 35 shows the direct comparison between the two test modes for each of the three nodes.

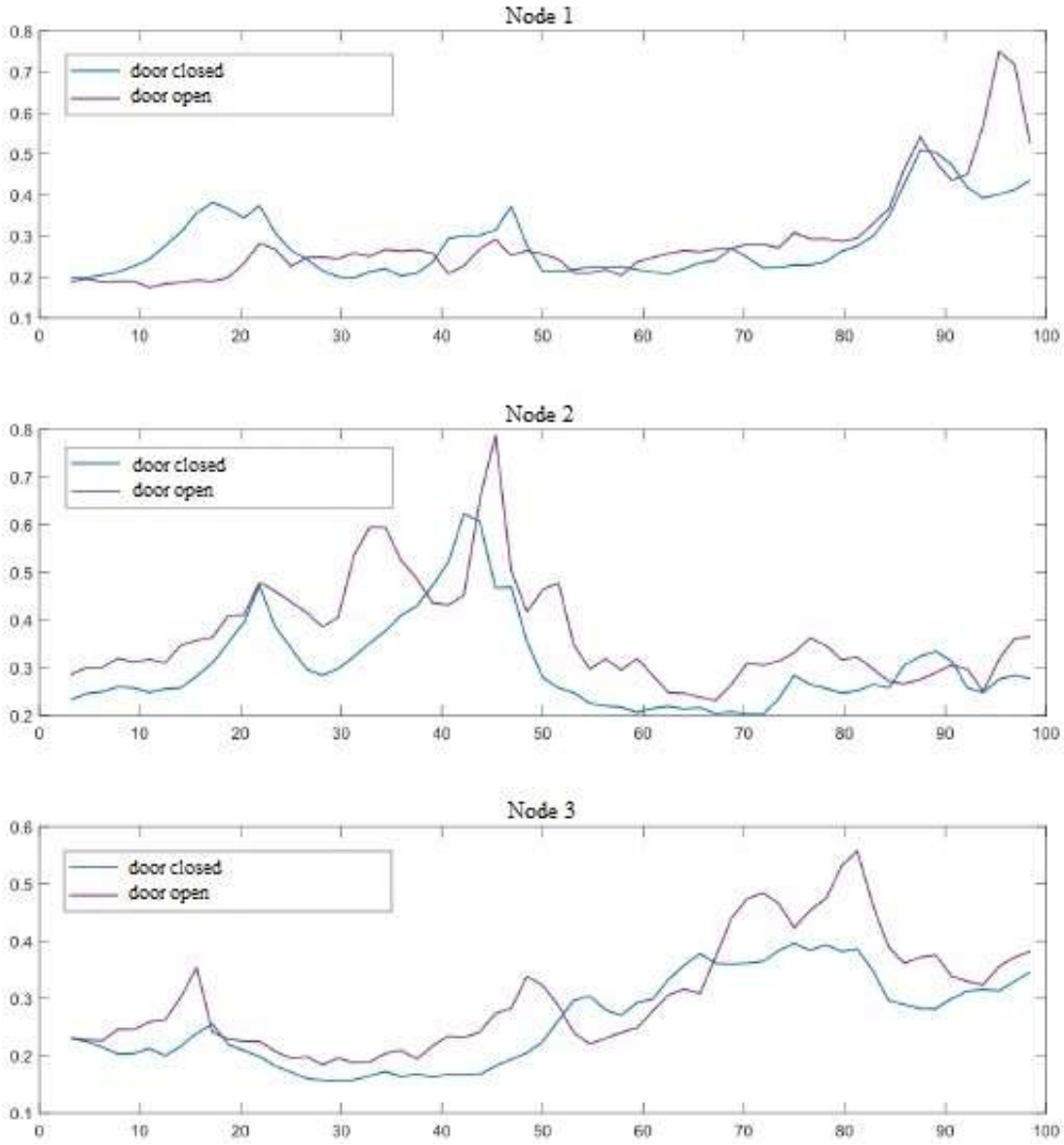

Figure 35: Comparison of trials.

2.4.6 Discussion

As far as the test carried out on the bar is concerned, it can be concluded that the results are in a good agreement with those obtained from the same system used only for signal sampling, in which the accelerometer basically saves the data in the memory and the signal post processing is entrusted to the PC.

The deviation of the modal frequencies from the theoretical ones is due in part to the weight of the node on the beam and in part to the frequency accuracy (since fc/N=200/128=1.56Hz).

The code written for the single node allows to considerably increase the performance of the system, since, unlike the "classic" solution, it allows to:

1. decentralize the post processing in the case of multiple nodes, which autonomously perform the frequency transformation, the search for the peaks and the eventual average of the signal;
2. radically reduce the amount of data coming from each single node.

As far as the hut is concerned, we obtain, as expected, that as the conditions of the structure vary, a significant change in the modal frequencies is obtained.

Chapter 3: Environmental Monitoring

In this chapter, the theme of Environmental Monitoring, introduced in the previous chapter (section 1.2), will be dealt with in detail.

Also in this case, the chapter begins with the literature review (section 3.1).

Subsequently, two case studies will be presented. Both refer to buildings actually demolished, but the first (section 3.2) is a completely preliminary work, while the second (section 3.3) has a greater degree of detail than the first, and was born following the good results provided by this last.

3.1 LITERATURE REVIEW

Despite what was said in the introduction (section 1.2), there is a field that is still too much neglected, that of construction sites. In fact, by carrying out a search through the Web of Science database, by inserting the keywords “construction site” and “dust pollution” from 1973 (the year in which the first document appears) to now, only 400 articles have been published. Among these, 333 have been published since 2005. The areas of greatest interest are those of environmental science and earth and planetary sciences, with 40.2% and 13.1%, respectively. Instead, the engineering field covers only 11.9% (Figure 36). An in-depth study of the state of the field was carried out precisely within this range, noting the presence of only 58 items.

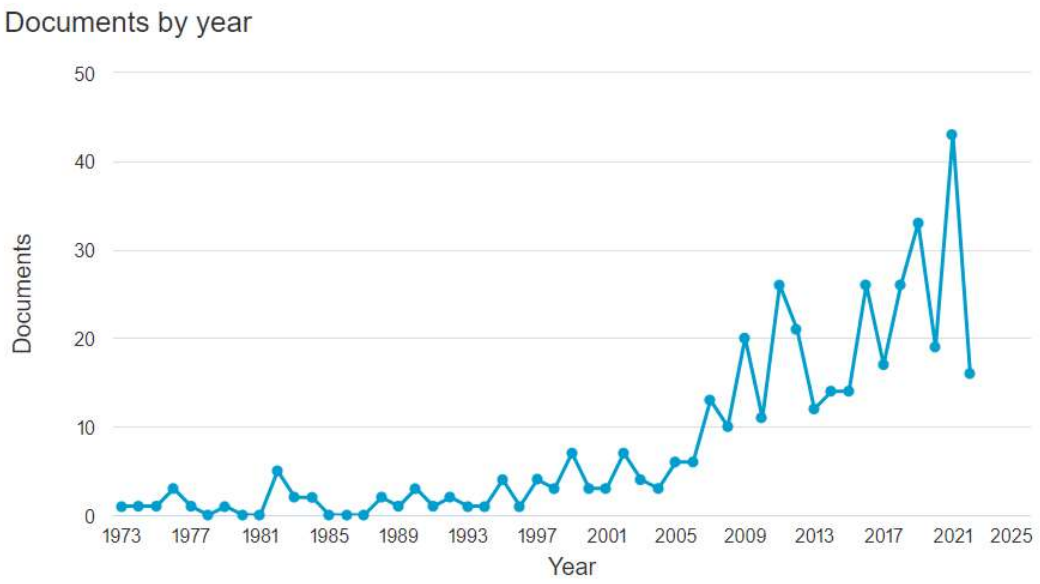

(**a**)

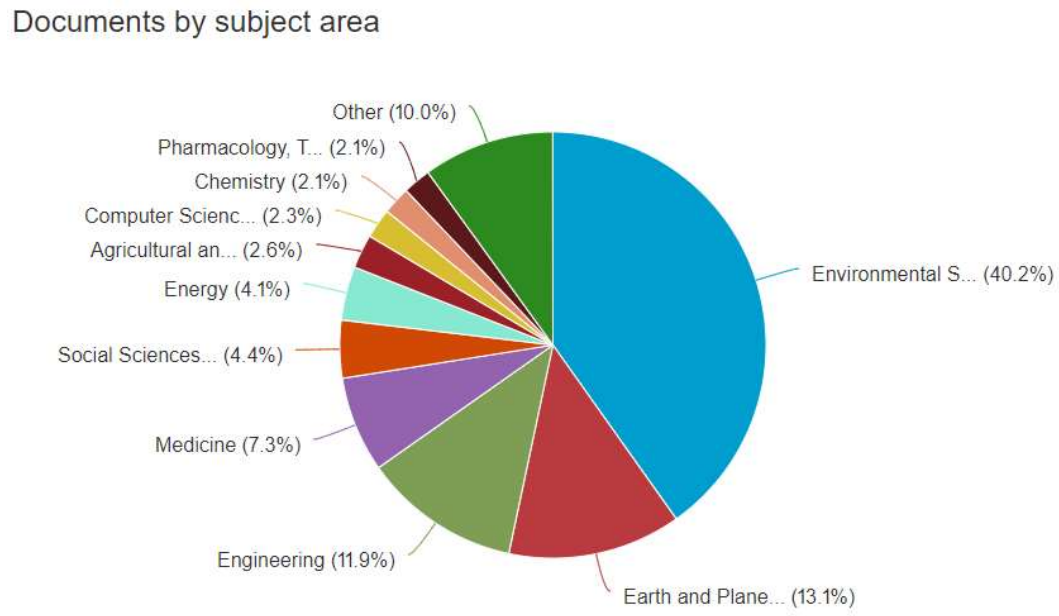

(**b**)

Figure 36: Analysis of the publications in the Web of Science database according to the keywords "construction site " and "dust pollution" - (**a**) the trend of publications over the years, (**b**) documents by disciplinary area (Scopus database).

Among the most recent, relating to the last two years (2021 and 2022), some are particularly interesting for the purposes of this paper. For example, in [70], the problem of the production of fine powders on site is addressed. In particular, a methodology is defined to reduce pollution from such dusts through the combined action of in situ measurements and application of the law of dust diffusion. It is also highlighted that research on the impact of PM on workers follows three main lines, namely the monitoring of powders, the control and prevention of the production of such powders during processing, and the effects on health. Instead, paper [71] aims to highlight the potential of the use of Internet of Things sensors for monitoring as support visualization in construction. Additionally, in [72] a high importance is given to the monitoring of construction site dust to support political decision-makers in their choices. To this end, a dust detection method for a construction site is tested. This method is based on a prior knowledge min-max k-means clustering algorithm. Then, paper [73] focuses on fine dust risk mitigation measures, not only for construction site operators but also for users and residents. Therefore, experiments with water systems for dust suppression in Rostov-on-Don (Russia) were conducted. In [74], on the other hand, an earthwork construction is analyzed in detail by monitoring workers exposed to dust during the execution of this task. Subsequently, the authors quantified the health risks for workers by defining an effective evaluation system. Finally, paper [75]

summarizes the results of the study of the distribution and concentration of fine dust released during construction production. Finally, the solution presented in [76] links the concept of urban design in construction sites to an innovative integrated monitoring system.

Although the study of the state of the field has revealed the presence of a limited number of studies on the topic of interest, illustrated and summarized in Table 1, the need to identify strategies capable of reducing the emissions of dangerous substances into the atmosphere, increasing the consumption of non-renewable resources, and decreasing noise pollution is increasingly pressing. This will lead to a radical change in perspective on the construction site and its design, but will also facilitate the change in trend required by the Sustainable Development Goals of the 2030 Agenda [77].

Table 3: Main recent references. In the table, the aim of the research and the results are reported.

Reference, Year	*Aim of the Research*	*Results*
[70], 2022	- To propose a new method of reducing construction dust pollution through a reasonable site layout plan	- Average dust concentration exposed to workers and total transportation cost were significantly reduced by 60.62% and 44.3%, respectively, thanks to the new method
[71], 2022	- To explore how sonification can support visualization in construction planning to decrease construction transport disturbances	- The low-cost sensors used could capture "good enough" data; - The use of sonification for representing these data is interesting and a possible useful tool in urban and construction transport planning
[72], 2021	- To propose a construction site dust detection method based on prior knowledge min-max k-means clustering algorithm	- Timely detect construction site dust could improve the ability of government supervision departments to monitor construction dust pollution
[73], 2021	- To discusse a method for suppressing dust emission on a construction site	- The amount of fine dust PM 2.5–PM 10 pollution reduced under the influence of a water fog gun with a magnetic nozzle equipment; - The concentration of particles in the air reduced by almost 2 times, depending on the height of the equipment's impact
[74], 2021	- To establish a health risk evaluation system based on the measured data and difference in the working contents of the works in the earthwork construction phase; - To base the health risk evaluation system on both measurements of dust exposure and the quantification of health risks	- The protective mask and spray dust control system reduced the health risk by 67.54% and 38.56%, respectively; - The health risks for the use of both measures could be reduced by 76.89%; - Effective dust control measures were proposed according to the results of this study, which provides references for workers to strengthen dust-proof works
[75], 2021	- To summarize the results of the study of fine dust distribution and concentration released during construction production	- The functional analysis of the amount of fine dust PM 2.5 and PM 10 released during the local construction; - Data knowledge allows us to determine the most dangerous construction works that affect the total environmental pollution in the working and sanitary protection areas
[76], 2022	- To develop a new integrated system for monitoring the environment. The system uses a wireless sensor network environment monitoring system IoT platform with embedded internal processors	- Real-time supervision through a mobile terminal and computer terminal management platform; - Subsequent online guidance and regulation

For this required change, it appears important to manage the construction site adequately, implementing the planning of the works [78], installing mobile acoustic barriers, using less-polluting vehicles, implementing cleaning, and reducing the dispersion of dust and the use of fossil resources.

Moreover, the correct design and operational planning of the construction site allows the rational management of the works and reduction of risks [79]. As part of these activities, attention to polluting emissions is a research gap that needs to be investigated. In fact, in daily practice, to avoid the lifting and dispersion of dust into the atmosphere, the following actions are implemented:

1. the continuous wetting of the work area;
2. the coverage of deposits of dusty material (both deposited and transported);
3. the use of dust shields.

Regardless, these strategies are not always effective since they do not allow for the control of the amount of dust actually produced by the processes that are taking place. Furthermore, they are "qualitative" strategies not supported by an effective numerical confirmation of the benefits achieved thanks to their implementation. Moreover, this appears even more true when it is necessary to intervene in particular urban contexts where, inevitably, there is an increase in emissions. These situations include, for example, the demolition of buildings, a particularly frequent activity in areas such as L'Aquila, Italy, hit by the earthquake of 6 April 2009. This often happens because the lack of urban planning determines the occurrence of demolitions at the same time [80]. For all these reasons, it is necessary to focus attention on dust pollution produced during construction/reconstruction activities.

For all these objectives, this topic has been studied in depth from an engineering point of view, given the urgency, also on the part of this sector, to develop solutions strictly dedicated to the problem linked to dust emissions in critical situations for workers on construction sites. Thoroughly investigating this need and responding to it will also allow us to provide new ideas for those studies which, as mentioned above, today appear almost entirely the prerogative of sectors such as environmental sciences and earth and planetary sciences, allowing for a multidisciplinary approach to the problem.

Even in the case of environmental monitoring, we first investigated the IoT systems already present in the literature to verify if there were already some used in this sense. In particular, the system in [76] uses an IoT platform with embedded internal processors capable of monitoring dust, among other parameters. Environmental data are collected by the sensors and sent to the terminal node via ZigBee for real-time viewing on the host PC. The solution presented in [81], on the other hand, describes the prototype of an IoT system, based on sensors connected via Wi-Fi to an MCU node that forwards the data to the PC. Again, in [82], a system based on LoRaWAN technology is shown, where data are sent to the cloud for further processing. Finally, in [83] a sensor-based system is presented that uses a Raspberry as a server, which then also sends the data to the web for consultation.

In essence, therefore, the project of the systems presented, including that studied in the context of the PhD activity, follows a common standard scheme, which consists of having a certain number of sensors that communicate with a master, which in turn transmits the data for consultation. However, in the works cited, the various systems are designed and optimized for purposes other than that of our interest. In fact, in the conclusions of [81-82], an emphasis is placed on the fact that the developed system is aimed at the creation of smart cities, aiming at the integration with other monitoring systems. Similar conclusions are reached for [83]. In [76], however, the developed system responds to the need to monitor a single building from the point of view of energy consumption. Basically, all of these systems have been designed to be used for a long time, to monitor extremely large spaces and to integrate with existing systems. This is in order to create a city IoT network.

The needs underlying the research activity were instead diametrically opposed , and all the references' parameters are changed as a result.

The first parameter is the duration of the survey, since in the case in question there is no need for it to be as long as possible. Indeed, it tends to last a few days, as many as the demolition activity lasts.

Furthermore, for the our purposes, a system capable of covering large portions of land was not required. Instead, this work requires a system optimized to detect the data relating to small areas as precisely as possible in an area slightly larger than the building being demolished.

Finally, compatibility and subsequent integration with existing systems are beyond our scope. Rather, the system must be extremely lean, flexible, as well as easy to disassemble in order to be moved quickly to other sites of interest, regardless of location or condition. It follows that, in the case in question, geographical location becomes superfluous, while independence from the point of view of power supply becomes fundamental.

It is then quite clear that the system should be characterized by the ability to detect multiple values simultaneously in a short time in order to provide detailed information to better calibrate any interventions.

Definitively, the goal of our work was to fine-tune a system specifically designed, and herefore optimized, to meet these specific needs.

As a consequence of all that has been said, we have explored a particular area which, as we said, is still extremely neglected, despite the need for a radical change in the perspective from which the construction site is traditionally conceived and designed, as already highlighted above (especially bearing in mind the Sustainable Development Goals of the 2030 Agenda [77]).

3.2 CASE STUDY 1 – A PRELIMINARY WORK

In this entirely preliminary work, the emissions of fine particles into the atmosphere were detected and analysed. In particular, PM2.5 and PM10 were detected. The detection took place during the actual demolition of a building in L'Aquila.

Taking advantage of documents already developed, also in the field of structures and environmental monitoring [3,6-25], an electronic low voltage, low power and low battery sensory system has been developed.

The main results obtained will be shown below.

3.2.1 General System Overwiev

Dust detection was carried out using two nodes, each equipped with a specific sensor capable of detecting PM10 and PM2.5 particles. The data collected were stored in a special memory and collected at the end of the single working day to be transferred to a PC and analyzed.

In Figure 37 and Figure 38 the diagram and the photo of the single node are shown, respectively.

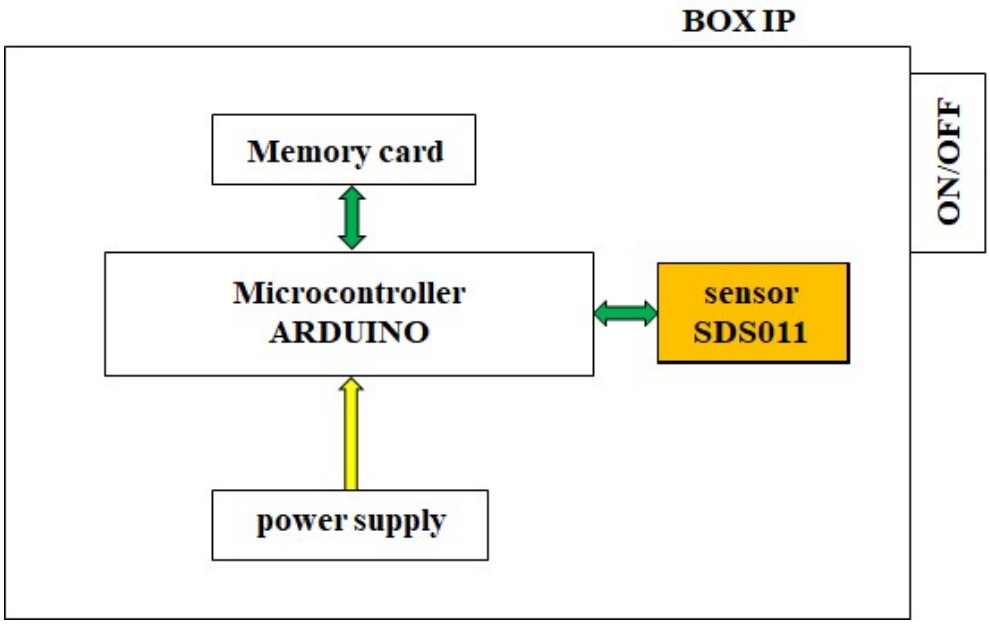

Figure 37: Internal architecture of the proposed node.

Figure 38: Photo of the proposed node.

3.2.2 Experimental Set Up

The building object of this work is located between two streets in L'aquila, that are Via Roma and Via Lopardi, which are very different in conformation. In particular, while Via Roma looks like a narrow street and often affected by the wind, Via Lopardi shows an open space that allowed to position the pump for the emission of water. The presence of this pump is decisive. In fact, sprinkling the building in demolition with

water allows to contain the dust, considerably reducing its dispersion into the atmosphere.

The two nodes were placed one on each route and this made it possible the monitoring of the two situations - with or without water - at the same time.

In Figure 39 the location of the nodes is shown, while in Figures 40 and 41 the photos of the positioning of the nodes are shown.

Figure 39: Node location map.

Figure 40: Node 1 location.

Figure 41: Node 2 location.

As already mentioned, the nodes are turned on at the beginning of each working day and turned off at the end of the same to extract the data. The results are shown in the next paragraph.

3.2.3 Results

Following figures (from Figure 42 to Figure 45) show the results at the end of two working days (02/27/2021 and 03/03/2021).

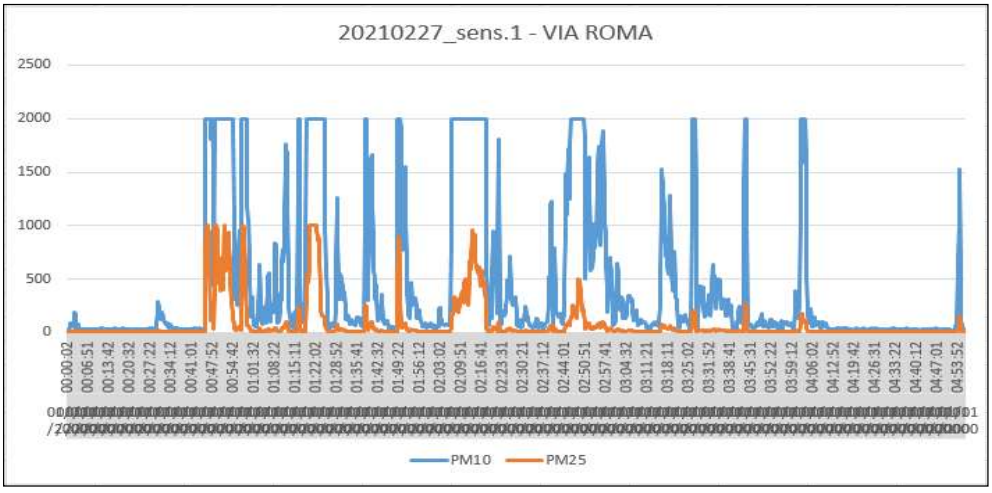

Figure 42: 27/02/2021 experimental results on Via Roma.

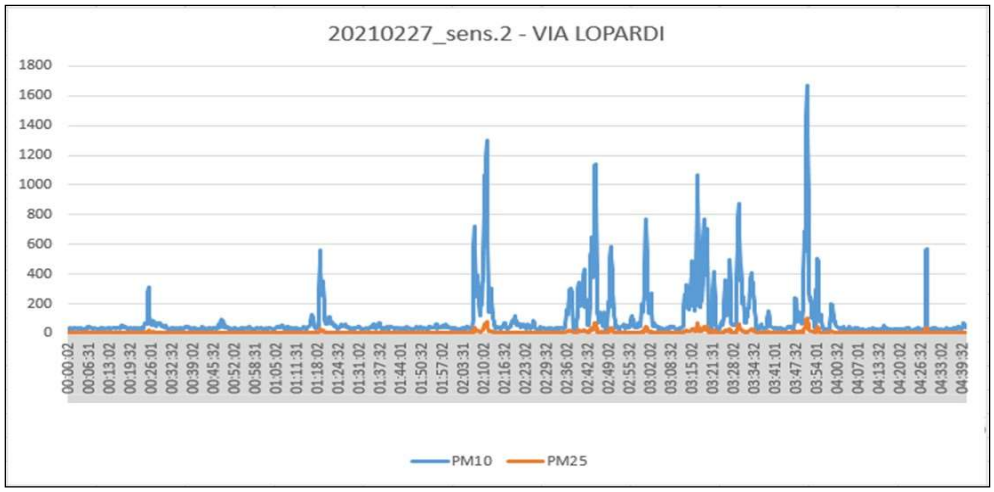

Figure 43: 27/02/2021 experimental results on Via Lopardi.

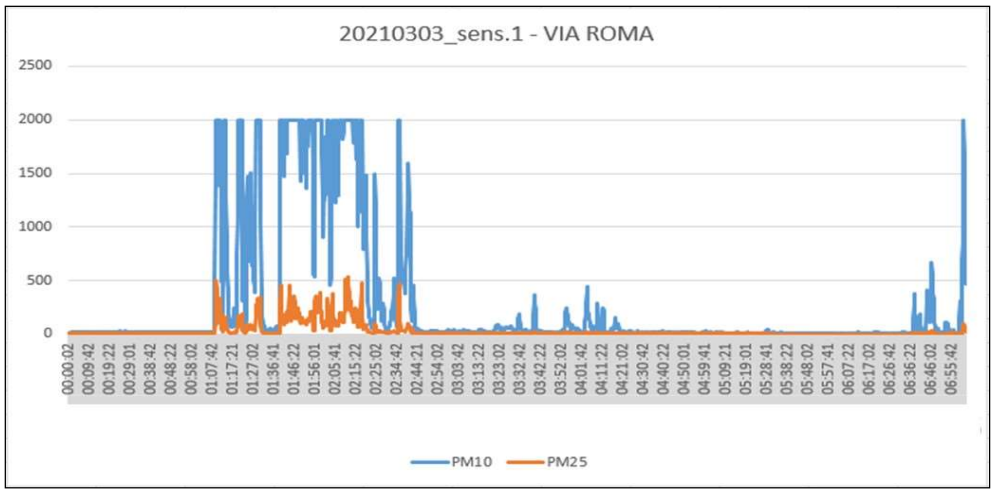

Figure 44: 03/03/2021 experimental results on Via Roma.

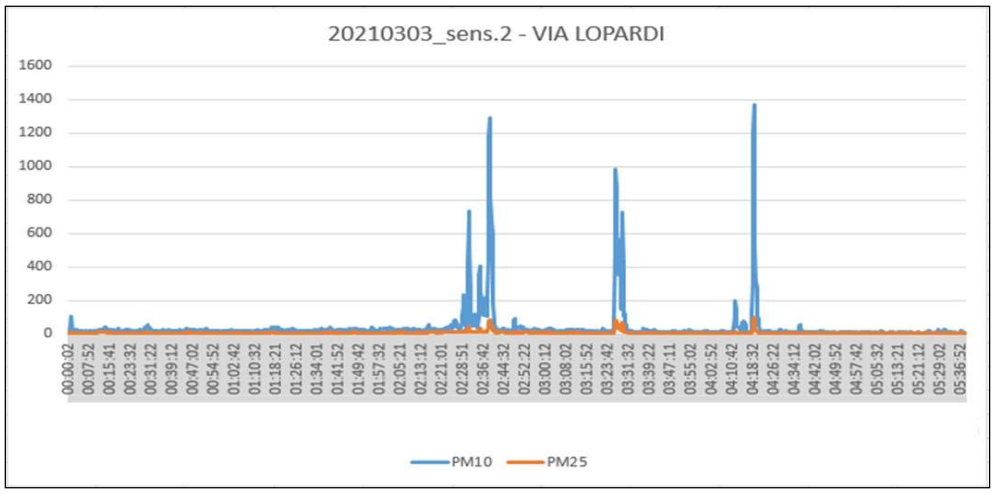

Figure 45: 03/03/2021 experimental results on Via Lopardi.

As it can be seen, when the demolition of a building is in progress, there is a sharp rise in the levels of PM10 and PM2.5 particles. However, the data collected on Via Lopardi, where the demolition takes place at the same time as the jet of water,

remains considerably below those on Via Roma, where even the PM10 level exceeds the threshold allowed by the sensors.

3.3 CASE STUDY 2 – IN-DEPTH ANALYSIS OF THE ENVIRONMENTAL MONITORING

Starting from the reflections made in the Introduction (section 1.2), and from the comforting results achieved with the preliminary work, we decided to continue with the study of PM10 and PM2.5 emissions during the demolition of buildings on construction sites. For this purpose, a system has been devised which, as will be seen below, has much better performance than the previous one.

Moreover, in addition to the improvement of the purely technical performances, and starting from what is reported in section 3.1, the novelty of this system lies in having opened, in the opinion of the authors, a new scenario on which there will be much to investigate based on the results achieved . In fact, these results demonstrate how inconsiderate the inattention shown up to now towards construction sites has been, in which, especially during activities such as demolitions, the values of PM 2.5 and PM 10 are - as will be seen later - well beyond the health protection limit, and remain so for the entire working day, making the matter even more serious.

3.3.1 Materials and Methods

Figure 46 shows the block diagram of the research method followed in this work.

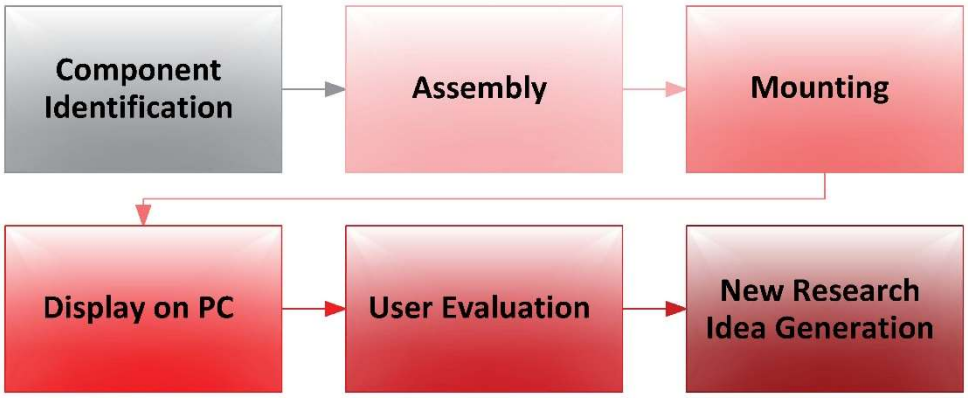

Figure 46: Research method block diagram.

First, the most suitable components in terms of sensors and data loggers were identified. The selection criteria were based on the evaluation of the best compromise between accuracy and cost-effectiveness. Then, we moved on to the assembly phase. In particular, each sensor was positioned inside an IP box, suitably powered, and

connected wirelessly to the other elements of the system. The system thus created is hereinafter referred to as the "node". The third phase was mounting, that is, the in situ assembly of the various nodes and the system as a whole. The next phase was to view the data on the PC. After reading them, the interpretation and evaluation of the results followed (fifth phase), and from these, the future developments of the present research were hypothesized. The scheme shown in Figure 46 could, however, turn into an infinite loop. The development of new ideas, in fact, could lead to a possible re-evaluation of the sensors best suited to the new needs, to the subsequent assembly, and so on.

Following the previously described scheme, a preliminary study related to the detection of dust during the demolition of a building was conducted and presented in [84]. Since the results have been satisfactory, we have deepened the analysis. As mentioned earlier, a more complex and performing system was therefore developed. Figure 47 shows a general block scheme of this system.

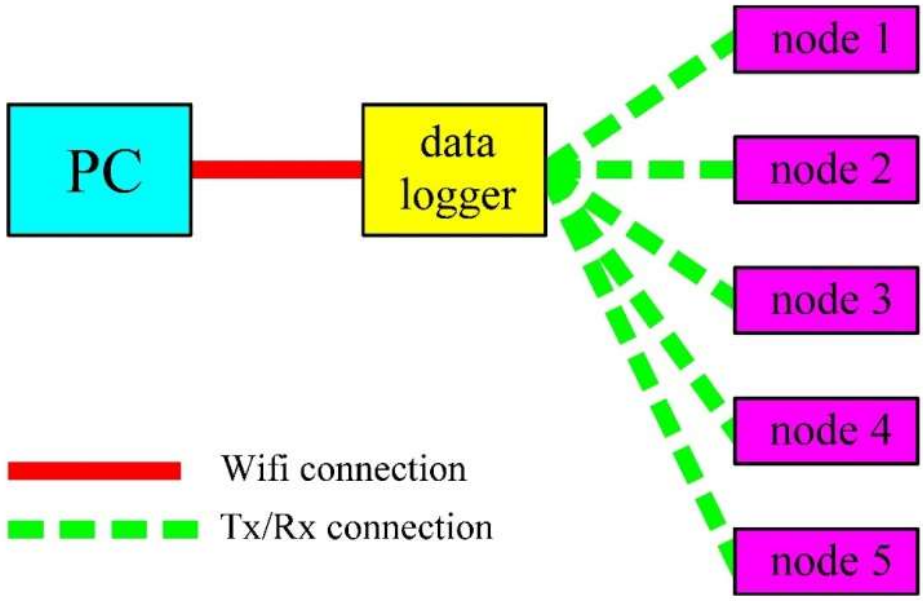

Figure 47: System general block scheme.

The developed system as a whole is characterized by its economy and extreme simplicity of use. Furthermore, the returned data are easily usable to anyone in possession of the appropriate credentials.

Five nodes have been developed, each positioned at different distances from the site of interest. This made it possible to have a greater number of information, and above all to study how the impact of dust changes as a function of the distance.

Furthermore, with respect to the solution proposed in [84], the memory on board of the nodes has been eliminated. In that case, in fact, the data were downloaded manually, physically taking the memory from each single node at the end of each acquisition period (typically a working day). This obviously meant that the single node had to be necessarily positioned in places that were always easily accessible. It also increased the risk of damage to the nodes themselves.

The nodes presented in this work, instead, do not store the data on board, but have the ability to continuously send them to the data logger which, in turn, transmits them to the PC. Furthermore, as we will see in more detail, the data will be available to anyone with the appropriate access credentials.

The characteristics of the whole system from the point of view of accuracy, precision, and durability are, however, related to the intrinsic characteristics of the sensors used. As described in this paper, one of the objectives of the developed system was it was to be inexpensive. This imposed us to use low-cost sensors. Among the available ones, we chose the SDS011 sensor, widely disseminated and documented in the literature [81-83,85-88], even with extremely recent articles which have dealt well with the issue of its performance. In particular, in [87], which constitutes a review of low-cost sensors, the SDS011 sensor is judged to be one of the best performing. More specifically, from the point of view of accuracy and precision, the solution shown in [88] emphasizes that accuracy falls within the range of 81–98%, while the accuracy is an average of 1 min data. As far as durability is concerned, in [89] it is noted that the life cycle of the sensor is 8000 h. This duration, apparently not exceptional in the case of prolonged use, does not compromise the purpose of our work. The demolition activity, in fact, has a limited duration in terms of days, after which it makes no sense to keep the system (and therefore the sensor) running.

In the following, the characteristics of each system component of the block will be detailed.

3.3.1.1 System Nodes

As already mentioned, the system nodes represent the elements capable of effectively detecting the dust present in the air, with particular reference, in the case in question, to PM2.5 and PM10. Figure 48 shows the diagram of a single node (a) and a photo reference (b).

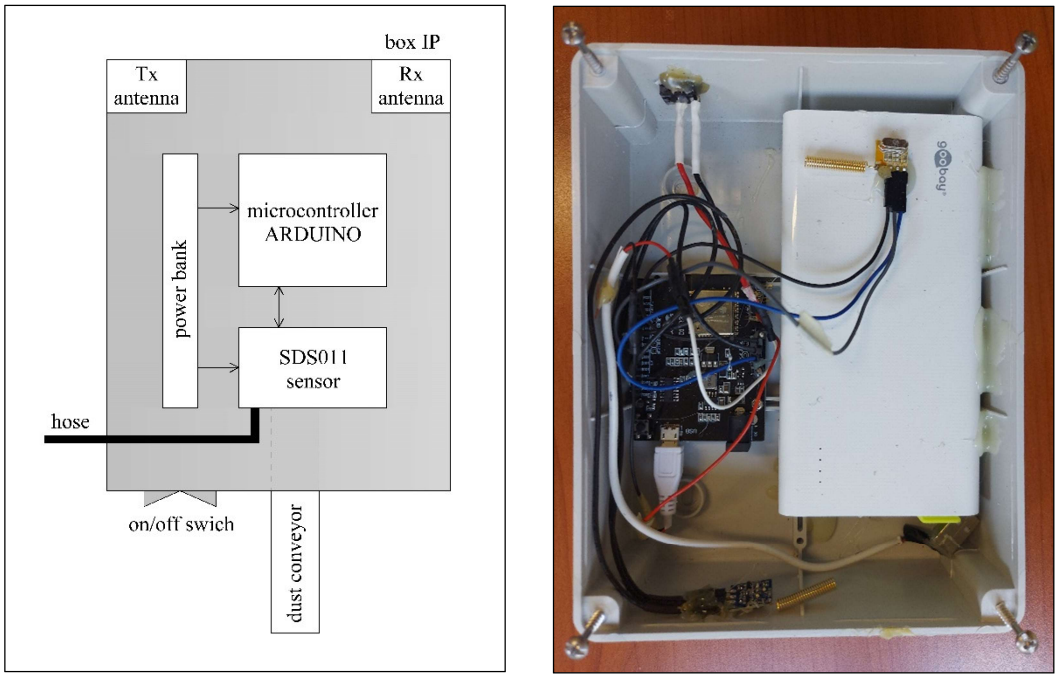

(**a**) (**b**)

Figure 48: (**a**) Scheme of a single node, (**b**) photo of a single node.

Dust detection takes place by employing a specific air quality sensor, named SDS011 [89]. Its operation is based on the principle of laser diffusion. Basically, when the particles cross the detection area, the diffusion of light is induced. This light is then suitably transformed into electrical signals which are subsequently amplified and processed so to have the required values.

This sensor is also characterized by both high precision and reliability, thanks to the laser detection, and a fast response (lower than 10 s). Furthermore, it has a very high resolution of 0.3 $\mu g/m^3$ and is easily integrated.

Figure 49 shows a picture of the sensor, while Table 3 gives the related main technical parameters

Figure 49: SDS011 sensor.

Table 4: Main parameters of the SDS011 sensor.

Measurement parameters	PM2.5,PM10
Range	0.0-999.9 μg /m³
Rated voltage	5V
Rated current	70mA±10mA
Sleep current	<4 mA
Temperature range	Storage environment：-20 ~ +60℃ Work environment：-10 ~ +50℃
Umidity range	Storage environment：Max 90% Work environment：Max 70%
Air pressure	86kPa~110kPa
Corresponding time	1s
Serial data output frequency	1Hz
Minimum resolution of particle	0.3 μm
Relative error	Maximum of ± 15% and ±10μg/m³

As can be seen, the range indicated in Figure 4 indicates the upper limit as 999.9 μg/m^3. However, from the results shown in the figures, it can be seen that, in some cases, the level of dust (both PM 2.5 and PM 10) detected often exceeds this value. Having proved the effectiveness of the tests carried out, as well as the correctness of the results obtained, the conclusion was that the indicated range is probably the one that guarantees the optimal performance of the sensor in terms, for example, of expected margins of error. Furthermore, it is important to underline that this aspect is ultimately absolutely irrelevant in relation to the purposes of this work. In fact, the aim of the latter was to study whether and for how long the level of dust exceeds the values set by WHO and Europe, both of which are in any case well below the aforementioned range limits.

The previously described sensor is connected to an Arduino microcontroller. The latter's task is twofold. In fact, it translates the detected quantities of PM 10 and PM 2.5 into numerical form and subsequently sends these data to the data logger through the Tx/Rx antennas present inside the node itself.

Finally, all the elements described above are placed in an appropriate IP-grade box. The operation of the node can be regulated from the outside through an on/off switch, and the power supply is ensured by a 10,000 mAh power bank, also mounted inside the IP box.

From a practical point of view, then, when the node is switched on, the dust is conveyed towards the fan integrated in the sensor. Subsequently, thanks to the microcontroller, the quantities of PM 2.5 and PM 10 are transformed into a numerical form and sent to the data logger. The dust is finally expelled through the hose.

3.3.1.2 Data Logger

Figure 50 shows the diagram of the data logger (a) and a reference photo (b).

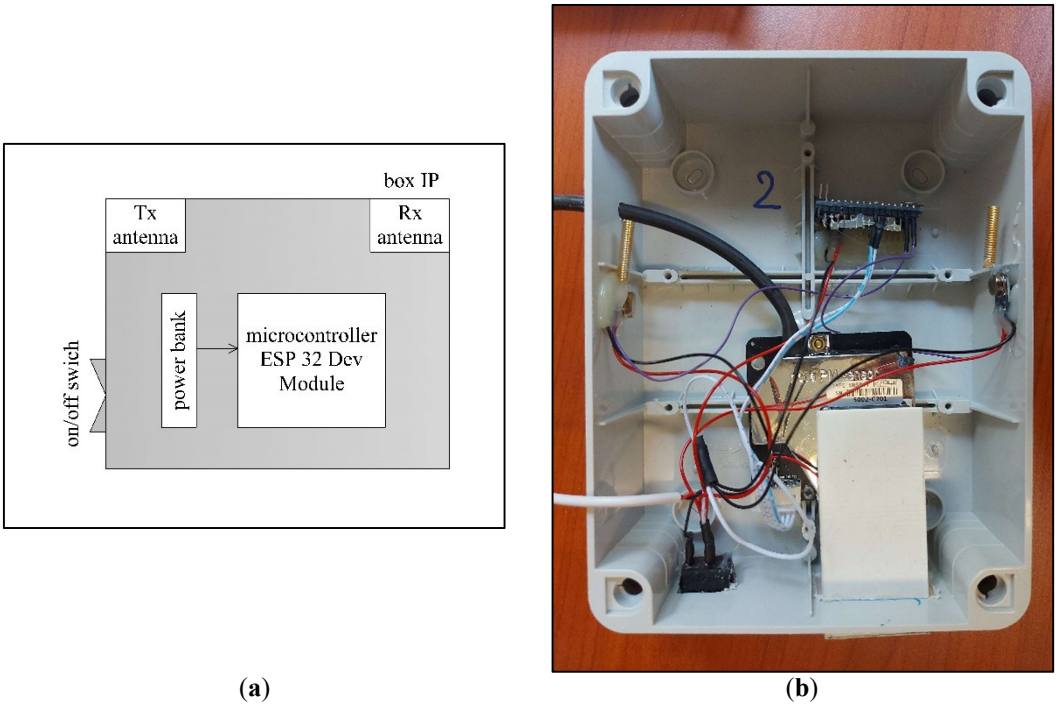

(**a**) (**b**)

Figure 50: (**a**) Data logger scheme, (**b**) data logger photo.

The data logger's task is, as already mentioned, to receive data from the microcontroller of each single node through the Tx/Rx antennas. In addition to this, the data logger takes care of making these data available to users by sending them to the PC using this time a Wi-Fi connection.

In this case, data loggers and antennas are mounted inside an IP box. The power supply is also ensured by a power bank. However, during the laboratory tests it emerged that the data logger had a much higher consumption than the single nodes. For this reason, in this case we have chosen to power it with a 20,000 mAh power bank to guarantee its operation for about three days.

3.3.1.3 Data Consultation Platform

The Ubidots platform was used to consult the data. It is characterized by a high easiness of use; it is open-source (at least in the basic version, more than sufficient for this work); and it allows the real-time viewing of the data received in the form of graphs. It also allows the download of the corresponding .csv file. To be able to use this platform, you must simply create your account and set your username and password. Obviously, the data can be consulted on any PC (or even by phone) and by anyone in possession of the set credentials.

Figure 51 shows a screen of the platform home page.

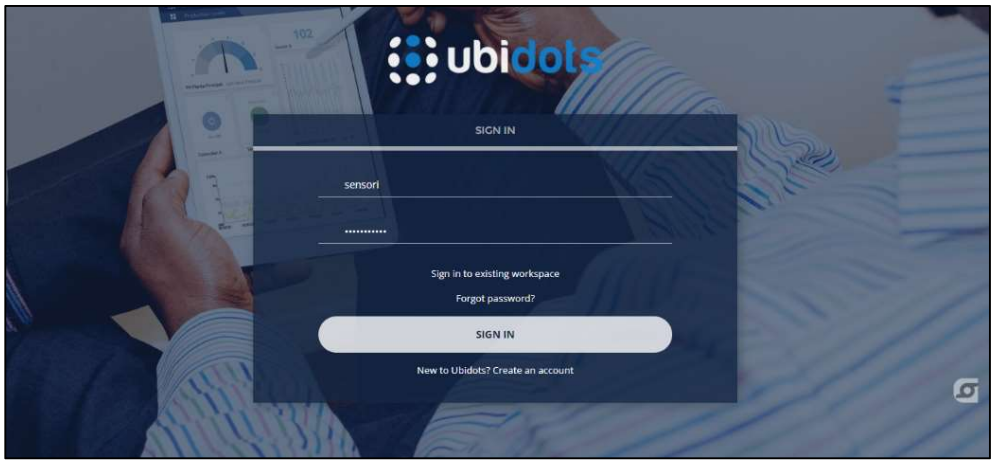

Figure 51: Ubidots home page.

3.3.1.4 The Case Study—Experimental Set Up

In the case study described here, five nodes were used. They were placed near a building located in a hamlet of L'Aquila which was really demolished following the serious damage suffered in the earthquake of 6 April 2009 in L'Aquila. This building is located in the historic center of Roio, near L'Aquila, between via San Leonardo and via Madonna di Roio, in an area that is not densely populated and characterized by being in the vicinity of construction sites used in the reconstruction of buildings damaged by the earthquake. Immediately around the construction site, there is an absence of sensitive receptors. The working phase of interest for this study is the one

that has the greatest impact in terms of fine dust pollution, namely the phase of demolition of the aggregate. For this reason, dust monitoring will be carried out for the entire duration of the process.

The building object of interest consists of an aggregation of several buildings spread over two levels, with as many real estate units. From a construction point of view, it is made up of load-bearing walls made of disordered stone masonry and the roof is wooden with tiles at the top. The criticism found to be taken into consideration with regard to the production of powders are the limited external spaces with the possible creation of the tunnel effect and consequent stagnation of the powders and inadequate dispersion. Figure 52 shows both the plan of the area of interest with the location of the system elements (nodes and data logger), and the photos of each of them after installation.

Keeping in mind the limitations related to technology widely discussed in the paper, the exact location of the nodes is the result of a careful evaluation aimed at reconciling different needs. On the one hand, there is a clear need intrinsic to the present work to understand how the measurements change as the distance and wind vary (which has also led us to the new ideas for future developments reported in the conclusions). On the other hand, we have also considered the practical need to have easily accessible physical supports, which for the most part do not fall into private areas and do not hinder the daily activities of the area's inhabitants.

Figure 52: (**a**) Plan of the area; (**b**) node installation 1; (**c**) node 2 and data logger installation; (**d**) node installation 3; (**e**) node installation 4; (**f**) node installation 5.

The type of demolition that the building company undertook was the traditional uncontrolled type with a hydraulic grapple, followed by a recovery and reuse of the area. Figure 53 shows some stages of the demolition.

Figure 53: Three different stages of demolition.

The positive aspect linked to this practice is the speed in carrying out the work. On the other hand, there is a high risk for the operators, both for the noise produced and for the vibrations and dust generated. This last risk is generally mitigated by using a manual lance to move along the demolition front.

3.3.2 Results

The demolition activity was monitored on two consecutive days, in particular 23 and 24 June 2022. The system was then left active until the power banks were unloaded in order to have a direct comparison between the measurements made during the demolition and activities suspended for the weekend.

In the rest of this section, the analysis of about 3000 values (300 of PM2.5 and 300 of PM10 for each of the five nodes) considered the most significant is presented.

The measured values are graphically represented in Figures 54–56. In the same graphs, the threshold lines set by Europe (in green) and the WHO (in red) are reproduced to facilitate an immediate comparison of the situation.

3.3.2.1 23 June 2022: results

Figure 54 shows the data related to the day of 23 June 2022. In particular, the survey starts at 11:29 (immediately after the installation of the system) and continues uninterrupted until about 17:00, i.e., until the end of working hours. Figure 22 shows the results relating to PM2.5 (a) and PM10 (b).

As can be seen, the trends of the graphs are absolutely superimposable. In effect, this means that the demolition activity involves an increase in both types of particulate matter.

Furthermore, the maximum peak of the survey is obtained from node 5. This is not accidental since the demolition activities started right from the part of the building immediately next to it.

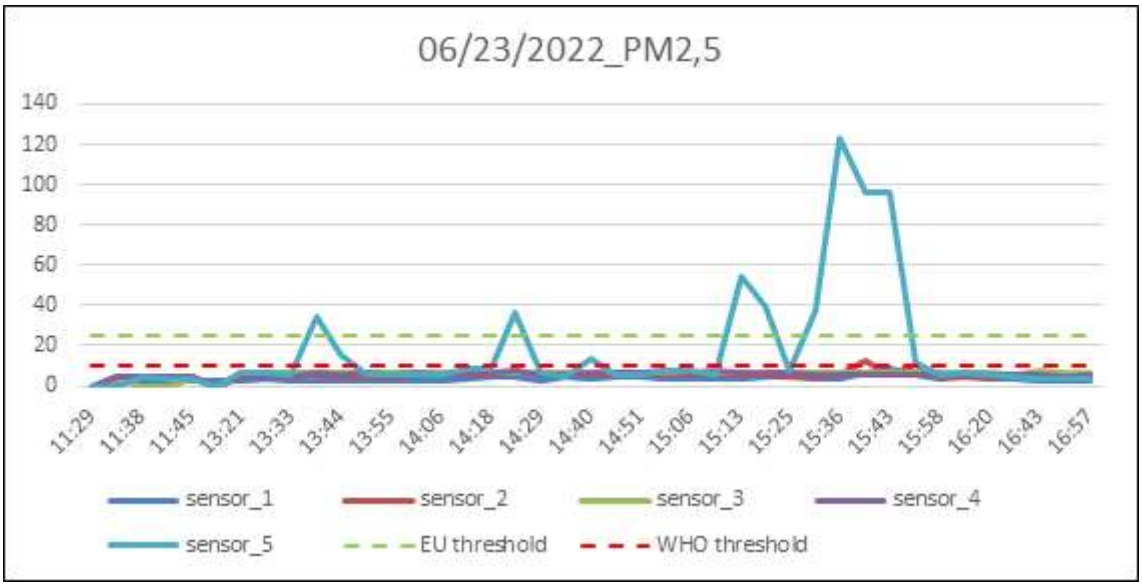

(**a**)

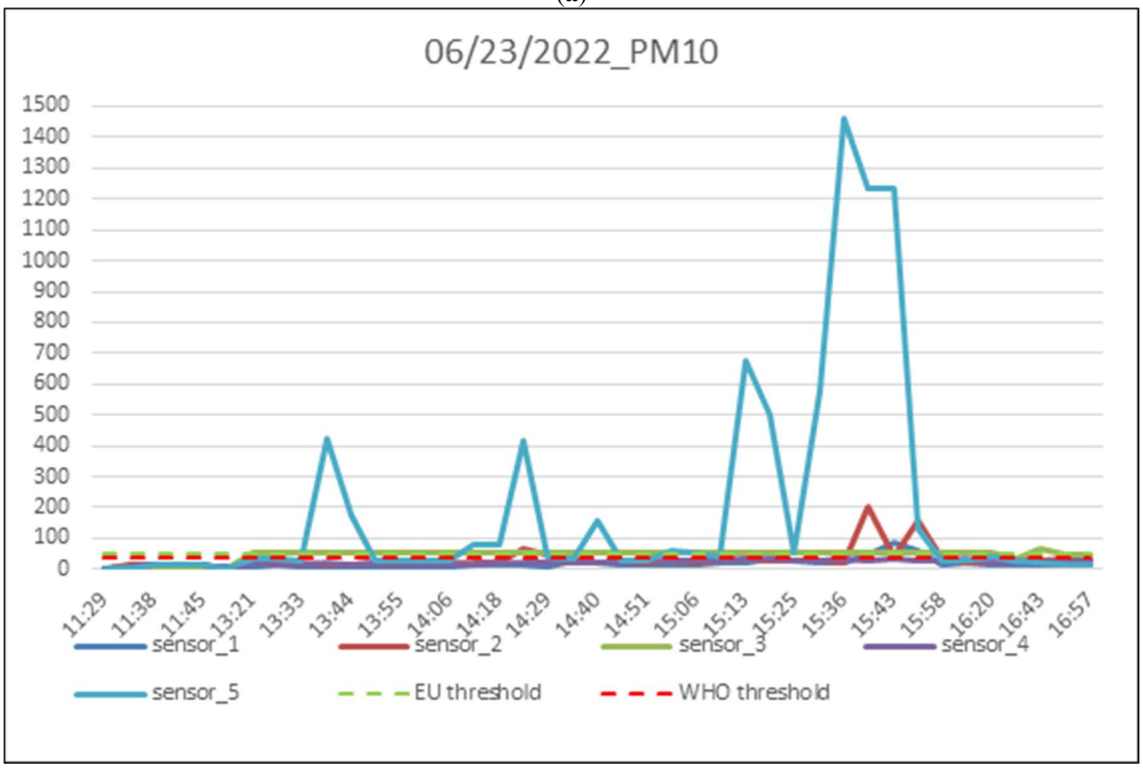

(**b**)

Figure 54: (**a**,**b**) Comparison between data recorded during active demolition work and after demolition work s stopped.

3.3.2.2 24 June 2022: results

Figure 55 below shows the data relating to 24 June 2022. In this case, the survey started at 9:30 a.m. and ended at approximately 5:20 p.m.

As before, Figure 55 shows the results for PM 2.5 (a) and PM 10 (b).

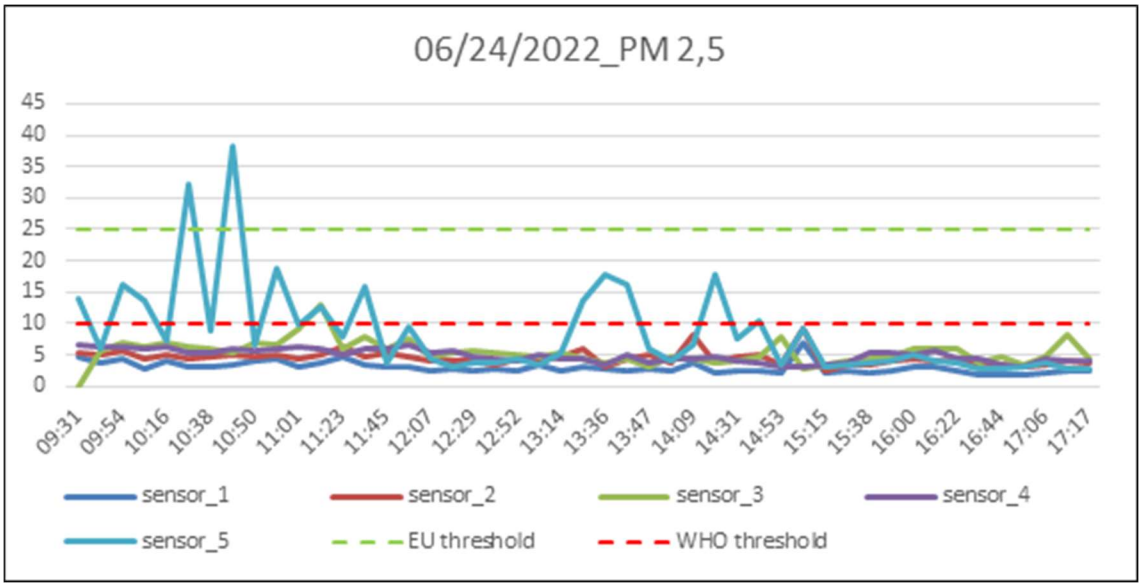

(**a**)

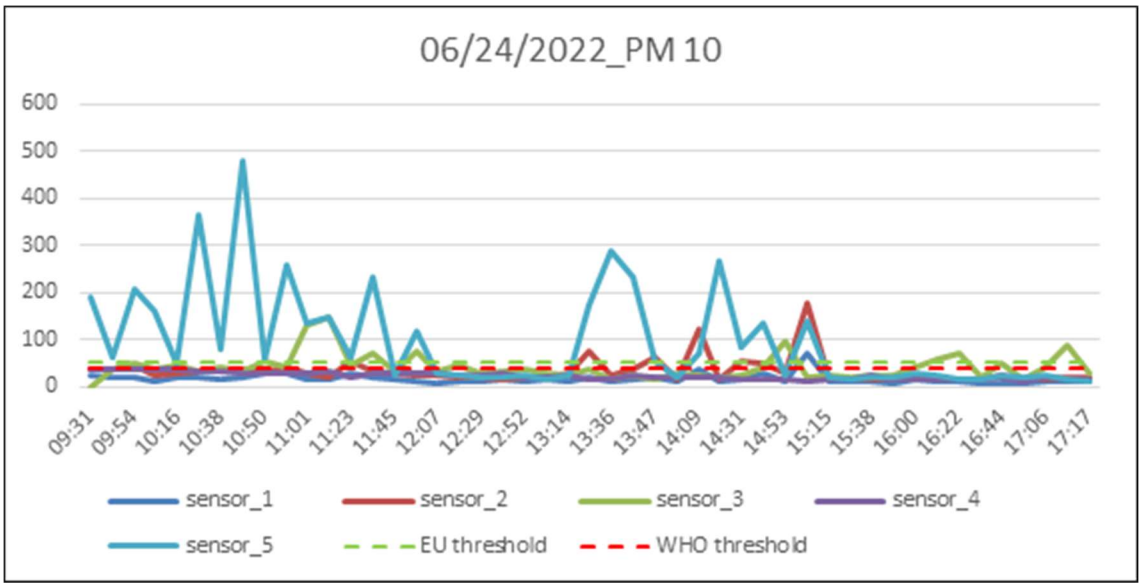

(**b**)

Figure 55: Result of the measurements of PM 2.5 (**a**) and PM 10 (**b**) on 24 June 2022.

In this case, all the nodes returned values that, in some moments, exceeded the thresholds set by the relevant regulations.

The exception is node 4, which does not seem to detect amounts of PM beyond the threshold. Most likely, this could be due to the action of the wind. The implications

of the wind in the detection of dust could constitute a future further development of the present work.

3.3.2.3 Results of the Surveys with Standstill Activities

Finally, Figure 56 shows the dust levels detected outside working hours.

Specifically, the values obtained on 24 June, starting at around 1:00 pm and subsequently, those obtained on 25 June (Saturday), a non-working day, are represented. On this day, the survey continued until 11:10 am, the time when the system stopped working due to the power bank being unloaded.

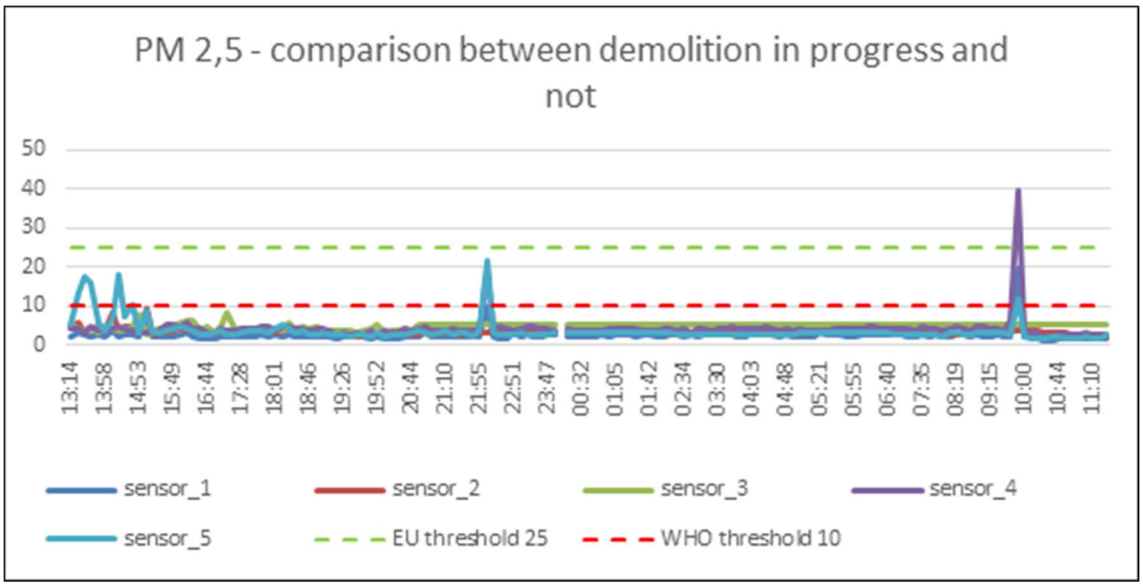

(**a**)

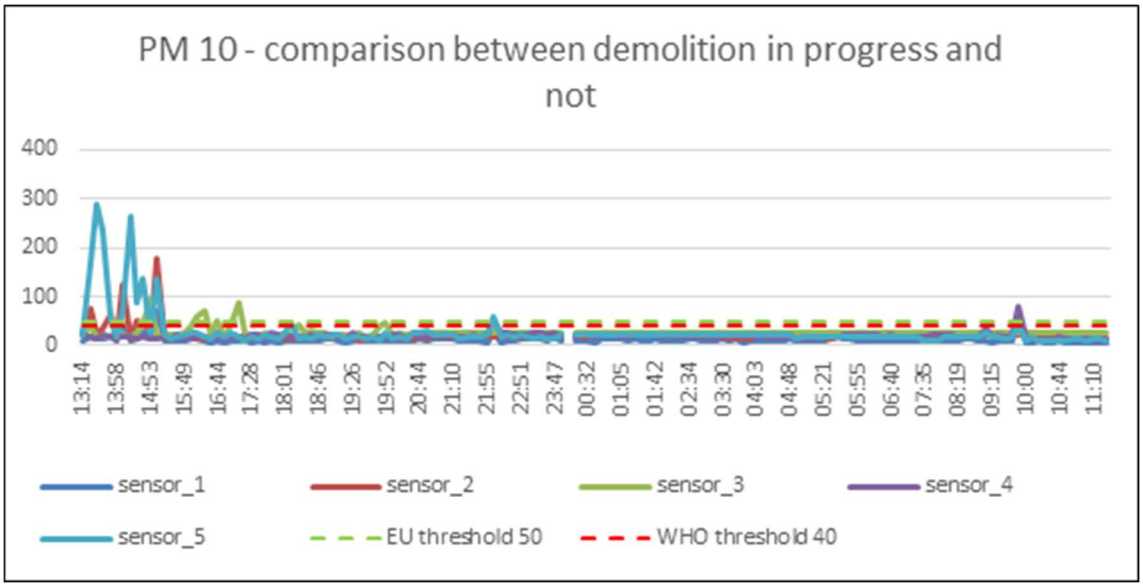

(**b**)

Figure 56: Result of the measurements of PM 2.5 (**a**) and PM 10 (**b**) at a standstill.

As can be seen, on the 24th there are still isolated peaks of fine dust. This is probably due to the fact that the powders need a certain amount of time to settle definitively.

In fact, on the 25th, the situation appears considerably calmer, and the level of dust in the air remains well below the permitted limits. The only noteworthy moment, albeit characterized by values well below those detected during the demolition, is detected by node 4 around 10:00. However, remembering that we are on a public road, it cannot be excluded that a vehicle passed at that moment.

3.3.2.4 Final Comparisons

Finally, in Tables 3 and 4, and in Figure 57, the average of the values measured over the three days is shown.

Table 5: Detected average of the PM2.5.

DATA	s1_PM2,5 (µg/m^3)	s2_PM2,5 (µg/m^3)	s3_PM2,5 (µg/m^3)	s4_PM2,5 (µg/m^3)	s5_PM2,5 (µg/m^3)
06/23/2022	3.512	5.134	5.400	5.573	17.293
06/24/2022	2.949	4.506	5.387	4.855	8.649
06/25/2022	2.615	3.402	5.010	4.399	2.951

Table 6: Detected average of the PM10.

DATA	s1_PM10 (µg/m^3)	s2_PM10 (µg/m^3)	s3_PM10 (µg/m^3)	s4_PM10 (µg/m^3)	s5_PM10 (µg/m^3)
06/23/2022	17.810	31.995	43.998	21.912	193.551
06/24/2022	16.602	33.374	41.309	22.730	96.283
06/25/2022	10.749	19.417	24.200	19.442	17.883

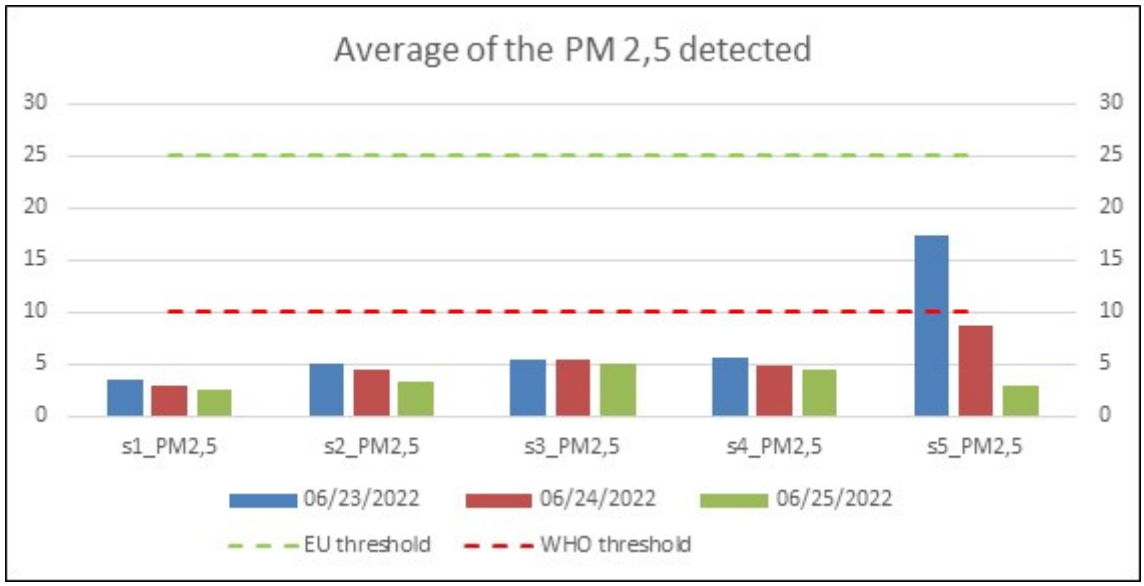

(**a**)

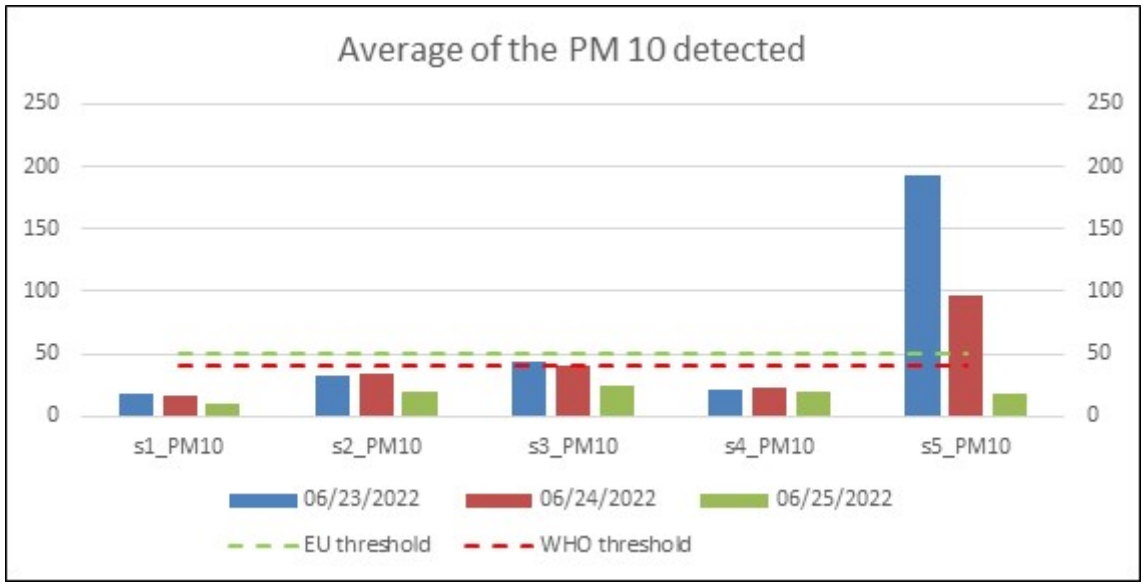

(**b**)

Figure 57: Average of the detected value of PM 2.5 (**a**) and PM 10 (**b**) at a standstill.

The reported values give further confirmation of the fact that node 5, the node closest to the site of interest, is the one that detects the highest values.

Chapter 4: Analysis

In this chapter the results reported for each of the topics covered in this thesis are commented. In particular, section 4.1 deals with the results of the studies conducted on Structural Monitoring, both from the point of view of synchronization, and from the point of view of the damage index, and finally from the point of view of modal frequencies. In section 4.2, on the other hand, the results obtained in the context of Environmental Monitoring are critically analysed.

4.1 STRUCTURAL MONITORING

From the point of view of synchronization (section 2.2), the experimental results lead us to conclude that, effectively, thanks to the use of the RS485 protocol, communication between nodes and masters takes place in a synchronized manner. In fact, as can be seen from Figure 6, all samples of the nodes of the proposed monitoring system are synchronized.

As far as the study on the damage index (section 2.3) is concerned, the results shown in section 2.3 are extremely comforting. Indeed, the values of the damage indicator have an increase of ten times, with only a 2.5mm engrave. Then, these results show that the proposed system, with synchronous samples between the two sensors, is able to detect damages in a monitored structure. However, the proposed monitoring system with a damage indicator approach will detect structural defects or damage after events such as earthquakes or landslides.

Finally, as regards the study of modal frequencies (section 2.4), from the results shown in section 2.4 we can conclude that, effectively, as the conditions of the structure vary, there is a variation in the modal frequencies. This was achieved thanks to an innovative system that moves data processing directly to the nodes.

In particular, in the first test conducted on the bar, important peaks can be seen between 26 and 28 Hz and between 43 and 52 Hz, approximately corresponding to the central modal frequencies of the bar. No wonder if the modes are slightly different from the theoretical ones, since the latter are the result of an analysis performed with accelerometers (having a different weight than the node used now) placed above the beam under examination. A different load on the bus leads, of course, to slightly

different modal frequencies. Furthermore, by performing an on board average of the transforms it is possible to save a much smaller number of samples (at most 128 instead of 1600) and better view frequencies with higher amplitude.

In the second type of test, instead, the main frequency is 53Hz, while all the others are less visible. It can therefore be seen how the position of the node influences the frequencies detected by the sensor.

In the third case, the lower frequency also emerges strongly, while the detection of the higher one is a little more problematic (which could be associated with the peak at 67 Hz, which however is very far from the 80 Hz hypothesized; moreover, the peak at 67 does not particularly stand out).

Finally, from an examination of the graphs of the fourth type of test, it can be seen that by increasing the number of samples the result becomes less corrupted by noise and the modal frequencies are more visible in the average of the signal.

In summary, therefore, as far as the test carried out on the bar is concerned, it can be concluded that the results are in line with those obtained from the same system used only for signal sampling, in which the accelerometer basically saves the data in the memory and the signal post processing is entrusted to the PC.

The deviation of the modal frequencies from the theoretical ones is due in part to the weight of the node on the beam and in part to the frequency accuracy (since fc/N=200/128=1.56Hz).

The code written for the single node allows to considerably increase the performance of the system, since, unlike the "classic" solution, it allows to decentralize the post processing in the case of multiple nodes (which autonomously perform the frequency transformation, the search for the peaks and the eventual average of the signal) and radically reduce the amount of data coming from each single node.

Similarly, with regard to the study carried out on the shed, the experimental results confirm that the peaks relating to the modal frequencies of the structure are clearly visible, and change as the conditions of the structure vary. It is also obtained, as expected, that as the conditions of the structure vary, a significant change in the modal frequencies is obtained.

4.2 ENVIRONMENTAL MONITORING

With regard to environmental monitoring, the experimental results of the preliminary test (section 3.2) show that, when a building is being demolished, there is

indeed a sharp increase in the levels of PM10 and PM2.5 particles. However, the data collected on via Lopardi, where the demolition takes place at the same time as the jet of water, remains considerably lower than those of via Roma, where even the PM10 level exceeds the threshold allowed by the sensors.

In the deepening of the environmental monitoring study (section 3.3), an evolution of the system capable of detecting PM 2.5 and PM 10 particles emitted during the demolition of a building was presented. This system makes it possible to evaluate the real level of dispersed dust, keeping the possibility of exceeding of the thresholds set by both Europe and the WHO under control.

The system is based on the use of five nodes, each equipped with an Arduino microcontroller and an SDS011 sensor, characterized by great sensitivity for the detection of dust. The nodes communicate with the data logger, then with another microcontroller in charge of sending the data to the PC, the ESP 32 Dev Module. Thanks to the system under examination, the problem of data storage is overcome. In fact, there is no longer the need to store the data directly onboard; instead, the same data are sent and stored directly in a special database. This eliminates the need to have a memory card for each node and, above all, the need to intervene directly on the node with the risk of damaging it. Furthermore, this allows you to position each single node, even in places that are not easily accessible on a continuous basis.

The system is also capable of handling a large amount of data. In the proposed system, 10 values (one of PM 2.5 and one of PM 10 for each of the five sensors) were acquired at approximately 4 min intervals for nearly three consecutive days. However, it should be specified that the system would also be able to withstand a further increase in the data itself, due, for example, to an increase in the total number of nodes or to an increase in the parameters detected for each node (for example, by inserting an anemometer that allows the detection of wind direction). In fact, the proposed system stopped working not because it was saturated, but simply because the power bank was unloaded. This means that, using other solutions, such as better-performing power banks or, if the conditions apply, alternative energies, the life of the system is theoretically infinite.

Furthermore, the high precision of the data collected makes the system particularly sensitive and precise. Parallel to the study presented here, in fact, an experiment was conducted using commercial sensors commonly purchased on the

internet, and positioned near some of those presented here. The result of the surveys in this case was extremely disappointing and not very significant. While the system proposed here has returned significant values in relation to the various moments of the activity, the values detected by the commercial sensors were significantly flattened, denoting a much lower sensitivity than the proposed nodes.

The proposed system is also extremely versatile and can be used whenever it is necessary to detect possible dangerous situations related to the emission of fine dust into the atmosphere. In this case, it was used to monitor the demolition of a building damaged by the L'Aquila earthquake, but it could easily be used in any other situation where such monitoring is necessary.

It must be said that, at present, an intrinsic limit of the proposed system is given by the distance at which the nodes must be placed (about 25 m and in visibility) with respect to the data logger. However, for the needs dictated by the case in question, this was not a problem but certainly among the future developments of the system, we can also include overcoming this difficulty.

Furthermore, considering that the results are made available in real time, they will allow workers in the trade to make appropriate assessments in order to protect both the people who live or in any case may be in the vicinity of the site for various reasons and workers as much as possible through appropriate prevention and protection measures. In fact, the ability to monitor the emission production in real time allows the site safety coordinator and also the employer to take timely decisions to safeguard the wellbeing of workers. For example, as soon as any critical conditions arise, it will be possible to promptly switch on an additional lance or a new sprayer or even to temporarily suspend work. Moreover, given the windy conditions of the site, a different work schedule can be defined to better distribute the demolition phases in order to reduce emissions. Ultimately, the focus on the particular issue of dust produced by urban demolition and reconstruction sites can be particularly important to promote awareness among all actors in the construction industry and to spread a culture of prevention and safety.

Ultimately, given the interesting reflections that this work has aroused, the future developments of this research may also be significant and continue to involve various engineering sectors in a transversal manner.

Chapter 5: Conclusions

In this final chapter, conclusions are drawn. Among other things, the strengths and weaknesses of the new systems described are underlined, as well as what future research prospects could be.

Also in this case, the chapter will be divided into two parts: section 5.1 will deal with Structural Monitoring, section 5.2 will deal with Environmental Monitoring.

5.1 STRUCTURAL MONITORING

As for synchronization, a new electronic sensory system for synchronization has been presented in section 2.2. The system is based on one master device and N nodes that are synchronized through RS485 bus. The system can acquire a large number of samples with high speed. The monitoring system has been tested with one master and two nodes to verify the synchronization between the samples.

In the future, the system may be readapted for a larger scale. In fact, it can be enriched with a higher number of nodes. These nodes, thanks to the use of the RS485 communication protocol, will communicate simultaneously with the master and can also be placed at a great distance (even hundreds of meters away) from it.

The results of this research were presented in [25,69].

With regard to the damage index, an IoT monitoring system for structural health is presented. The IoT system, with application in Smart Buildings, allows for the measurement of the main parameters for evaluating the damage indicator. The system is based on the microcontroller Sam3X8E ARM cortex-M3 and high-resolution digital accelerometers ADXL355. Furthermore, thanks to the use of an SD card and DMA, the system allows for the acquisition of a high number of samples and communicates through the RS485 to the master device.

The reliable results have been ensured with the high synchronization between the sensors and their high resolution. Instead, the problems of the traditional analog sensors used in the typical monitoring systems have been eliminated with the use of the digital accelerometers. Therefore, the proposed monitoring system is cheaper than an analog solution.

The system has been used to evaluate damage in an aluminum bar locked in a bench vice. The test gave the possibility to assess, with the developed system, its capability of damage identification. An engraving was realized in the structure for comparing the evaluated damage indicator in both conditions.

Therefore, to implement a structural health monitoring system, our studies confirmed that the detection of any type og damage is important. Future development of the proposed system will concern the installation of the device on real structures, such as buildings.

The results of this research were presented in [90-91].

Finally, regarding the study of modal frequencies, a new code for the structural health monitoring system was developed in this study. This code allows you to:

1. sampling the input data to the accelerometer (with modifiable sampling frequency and duration);
2. save the sampled data inside the flash;
3. perform the FFT of N samples (with N < 128), in which however the following parameters can be set
   - number of samples for each FFT (4, 8, 16, 32, 64 or 128);
   - ype of FFT to execute (1.3, 1.4.1, 1.4.2);
   - options to activate: ControlMagnitude(1.5.1), Fitting(1.5.2), find-Peaks(1.6) and average of results(AVERAGE_RESULT);
4. implement communication between nodes and masters;
5. retrieve accelerometer data, FFT results (peaks only if FIND_PEAKS is on), and average results.

The presented work allows to decentralize data processing by performing the post processing on board. This decreases the costs of the monitoring system, which no longer needs the use of an external device for processing the accelerometric data.

It also allows you to significantly reduce the data flow between nodes and masters, especially if the results are averaged.

Furthermore, the work lends itself to interesting future developments, capable of improving the characteristics of what is presented here, such as:

- resolution of the problems present in the accelerometer, which has shown that it suffers from disturbances due to the network frequency;

- increase of the baud rate in the communication between nodes and master (limited to 1200 in the tests carried out due to communication problems);
- implementation of advanced techniques in the calculation of the FFT;
- improvement of the search of the peaks in the pier such as to find only the significant ones.

The results of this research were presented in a degree thesis of which I was co-supervisor.

5.2 ENVIRONMENTAL MONITORING

The preliminary work related to environmental monitoring consisted in the study of a practical case of detection of the dust emitted during the demolition of a building. Working in the same conditions, the particular position of the building made it possible to monitor two opposite situations: emissions with or without the presence of water jets. Experimental data confirm that carrying out a demolition with simultaneous emission of water jets helps to keep emissions lower.

In future works, it will be interesting to add further nodes to monitor the surrounding areas, so to verify how far emissions continue to remain high. Furthermore, the final aim is to get to fine-tune an "intelligent" system that sends alerts to the personnel working on site, signaling the potential danger when excessively high emissions are present for too long. Finally, it will be interesting to understand how to intervene to further improve working conditions.

The results of this research were presented in [84].

In the next phase of study, an electronic system for the sensing of fine dust has been fine-tuned. In particular, the system detects the quantities of PM 2.5 and PM 10 emitted during the demolition of a building located in L'Aquila that was severely damaged following the 2009 earthquake. The system is based on a data logger that receives data from five nodes equipped with dust sensors. These data are transferred in real time to the PC and, at the same time, stored for future consultations. The experimental results confirmed how critical the demolition of a building is from the point of view of the emission of fine particles.

The strengths of the system presented essentially reside in the cost-effectiveness, simplicity of use, the ability to manage a large amount of data, the high accuracy of the surveys, and versatility.

There are certainly some weaknesses: first of all, the need for nodes and data loggers to be placed in perfect visibility and at a distance of no more than 25 m.

The future developments of this work will concern the monitoring of further construction sites, even more complex ones, in order to further expand the proposed system (both from the point of view of the number of nodes and from that of the number of parameters detected by each of them) to overcome the problems that have emerged and, ultimately, to confirm and enrich the good results obtained so far.

The results of this research were presented in [92].

List of Publications

- **Paolucci, R.**; Rotilio, M.; Ricci, S.; Pelliccione, A. *A Sensor Based System for Dust Containment and in the Construction Site.* Energies 2022, 15(19), 7272; https://doi.org/10.3390/en15197272.
- Pantoli, L.; Alaggio, R.; **Paolucci, R.**; Di Battista, L.; Ferri, G. *Sensors and Interfaces for Structural Health Monitoring.* In Lecture Notes in Electrical Engineering book series (LNEE,volume 918) - AISEM 2021: Sensors and Microsystems pp 295–300, doi: 10.1007/978-3-031-08136-1_46.
- **Paolucci, R.**; Ferri, G.; Alaggio, R.; Cirella, R.; Stornelli V. *Structural Health Monitoring: a system for the correct syncronization of the sensors.* In Proceedings of the 6th International Conference on Smart and Sustainable Technologies (SpliTech), Split and Bol, Croatia (Hybrid), 8-11 September 2021, doi: 10.23919/SpliTech52315.2021.9566353
- **Paolucci, R.**; Rotilio, M.; De Berardinis, P.; Ferri, G.; Cucchiella F.; Stornelli, V. *Electronic System for Monitoring of Dust on Construction Sites for the Health of Workers.* In Proceedings of the 15th International Conference on Advanced Technologies, Systems and Services in Telecommunications (TELSIKS), Nis, Serbia, 20-22 October 2021, doi: 10.1109/TELSIKS52058.2021.9606281.
- Muttillo, M.; Stornelli V.; Alaggio, R.; **Paolucci, R.**; Di Battista, L.; de Rubeis, T.; Ferri, G. *Structural Health Monitoring: an IoT sensor system for structural damage indicator evaluation.* Sensors 2020, 20(17): 4908; https://doi.org/10.3390/s20174908
- **Paolucci, R.**; Muttillo, M.; Di Luzio, M.; Alaggio, R.; Ferri, G. *Electronic Sensory System for Structural Health Monitoring Applications.* In Proceedings of the 5th International Conference on Smart and Sustainable Technologies (SpliTech), Virtual, 23-26 September 2020, doi: 10.23919/SpliTech49282.2020.9243798.
- Fazzini, G.; Chiulli, D.; Muttillo, M.; Paolini, P.; Barile, G.; **Paolucci, R.**; Leoni, A.; Ferri, G. *Print On Air: FDM 3D Printing Without Supports.* In Proceedings of the II Workshop on Metrology for Industry 4.0 and IoT (MetroInd4.0&IoT), Naples, Italy, 04-06 June 2019, doi: 10.1109/METROI4.2019.8792846.
- Leoni, A.; Barile, G.; Muttillo, M.; Pantoli, L.; Stornelli V.; Ferri, G.; **Paolucci, R.**; Di Vita, L. *A Spherical Directional Anemometer Sensor System.* In Proceedings of the Eurosensors 2017, Paris, France, 03–06 September 2017, https://doi.org/10.3390/proceedings1040388.

Bibliography

1. Ooijevaar, T.H. Vibration Based Structural Health Monitoring of Composite Skin-Sti_ener Structures. Ph.D. Thesis, Universiteit Twente, Enschede, The Netherlands, March 2014.

2. Li, H.; Ren, L.; Jia, Z.; Yi, T.; Li, D. State-of-the-art in structural health monitoring of large and complex civil infrastructures. J. Civ. Struct. Health Monit. 2015, 6, 3–16.

3. Ko, J.; Ni, Y. Technology developments in structural health monitoring of large-scale bridges. Eng. Struct. 2005, 27, 1715–1725.

4. Eun-Min, C.; Hyung Jin, J.; Dan Ki, Y.; Si Hyun, P.; Hyung Jin, H.; Kil Yong, C.; Heun Woo, C.; Hyo Chang, C.; Cheol Min, L. Reliability of Low-Cost, Sensor-Based Fine Dust Measurement Devices for Monitoring Atmospheric Particulate Matter Concentrations. Int. J. Environ. Res. Public Health 2019, 16, 1430.

5. Xiaoling, Z.; Liyin, S.; Lei, Z. (2015). Life cycle assessment of the air emissions during building construction process: A case 479 study in Hong Kong. Renew. Sust. Energ. Rev. 2015, 17, 160-169, https://doi.org/10.1016/j.rser.2012.09.024.

6. Cigada, A.; Moschioni, G.; Vanali, M.; Caprioli, A. The measurement network of the San Siro Meazza stadium in Milan: Origin and implementation of a new data acquisition strategy for structural health monitoring. Exp. Tech. 2010, 34, 70–81.

7. Ni, Y.; Xia, Y.; Liao, W.; Ko, J. Technology innovation in developing the structural health monitoring system for Guangzhou New TV Tower. Struct. Control Health Monit. 2009, 16, 73–98.

8. Velmurugan, R.; Balaganesan, G. Modal analysis of pre and post impacted nano composite laminates. Lat. Am. J. Solids Struct. 2011, 8, 9–26.

9. Muttillo, M.; Di Battista, L.; de Rubeis, T.; Nardi, I. Structural health continuous monitoring of buildings—A modal parameters identification system. In Proceedings of the 4th International Conference on Smart and Sustainable Technologies (SpliTech), Bol (Island of Brac) and Split, Croatia, 18–21 June 2019.

10. Lifshitz, J.; Rotem, A. Determination of Reinforcement Unbonding of Composites by a Vibration Technique. J. Compos. Mater. 1969, 3, 412–423.

11. Kim, J.; Ryu, Y.; Cho, H.; Stubbs, N. Damage identification in beam-type structures: Frequency-based method vs mode-shape-based method. Eng. Struct. 2003, 25, 57–67.

12. Gomes, G.; Ancelotti, A.; da Cunha, S. Residual stress prediction in porous cfrp using artificial neural networks. Compos. Mech. Comput. Appl. Int. J. 2018, 9, 27–40.

13. Cawley, P.; Adams, R. The location of defects in structures from measurements of natural frequencies. J. Strain Anal. Eng. Des. 1979, 14, 49–57.

14. Aloisio, A.; Di Battista, L.; Alaggio, R.; Antonacci, E.; Fragiacomo, M. Assessment of structural interventions using Bayesian updating and subspace-based fault detection methods: The case study of S. Maria di Collemaggio basilica, L'Aquila, Italy. Struct. Infrastruct. Eng. 2020, 17, 141–155.

15. Aloisio, A.; Di Battista, L.; Alaggio, R.; Fragiacomo, M. Sensitivity analysis of subspace-based damage indicators under changes in ambient excitation covariance, severity and location of damage. Eng. Struct. 2020, 208, 110235.

16. Khan, I.; Choi, S.; Kwon, Y. Earthquake Detection in a Static and Dynamic Environment Using Supervised Machine Learning and a Novel Feature Extraction Method. Sensors 2020, 20, 800.

17. Quqa, S.; Landi, L.; Diotallevi, P. Real time damage detection through single low-cost smart sensor. In Proceedings of the 7th International Conference on Computational Methods in Structural Dynamics and Earthquake Engineering (COMPDYN), Crete, Greece, 24–26 June 2019.

18. Valenti, S.; Conti, M.; Pierleoni, P.; Zappelli, L.; Belli, A.; Gara, F.; Carbonari, S.; Regni, M. A low cost wireless sensor node for building monitoring. In Proceedings of the IEEEWorkshop on Environmental, Energy, and Structural Monitoring Systems (EESMS), Salerno, Italy, 21–22 June 2018.

19. Liu, L.; Zhang, Y. Design of greenhouse environment monitoring system based on Wireless Sensor Network. In Proceedings of the 3rd International Conference on Control, Automation and Robotics (ICCAR), Nagoya, Japan, 22–24 April 2017.

20. Barile, G.; Leoni, A.; Pantoli, L.; Stornelli, V. Real-Time Autonomous System for Structural and Environmental Monitoring of Dynamic Events. Electronics 2018, 7, 420.

21. Pantoli, L.; Muttillo, M.; Ferri, G.; Stornelli, V.; Alaggio, R.; Vettori, D.; Chinzari, L.; Chinzari, F. Electronic system for structural and environmental building monitoring. In Lecture Notes in Electrical Engineering; Springer: Cham, Switzerland, 2019; Volume 539, pp. 481–488.

22. Ghosh, A.; Raha, A.; Mukherjee, A. Energy-Effcient IoT-Health Monitoring System using Approximate Computing. Internet Things 2020, 9, 100166.

23. Luan, H.; Leng, J. Design of energy monitoring system based on IOT. In Proceedings of the 28th Chinese Control and Decision Conference (CCDC), Yinchuan, China, 28–30 May 2016.

24. De Rubeis, T.; Muttillo, M.; Nardi, I.; Pantoli, L.; Stornelli, V.; Ambrosini, D. Integrated Measuring and Control System for Thermal Analysis of Buildings Components in Hot Box Experiments. Energies 2019,12, 2053.

25. Paolucci, R.; Muttillo, M.; Di Luzio, M.; Alaggio, R.; Ferri, G. Electronic Sensory System for Structural Health Monitoring Applications. In

Proceedings of the 5th International Conference on Smart and Sustainable Technologies (SpliTech), Virtual, 23–26 September 2020.

26. Schubel, P.; Crossley, R.; Boateng, E.; Hutchinson, J. Review of structural health and cure monitoring techniques for large wind turbine blades. Renew. Energy 2013, 51, 113–123.
27. Diamanti, K.; Soutis, C. Structural health monitoring techniques for aircraft composite structures. Prog. Aerosp. Sci. 2010, 46, 342–352.
28. Guo, H.; Xiao, G.; Mrad, N.; Yao, J. Fiber Optic Sensors for Structural Health Monitoring of Air Platforms. Sensors 2011, 11, 3687–3705.
29. Fu, Y.; Liu, J.; Wei, Z.; Lu, Z. A two-step approach for damage Identification in plates. J. Vib. Control 2014, 22, 3018–3031.
30. Gomes, G.F.; Mendéz,Y.A.D.; Alexandrino, P.D.S.L.; da Cunha, S.S., Jr.; Ancelotti, A.C., Jr. The use of intelligent computational tools for damage detection and identification with an emphasis on composites—A review. Compos. Struct. 2018, 196, 44–54.
31. Heslehurst, R. Defects and Damage in Composite Materials and Structures; CRC Press, Taylor & Francis Group: Boca Raton, FL, USA, 2017.
32. Gopalakrishnan, S.; Ruzzene, M.; Hanagud, S. Computational Techniques for Structural Health Monitoring; Springer: Berlin/Heidelberg, Germany, 2011.
33. Mufti, A. Structural Health Monitoring of Innovative Canadian Civil Engineering Structures. Struct. Health Monit. Int. J. 2002, 1, 89–103.
34. Wang, Y.; Lynch, J.; Law, K. A wireless structural health monitoring system with ultithreaded sensing devices: Design and validation. Struct. Infrastruct. Eng. 2007, 3, 103–120.
35. Hu, X.; Wang, B.; Ji, H. AWireless Sensor Network-Based Structural Health Monitoring System for Highway Bridges. Comput. Aided Civ. Infrastruct. Eng. 2012, 28, 193–209.
36. ADXL355 Datasheet and Product Info. Analog Devices. Available online: https://www.analog.com/en/ products/adxl355.html (accessed on 4 June 2020).
37. González, S.; Jiménez, J.C.; Guevara, R.; Palacios, I. IoT-based microseismic monitoring system for the evaluation of structural health in Smart cities. In Proceedings of the Ibero-American Congress Smart Cities (ICSC-CITIES), Soria, Spain, 26–27 September 2018; pp. 1–13.
38. Lee, J.; Khan, I.; Choi, S.; Kwon, Y. A Smart IoT Device for Detecting and Responding to Earthquakes. Electronics 2019, 8, 1546.
39. Pierleoni, P.; Conti, M.; Belli, A.; Palma, L.; Incipini, L.; Sabbatini, L.; Valenti, S.; Mercuri, M.; Concetti, R. IoT Solution based on MQTT Protocol for Real-Time Building Monitoring. In Proceedings of the IEEE 23rd International Symposium on Consumer Technologies (ISCT), Ancona, Italy, 19–21 June 2019.

40. Wondra, B.; Malek, S.; Botz, M.; Glaser, S.; Grosse, C. Wireless High-Resolution Acceleration Measurements for Structural Health Monitoring ofWind Turbine Towers. Data-Enabled Discov. Appl. 2019, 3, 4.

41. Navabian, N.; Beskhyroun, S. An AutomatedWireless-Based System for Real-Time Health Monitoring of Civil Infrastructures. In Proceedings of the 2020 New Zealand Society for Earthquake Engineering Annual Technical Conference, Wellington, New Zealand, 22–24 April 2020.

42. Noel, A.; Abdaoui, A.; Elfouly, T.; Ahmed, M.; Badawy, A.; Shehata, M. Structural Health Monitoring Using Wireless Sensor Networks: A Comprehensive Survey. IEEE Commun. Surv. Tutor. 2017, 19, 1403–1423.

43. Gomes, G.; Diniz, C.; da Cunha, S.; Ancelotti, A. Design Optimization of Composite Prosthetic Tubes Using GA-ANN Algorithm Considering Tsai-Wu Failure Criteria. J. Fail. Anal. Prev. 2017, 17, 740–749.

44. Dixit, S.; Sharma, K. A Review of Studies in Structural Health Monitoring (SHM). In Proceedings of the Creative Construction Conference, Budapest, Hungary, 29 June–2 July 2019.

45. Jiang, S.; Zhang, C.; Zhang, S. Two-stage structural damage detection using fuzzy neural networks and data fusion techniques. Expert Syst. Appl. 2011, 38, 511–519.

46. Gui, G.; Pan, H.; Lin, Z.; Li, Y.; Yuan, Z. Data-driven support vector machine with optimization techniques for structural health monitoring and damage detection. KSCE J. Civ. Eng. 2017, 21, 523–534.

47. Gökda˘ g, H.; Yildiz, A. Structural Damage Detection Using Modal Parameters and Particle Swarm Optimization. Mater. Test. 2012, 54, 416–420.

48. Magalhães, F.; Cunha, A.; Caetano, E. Vibration based structural health monitoring of an arch bridge: From automated OMA to damage detection. Mech. Syst. Signal Process. 2012, 28, 212–228.

49. Bandara, R.; Chan, T.; Thambiratnam, D. Structural damage detection method using frequency response functions. Struct. Health Monit. Int. J. 2014, 13, 418–429.

50. Abdeljaber, O.; Avci, O.; Kiranyaz, S.; Gabbouj, M.; Inman, D. Real-time vibration-based structural damage detection using one-dimensional convolutional neural networks. J. Sound Vib. 2017, 388, 154–170.

51. Adams, R.; Cawley, P.; Pye, C.; Stone, B. A Vibration Technique for Non-Destructively Assessing the Integrity of Structures. J. Mech. Eng. Sci. 1978, 20, 93–100.

52. Van Overschee, P.; De Moor, P.; De Moor, B. Subspace identification problem. Automatica 1993, 29, 649–660.

53. Allahdadian, S.; Döhler, M.; Ventura, C.; Mevel, L. Towards robust statistical damage localization via model-based sensitivity clustering. Mech. Syst. Signal Process. 2019, 134, 106341.

54. Döhler, M.; Mevel, L.; Qinghua, Z. Fault detection, isolation and quantification from Gaussian residuals with application to structural damage diagnosis. Annu. Rev. Control 2016, 42, 244–256.

55. Jaishi, B.; Ren, W. Damage detection by finite element model updating using modal flexibility residual. J. Sound Vib. 2006, 290, 369–387.

56. Titurus, B.; Friswell, M. Damage detection using successive parameter subset selections and multiple modal residuals. Mech. Syst. Signal Process. 2014, 45, 193–206.

57. Döhler, M.; Mevel, L.; Hille, F. Subspace-based damage detection under changes in the ambient excitation statistics. Mech. Syst. Signal Process. 2014, 45, 207–224.

58. Deshmukh, A.; Shinde, U. A low cost environment monitoring system using raspberry Pi and arduino with Zigbee. In Proceedings of the 2016 International Conference on Inventive Computation Technologies (ICICT), Tamilnadu, India, 26–27 August 2016.

59. Novas, N.; Gázquez, J.; MacLennan, J.; García, R.; Fernández-Ros, M.; Manzano-Agugliaro, F. A real-time underground environment monitoring system for sustainable tourism of caves. J. Clean. Prod. 2017, 142, 2707–2721.

60. Kim, S.; Jeong, J.; Hwang, M.; Kang, C. Development of an IoT-based atmospheric environment monitoring system. In Proceedings of the 2017 International Conference on Information and Communication Technology Convergence (ICTC), Jeju Island, Korea, 18–20 October 2017.

61. Fusacchia, P.; Muttillo, M.; Leoni, A.; Pantoli, L.; Parente, F.; Stornelli, V.; Ferri, G. A Low Cost Fully Integrable in a Standard CMOS Technology Portable System for the Assessment of Wind Conditions. Procedia Eng. 2016, 168, 1024–1027.

62. Pantoli, L.; Paolucci, R.; Muttillo, M.; Fusacchia, P.; Leoni, A. A multisensorial thermal anemometer system. In Lecture Notes in Electrical Engineering; Springer: Cham, Switzerland, 2017; pp. 330–337.

63. Kychkin, A. Synthesizing a System for Remote Energy Monitoring in Manufacturing. Metallurgist 2016, 59, 752–760.

64. De Rubeis, T.; Nardi, I.; Muttillo, M.; Ranieri, S.; Ambrosini, D. Room and window geometry influence for daylight harvesting maximization—Effects on energy savings in an academic classroom. Energy Procedia 2018, 148, 1090–1097.

65. De Rubeis, T.; Nardi, I.; Muttillo, M. Development of a low-cost temperature data monitoring. An upgrade for hot box apparatus. J. Phys. Conf. Ser. 2017, 923, 012039.

66. Pantoli, L.; Muttillo, M.; Stornelli, V.; Ferri, G.; Gabriele, T. A low cost flexible power line communication system. In Lecture Notes in Electrical Engineering; Springer: Cham, Switzerland, 2017; pp. 413–420.

67. ATSAM3X8E - 32-bit SAM Microcontrollers, Microchip.com, 2020. [Online]. Available: https://www.microchip.com/wwwproducts/en/ATSAM3X8E. [Accessed: 4 - June - 2020].

68. Cypress [Online]. Available: https://www.cypress.com/documentation/datasheets/s25fl128ss25fl256s-128-mb-16-mb256-mb-32-mb-30v-spi-flash-memory. [Accessed: 13- Apr- 2020]

69. Paolucci, R.; Ferri, G.; Alaggio, R.; Cirella, R.; Stornelli V. Structural Health Monitoring: a system for the correct syncronization of the sensors. In Proceedings of the 6th International Conference on Smart and Sustainable Technologies (SpliTech), Split and Bol, Croatia (Hybrid), 8-11 September 2021.

70. Tao, G.; Feng, J.; Feng, H.; Feng, H.; Zhang, K. Reducing Construction Dust Pollution by Planning Construction Site Layout. Buildings 2022, 12, 531.

71. Rönnberg, N.; Ringdahl, R.; Fredriksson, A. Measurement and sonification of construction site noise and particle pollution data. Smart Sustain. Built Environ. 2020.

72. Jiang, Q.; Zhang, K. Research on construction site dust detection based on prior knowledge MinMax k-Means. In Proceedings of the 2nd IEEE International Conference on Artificial Intelligence and Industrial Design (AIID), Virtual, 28–30 May 2021.

73. Manzhilevskaya, S.; Petrenko, L.; Azarov, V. Monitoring Methods for Fine Dust Pollution During Construction Operations. In Proceedings of the International Scientific Conference Energy Management of Municipal Facilities and Sustainable Energy Technologies (EMMFT), Voronezh, Russia, 10–13 December 2019.

74. Luo, Q.; Huang, L.; Xue, X.; Chen, Z.; Zhou, F.; Wei, L.; Hua, J. Occupational health risk assessment based on dust exposure during earthwork construction. J. Build. Eng. 2021, 44, 103186.

75. Manzhilevskaya, S.; Petrenko, L.; Azarov, V. Vertical Distribution of Fine Dust During Construction Operations. In Proceedings of the International Scientific Conference Energy Management of Municipal Facilities and Sustainable Energy Technologies (EMMFT), Voronezh, Russia, 10–13 December 2019.

76. Zhang, D.; Ji, H.; Li, Z.; Ge, H. Design of Building Environment Detection System for Architectures Based on Internet of Things. Comput. Intell. Neurosci. 2022, 2022, 5438305.

77. United Nation, Department of Economic and Social Affairs Sustainable Development. Available online: https://sdgs.un.org/goals (accessed on 30 August 2022).

78. Rotilio, M. Strategies for overcoming critical post-disaster reconstruction: A case study. In Proceedings of the 4th International Conference on Preservation, Maintenance and Rehabilitation of Historical Buildings and Structures (REHAB), Barcelos, Portugal, 17–19 July 2019; pp. 539–551, ISBN 978-989-8734-41-9.

79. Rotilio, M.; Laurini, E.; Lucarelli, M.; De Berardinis, P. The maximization of the 4th dimension of the building site. Int. Arch. Photogramm. Remote Sens. Spat. Inf. Sci. 2019, XLII-4/W17, 15–20.

80. Alicandro, M.; Rotilio, M. UAV photogrammetry for resilience management in reconstruction plan of urban historical centres after seismic events. A case study. Int. Arch. Photogramm. Remote Sens. Spat. Inf. Sci. 2019, XLII-2/W11, 55–61.

81. Tagle, M.; Rojas, F.; Vásquez, Y.; Hallgren, F.; Lindén, J.; Kolev, D.; Watne, Å.K.; Oyola, P. Field performance of a low-cost sensor in the monitoring of particulate matter in Santiago, Chile. Environ. Monit. Assess. 2020, 192, 171.

82. Candia, A.; Represa, S.N.; Giuliani, D.; Luengo, M.A.; Porta, A.A.; Marrone, L.A. Solutions for SmartCities: Proposal of a monitoring system of air quality based on a LoRaWAN network with low-cost sensors. In Proceedings of the Congreso Argentino de Ciencias de la Informática y Desarrollos de Investigación (CACIDI), Buenos Aires, Argentina, 28–30 November 2018.

83. Kurnia, D.; Hadisantoso, F.S.; Suprianto, A.A.; Nugroho, E.A.; Janizal, J. Real-Time Air Quality Index Monitoring Experiments Using SDS011 Sensors and Raspberry Pi. In Proceedings of the 5th Annual Applied Science and Engineering Conference (AASEC), Virtual, 21–22 April 2020.

84. Paolucci, R.; Rotilio, M.; De Berardinis, P.; Ferri, G.; Cucchiella, F.; Stornelli, V. Electronic System for Monitoring of Dust on Construction Sites for the Health ofWorkers. In Proceedings of the 15th International Conference on Advanced Technologies, Systems and Services in Telecommunications (TELSIKS), Nis, Serbia, 20–22 October 2021.

85. Budde, M.; Schwarz, A.D.; Müller, T.; Laquai, B.; Streibl, N.; Schindler, G.; Köpke, M.; Riedel, T.; Dittler, A.; Beigl, M. Potential and Limitations of the Low-Cost SDS011 Particle Sensor for Monitoring Urban Air Quality. In Proceedings of the 3rd International Conference on Atmospheric Dust, Bari, Italy, 29–31 May 2018.

86. Budde, M.; Muller, T.; Laquai, B.; Streibl, N. Suitability of the Low-Cost SDS011 Particle Sensor for Urban PM-Monitoring. In Proceedings of the 3rd International Conference on Atmospheric Dust, Bari, Italy, 29–31 May 2018.

87. Alfano, B.; Barretta, L.; Del Giudice, A.; De Vito, S.; Di Francia, G.; Esposito, E.; Formisano, F.; Massera, E.; Miglietta, M.L.; Polichetti, T. A Review of Low-Cost Particulate Matter Sensors from the Developers' Perspectives. Sensors 2020, 20, 6819.

88. Chen, M.; Yuan, W.; Cao, C.; Buehler, C.; Gentner, D.R.; Lee, X. Development and Performance Evaluation of a Low-Cost Portable PM2.5 Monitor for Mobile Deployment. Sensors 2022, 22, 2767.

89. SDS011 Sensor Data Sheet. Available online: http://inovafitness.com/en/a/chanpinzhongxin/95.html (accessed on 22 March 2021).

90. Muttillo, M., Stornelli, V., Alaggio R., Paolucci R., Di Battista L., De Rubeis T.: Structural Health Monitoring: An IoT Sensor System for Structural Damage Indicator Evaluation. Sensors 20, 4908 (2020).

91. Pantoli, L.; Alaggio, R.; Paolucci, R.; Di Battista, L.; Ferri, G. Sensors and Interfaces for Structural Health Monitoring. In Lecture Notes in Electrical Engineering book series (LNEE,volume 918) - AISEM 2021: Sensors and Microsystems pp 295–300.

92. Paolucci, R.; Rotilio, M.; Ricci, S.; Pelliccione, A.; Ferri, G. A Sensor Based System for Dust Containment and in the Construction Site. Energies 2022, 15(19), 7272.

List of Figures

List of Tables